



# Shell International Deepwater Services B.V.

SIDS 98-0053

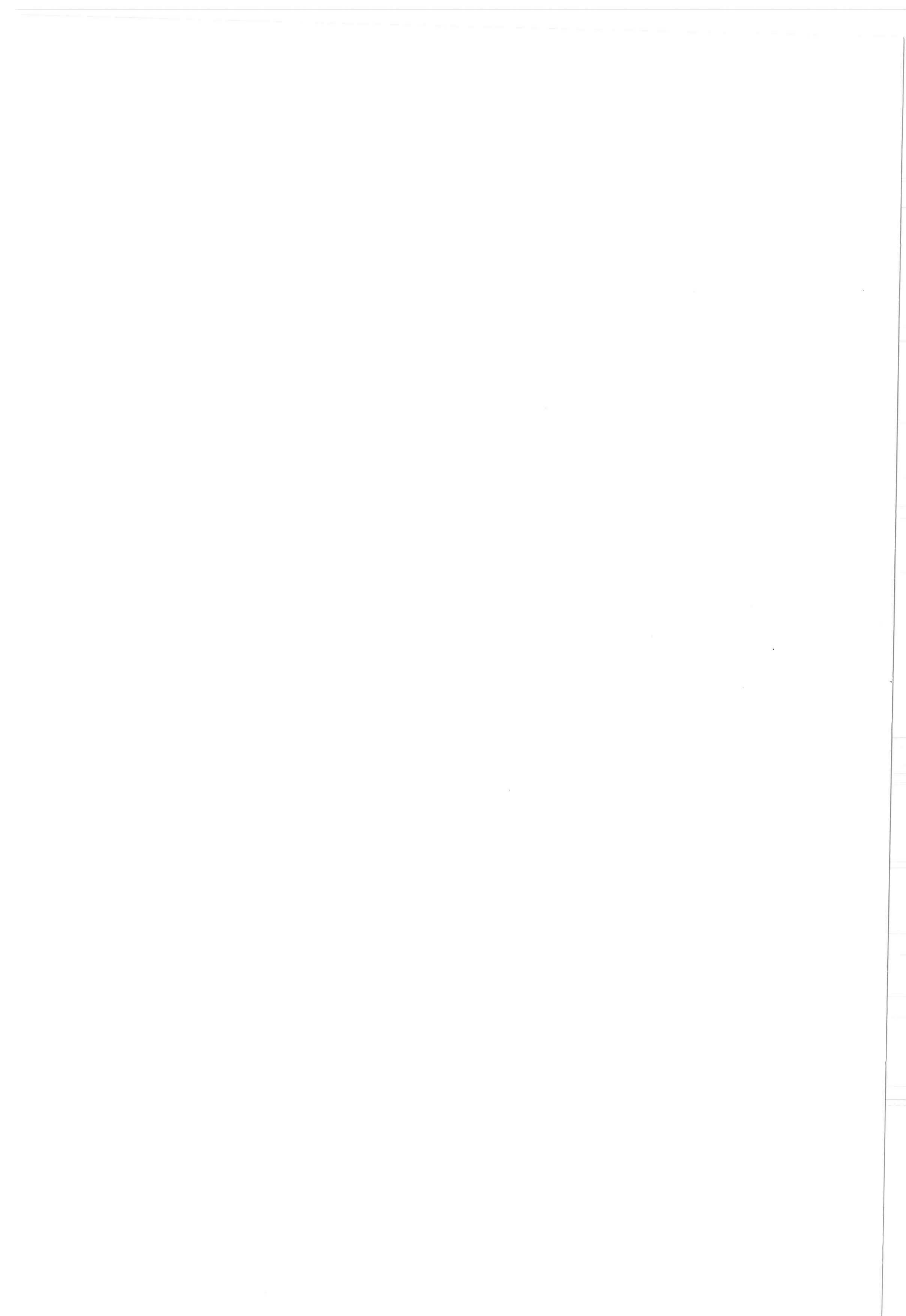
Student thesis report

## *Extreme Response of a Turret Moored Ship; A Frequency Domain Method*

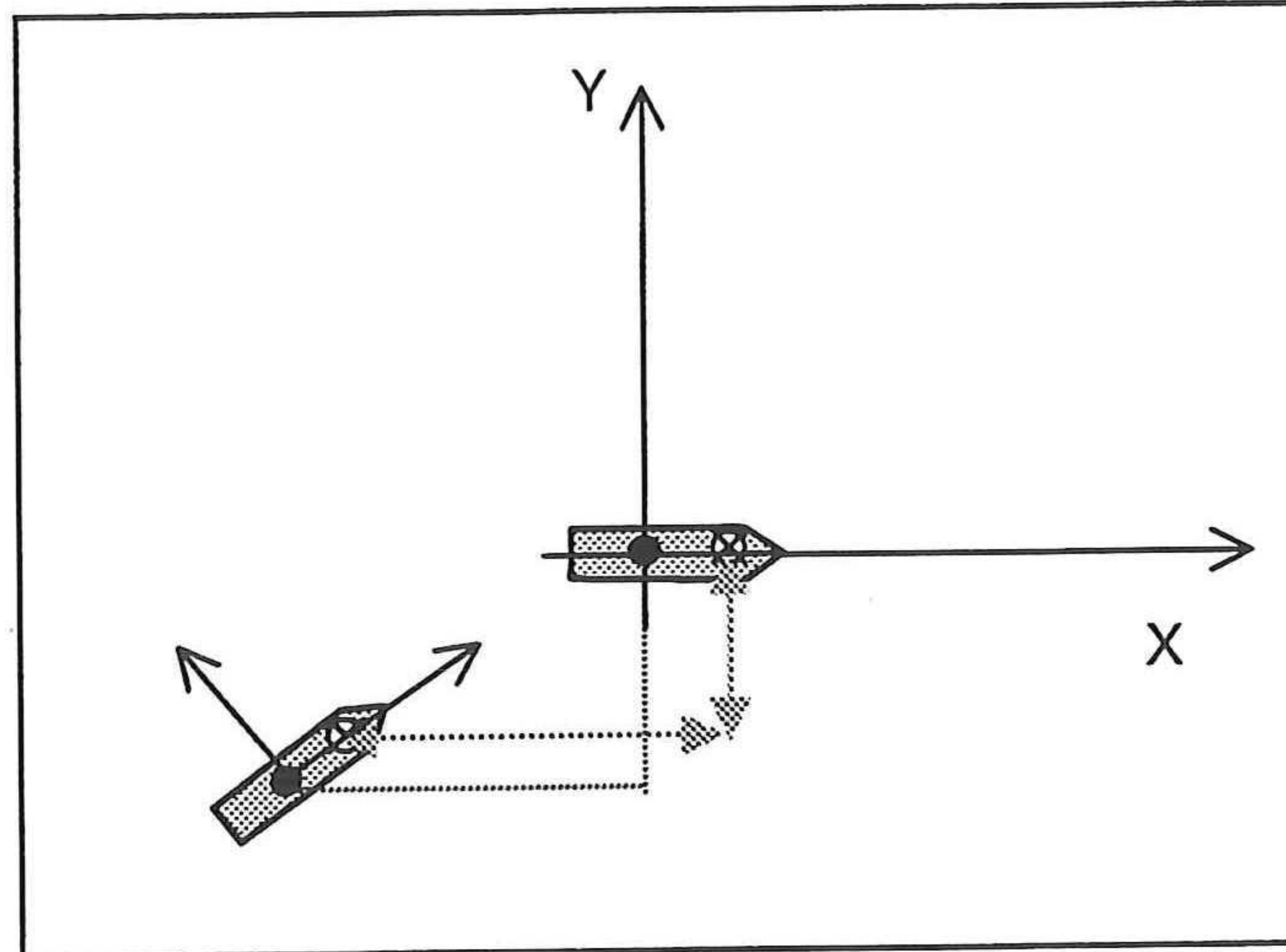
Louis Coulomb

October 1998

A1	23-Oct-98	For Review	L. Coulomb		
Rev	Date	Description	Originator		
REVISION STATUS			APPROVAL		



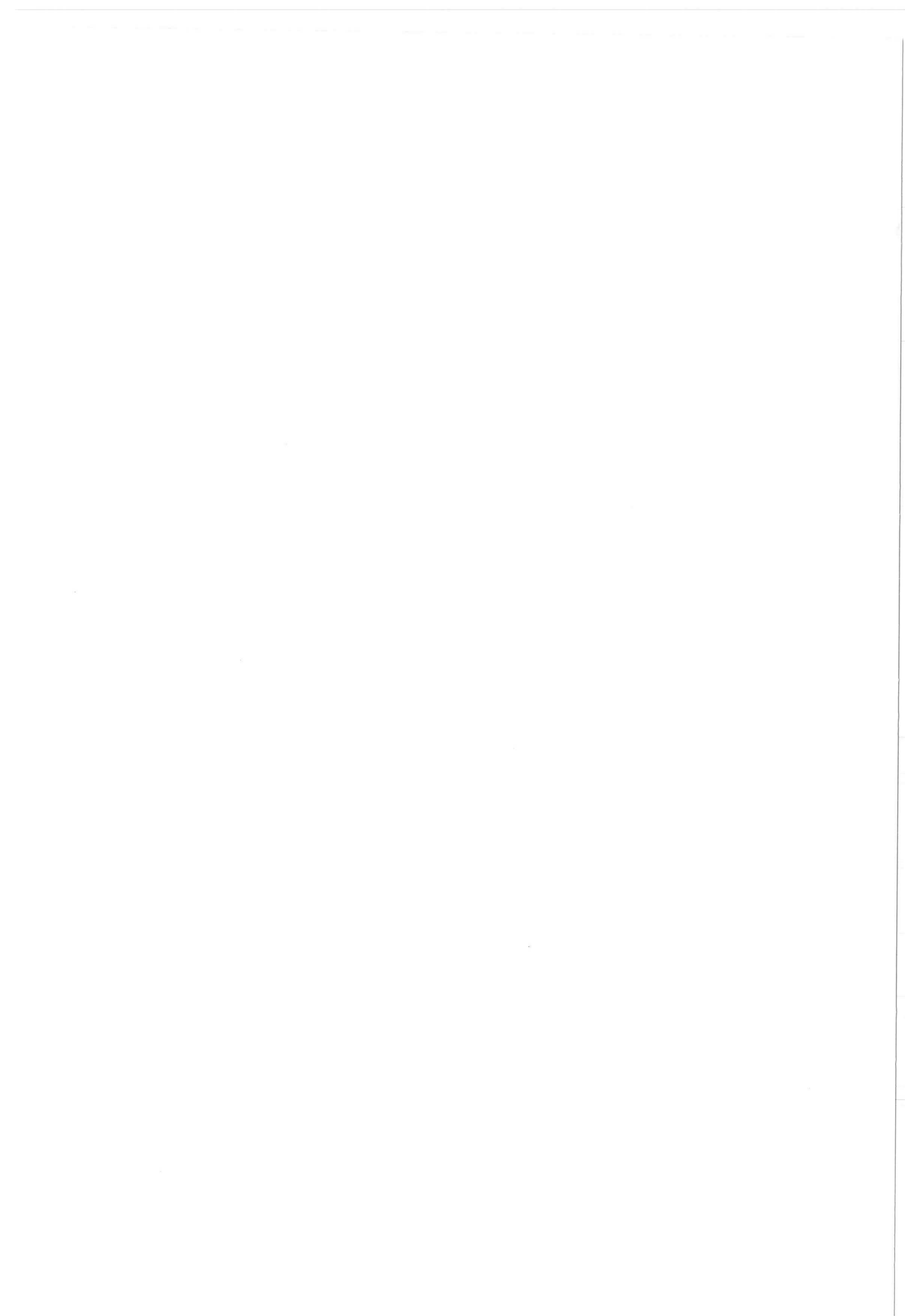
**Extreme Response of a Turret Moored Ship;  
A Frequency Domain Method**



*Final Report*

**October 1998  
Louis Coulomb**

Delft University of Technology  
Faculty of Civil Engineering  
Section Offshore Engineering



## PREFACE

This is the final report of my thesis project carried out at Shell International Deepwater Services (SIDS); I'm very grateful for the opportunity. I would like to thank the Metocean team for providing such a sound atmosphere to work in and, in particular, I want to thank Dr. Peter Tromans, my supervisor, for all his help and encouragement over the course of the eight month duration.

Furthermore, from the university, I want to thank the members of the exam committee, Prof. Vrouwenvelder, Prof. Battjes, Mr. Journee and Mr. Massie for their assistance and stimulating technical discussion during the meetings.

To briefly summarize the content of this report: much of chapters 2 through 3 covers some of the theory that underlies the calculation of the forces; chapter 4 presents the work I have done on static analysis of the system (under steady loads) and gives some results using the program that was written for it. Chapter 5 covers the theory for the dynamic analysis and gives the expressions for the dynamic response. Chapter six presents the theory for the first order reliability method as it relates to this project; chapter 7 gives some results of the "dynamic" program.



---

PREFACE.....	1
ABSTRACT .....	3
1. INTRODUCTION .....	4
1.1 The Context of the Problem .....	4
1.2 General Approach.....	5
2. DEFINITIONS .....	7
3. THE ENVIRONMENTAL FORCES .....	8
3.1 Steady wind and current .....	8
3.2 Waves.....	10
3.2.1 Spectral theory .....	10
3.2.2 First order wave forces.....	13
3.2.3 Second order wave drift forces .....	14
3.2.3.1 Low frequency wave drift forces .....	15
3.2.3.2 Mean wave drift forces .....	17
3.3 Unsteady Wind.....	18
3.3.1 Wind gust force .....	19
4. STATIC ANALYSIS.....	20
4.1 Mean offset and orientation.....	20
4.2 Program .....	22
4.3 Results.....	23
5. DYNAMIC ANALYSIS.....	25
5.1 Equations of motion .....	25
5.2 Modal superposition .....	25
5.2.1 Steady state response.....	27
5.1.2.1 First order dynamic response .....	29
5.1.2.2 Second order dynamic response .....	30
5.3 Coefficients of the equation.....	31
6. FIRST ORDER RELIABILITY METHOD .....	35
6.1 Transformations .....	35
6.2 Standardized response .....	36
6.3 The unit-variance normal space and the reliability index .....	38
6.4 Determining the design point.....	39
6.5 The first estimate of the design point.....	41
6.6 Extreme response .....	41
6.7 FORM: an optimization.....	42
6.8 Wave and wind histories .....	42
7. RESULTS AND ANALYSIS .....	44
7.1 The limit state function .....	44
7.2 The probability of exceedance (Q).....	44
7.3 CASE 1 .....	47
7.4 CASE 2.....	52
7.5 Concluding remarks .....	60
8. CONCLUSION.....	61
Nomenclature .....	62
References: .....	64
APPENDIX .....	65



**ABSTRACT**

A model has been developed to calculate extreme responses of turret moored ships. The responses are expressed in terms of the environmental parameters: waves, wind and current. Motions in the horizontal plane, surge, sway and yaw, are analyzed statically and dynamically.

The static analysis resolves the equilibrium position and heading about which the vessel oscillates. The dynamic analysis is a probabilistic one based on the first-order second-moment method. The frequency components of the ocean surface and turbulent wind processes, and their Hilbert transforms are transformed into a standardized form. A response, such as vessel offset, can be expressed in terms of the standardized variables. A constant value of that response then defines a limit state, a surface in the unit-variance normal space of the standardized variables. By an iteration process, we find the response corresponding to a prescribed probability of exceedance.

The point on the limit state surface with the highest probability is the "design point". This gives the combination of wave and wind most likely to generate the extreme response. The set of wind gust and wave components that occasioned the design-point-response can be retrieved, and together constitute metocean histories, "designer wave," that may be used for further design or analysis.

The algorithm is implemented in a program called TURRETDYN, which requires some time to find convergence in its iteration, but substantially less than its time domain counterpart. The results are compared with an existing time domain simulation program called DYNFLOAT. The project essentially demonstrates the applicability of this probabilistic method, particularly for preliminary evaluation and as a means to generate extreme-response statistics and designer waves.

1. The first part of the document discusses the importance of maintaining accurate records of all transactions. It emphasizes that every entry should be supported by a valid receipt or invoice to ensure transparency and accountability. This is particularly crucial for businesses operating in highly regulated industries where compliance is a top priority.

2. The second section delves into the various methods used for data collection and analysis. It highlights the need for robust systems that can handle large volumes of information efficiently. Modern software solutions offer advanced analytics capabilities, allowing users to identify trends and make data-driven decisions. However, it also notes the importance of data security and privacy, especially when dealing with sensitive customer information.

3. The third part of the document addresses the challenges of integrating different data sources. Many organizations struggle with siloed data, where information is scattered across various departments and systems. This can lead to inconsistent reporting and missed opportunities. The text suggests implementing a centralized data lake or data warehouse to facilitate seamless integration and provide a unified view of the organization's performance.

4. Finally, the document concludes by discussing the role of artificial intelligence (AI) in data management. AI-powered tools can automate repetitive tasks, such as data entry and cleaning, and provide predictive insights based on historical data. While AI offers significant benefits, it also raises concerns about job displacement and the need for upskilling the workforce. The text encourages organizations to embrace AI as a tool to enhance productivity and gain a competitive edge in the market.

## 1. INTRODUCTION

In recent years Floating Production, Storage and Offloading (FPSO) systems have become increasingly attractive for developing marginal fields with lives of less than 10 years. This is particularly so in the case of remote fields that lack the infrastructure, such as existing pipelines, to export the hydrocarbons. The better part of these are ship-shaped, single point moored FPSOs, predominantly turret moored whereby the ship can weathervane about the turret according to the prevailing environmental conditions. In fig 1.1 below such a system is shown; the turret, in fact, functions as a pivot around which the vessel can freely rotate. It is a single point moored (SPM) system because the catenary mooring lines are attached to the turret only. The advantage of such a system over traditional ones is that the vessel aligns itself with the environmental loads, reducing the total exposed surface, and thereby the load and the offset of the vessel.

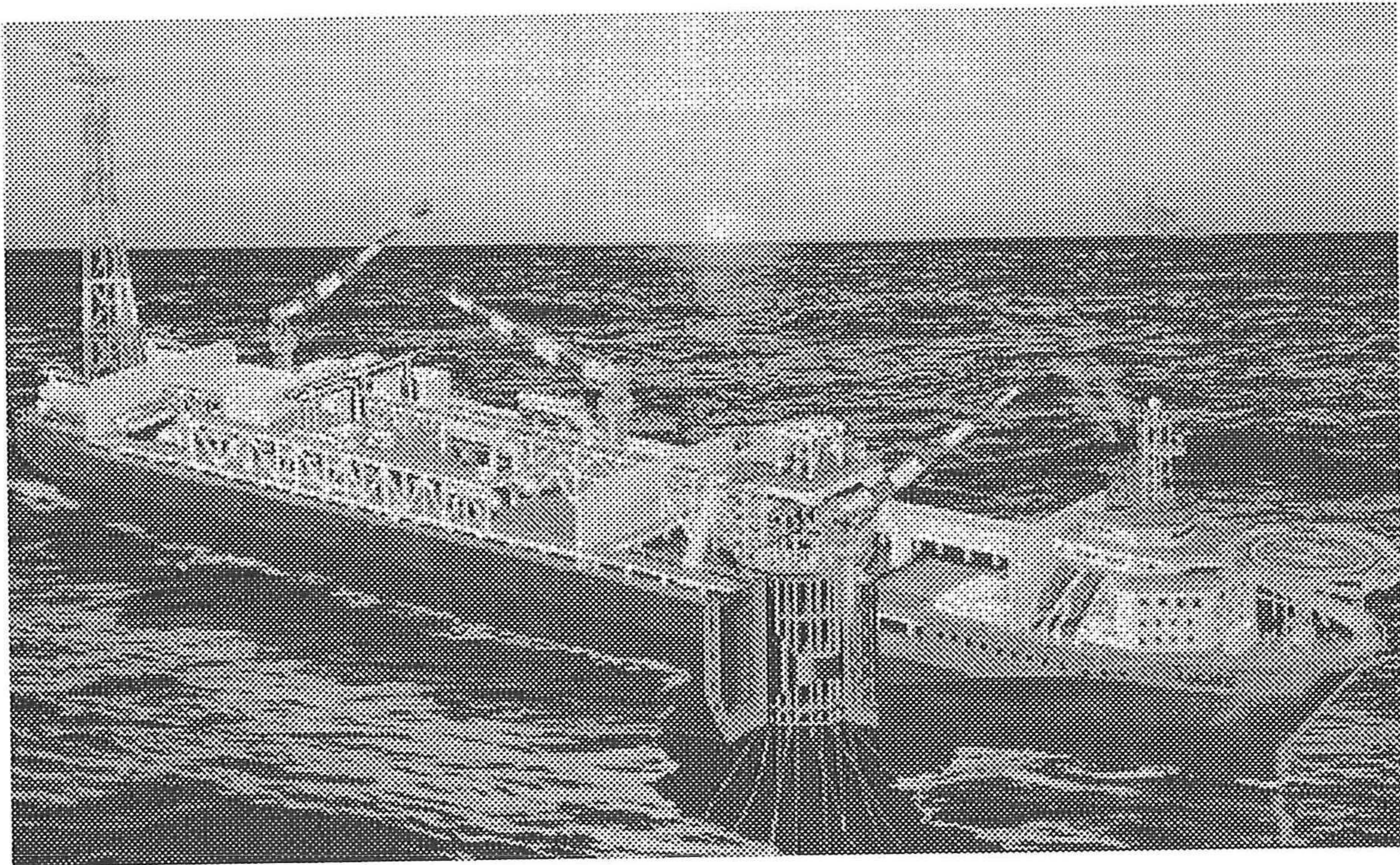


*Figure 1.1 A turret moored FPSO*

With advances in mooring technology, FPSO's can be applied to deep water developments. As these vessels move into deeper water with harsher environmental conditions, the importance of design environmental data becomes more and more critical: the riser system will dictate the maximum allowable offset, and the mooring system must be designed accordingly. Therefore, how the system responds to the environment, particularly extreme responses, and what environmental conditions occasion these, are crucial questions in the design process.

### 1.1 The Context of the Problem

At present, most available analysis tools to determine extreme responses of single point moored ships, that do not resort to empirical calibration factors, are based on time-domain simulation. At an initial design stage, parameters change rapidly as the design 'iterates' to a more definitive form; it is desirable, therefore, to have a tool that accommodates this speed of evolution and that can account for the parameters that are being considered.

Modern computing capacity can perform time domain calculations with an investment of time that may be acceptable where only one or two sea states are considered. Current methods, however, used to determine the joint meteorological and oceanographic (metocean) history that generates a most probable extreme response, are based not on individual sea states as the basic, independent event, but on storms, characterized by a set of four or five sea states. This method is response based in that the met-ocean signal that is determined is not derived directly from an extreme significant wave height and wind speed (corresponding to a particular return period) but to the most probable extreme response of the system. If 100 storms are analyzed, each storm being comprised of 4 or 5 sea states, the quantity begins to be intractable for time-domain simulation, and it is necessary then to move out of the time domain. Some of the most recent developments suggest that a better metocean signal for design is a "designer wave", a deterministic time history of surface elevation, wind and current that might be developed from such response based calculation.

Time domain simulation is not without merit in this age of high computer capacity. The frequency domain does not easily accommodate non-linearity in the system characteristics; a catenary mooring system is typically non-linear, in some cases very much so, and is very significant in the response calculation. The strengths of both methods can be deployed when the "designer wave" metocean signal is generated in the probabilistic or frequency domain, and used as input in a time domain simulation, where the non-linear characteristics of the system can be accounted for.

The subject of this project is the development of a probabilistic method that fulfills many of the above requirements for the analysis of turret moored tankers in a sea state.

## 1.2 General Approach

The system will be modeled in a simple fashion, as a rigid, floating body. The steady forces arising from wind and current can be determined using direction dependent coefficients, and the quadratic transfer functions for the mean drift force follow from hydrodynamic data files. These all are used in the static analysis in which we calculate the static offset and heading of the ship for given wave, wind and current data. This output will be some of the input for the dynamic analysis.

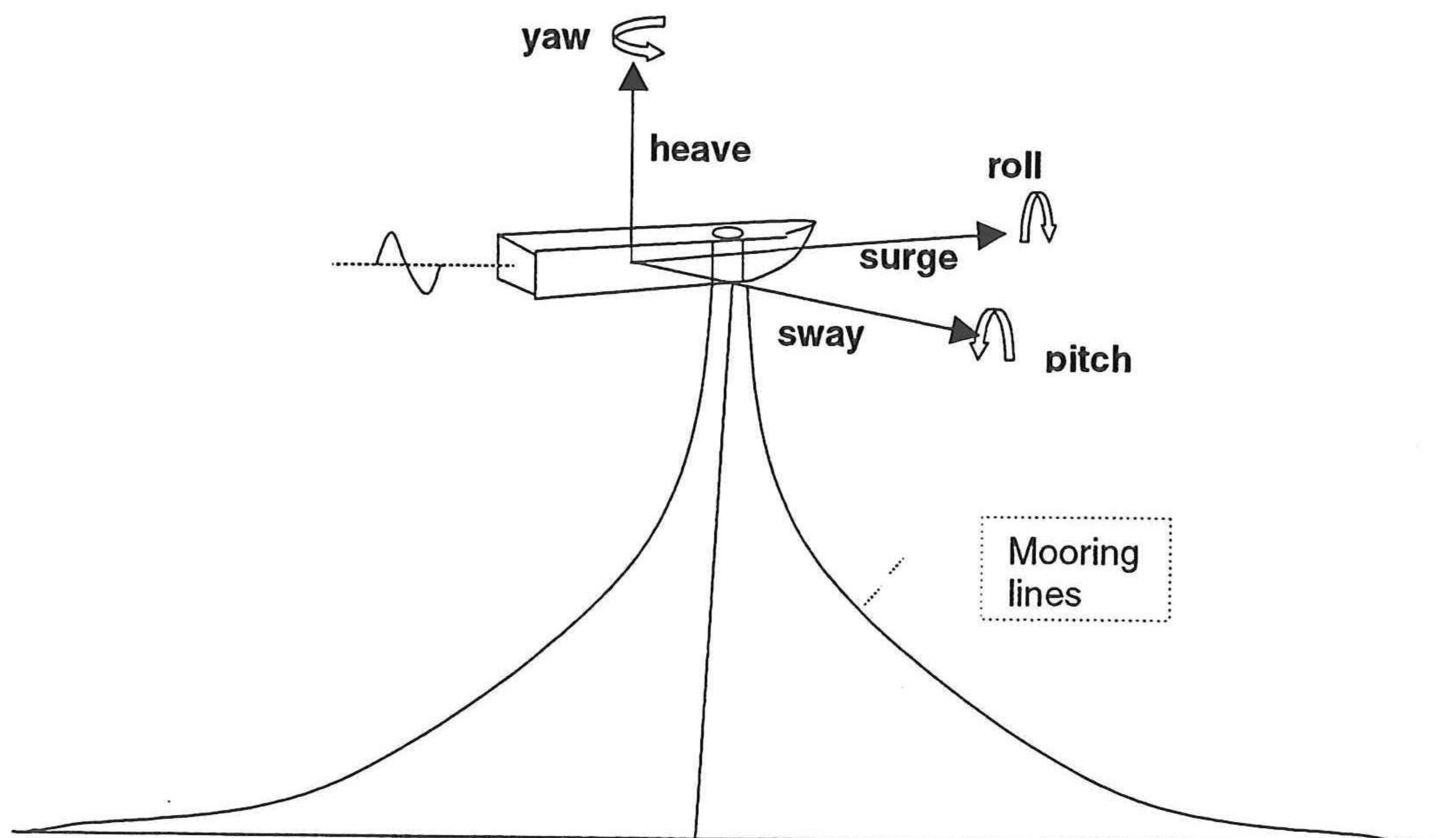
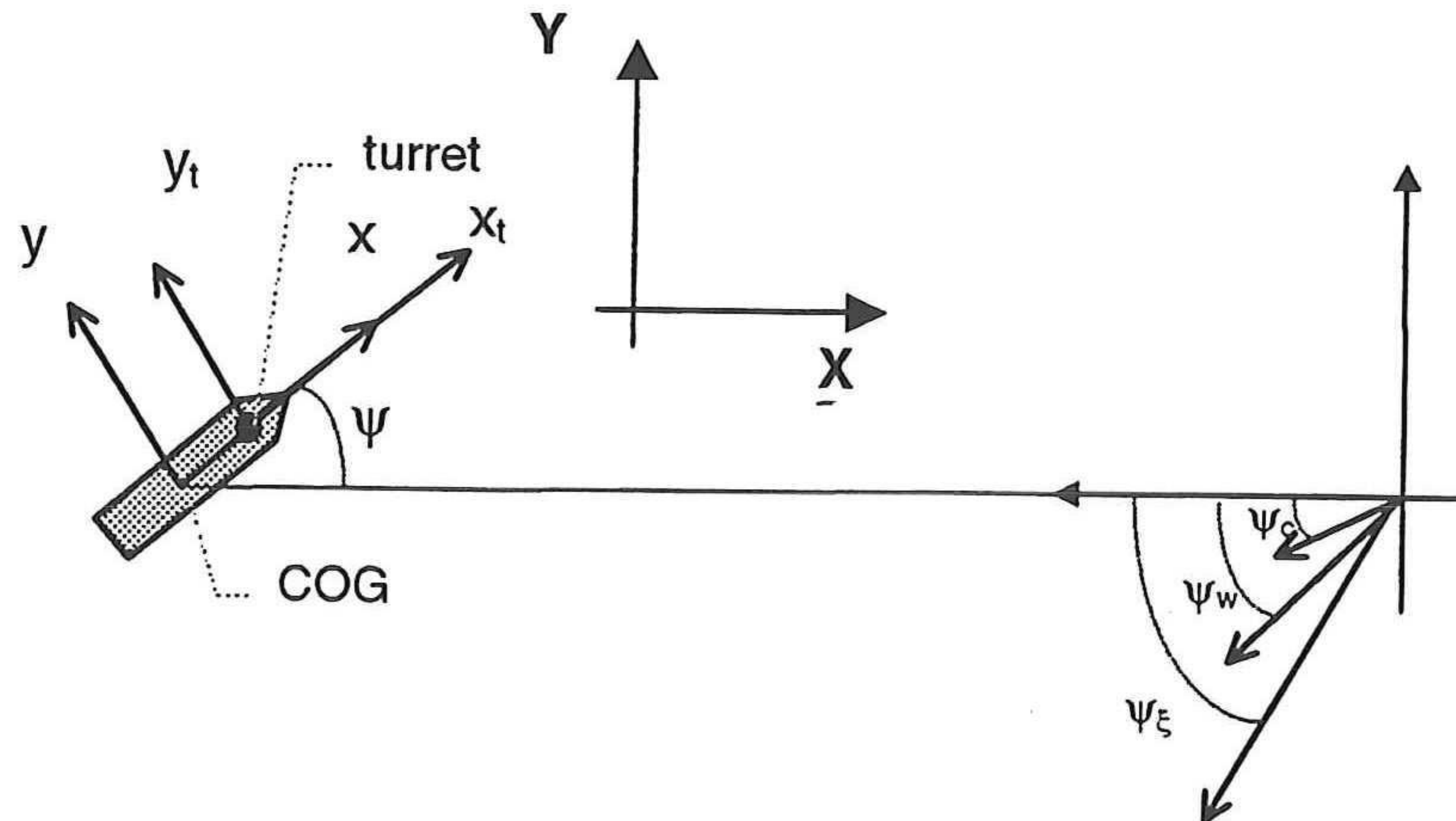


Figure 1.2 Rigid body motions

In the dynamic analysis, we consider only the horizontal motions, described by the three degrees of freedom, surge, sway and yaw (see figure 1.2). Naturally, data such as added mass and damping, and the first and second order transfer functions will have to be used for the relevant range of wave frequencies; these also can be obtained from the hydrodynamic data files. The mooring system will be characterized by a linear spring. The time varying environmental parameters will be expressed in terms of their corresponding spectrum (wind or wave) and transformed into a standardized form. From this point, the spectral response surface analysis may be applied to determine the extreme response (for a particular prescribed exceedance probability) and the metocean histories that generated it.

## 2. DEFINITIONS

Three co-ordinate systems will be used: the space fixed, global co-ordinate system  $(X,Y)$ , with its origin at the initial position (the unloaded case) of the center of gravity (COG), and two ship fixed, local co-ordinate systems, one with its origin in the COG  $(x,y)$  and the other with its origin in the center of the turret  $(x_t,y_t)$ . As we will be dealing only with motions in the horizontal plane in this study, it will suffice to express the co-ordinates in translations  $x$  and  $y$  (surge and sway), and rotation  $\psi$  (yaw), as shown in figure 2.1 below.



**Figure 2.1 Co-ordinate systems in the horizontal plane**

The directions of the environmental variables, current, wind and waves, are designated by  $\psi_c, \psi_w$  and  $\psi_\xi$  respectively. They are given with respect to the negative  $x$  direction of the global co-ordinate system; this is done to facilitate calculation in the program because the forces are given in terms of coefficients that depend on the relative heading of the ship, and because the ship weathervanes about the turret toward the prevailing environmental loads there would otherwise always be a 180 degree shift between ship and loads. This way the ship heading, in its equilibrium position, will have about the same value as the mean of the load directions.

The translatory rigid body motions are referred to as surge, sway and heave; the rigid body angular motions are referred to as roll, pitch and yaw. For now, we will only consider three degrees of freedom, namely surge, sway and yaw because they are often the most significant responses and need to be treated first. Heave, pitch and roll also play a role since they induce dynamic effects in risers and moorings, but they are not treated in this project.

Forces and moments are given with respect to the center of gravity.

### 3. THE ENVIRONMENTAL FORCES

The environmental parameters that play the most significant role in the response of a moored ship are:

- current
- waves
- wind

The forces the environment generates can be divided into steady and oscillatory:

*Steady:*

- mean wind and current forces.
- mean wave drift forces; proportional to the square of the wave amplitude.

*Oscillatory:*

- First order, wave frequency forces .
- Low-frequency forces, resulting from wind gusts and slowly varying wave forces occurring in irregular waves (also called difference frequency forces, as will be explained later).

We are dealing with a system of a ship and its mooring system, wherein the characteristics of the latter greatly influence its behavior, in particular the frequency range to which it is most responsive.

#### 3.1 Steady wind and current

The steady wind and current forces and moments are determined using empirically established coefficients as given by OCIMF [Oil Companies International Marine Forum, 1997]. These are given in non-dimensional form for a moored vessel in various draft and underkeel clearance conditions, as well as various water depth to draft ratios. The following non-dimensional coefficients are used:

$$\begin{aligned} C_x &= \text{longitudinal force coefficient} \\ C_y &= \text{lateral force coefficient} \\ C_{xy} &= \text{yaw moment coefficient} \end{aligned}$$

Note that these coefficients are valid in the local co-ordinate systems; for corresponding global forces a transformation must be carried out. *The coefficients account for the heading of the ship relative to the wind and current.*

**CURRENT:**

The equations for steady current are:

$$\begin{aligned} F_{x,cur} &= \frac{1}{2} C_{x,c} \rho_c U^2 L_{PP} T \\ F_{y,cur} &= \frac{1}{2} C_{y,c} \rho_c U^2 L_{PP} T \\ M_{xy,cur} &= \frac{1}{2} C_{xy,c} \rho_c (U L_{PP})^2 T, \end{aligned}$$

where  $\rho_c$  is the water mass density,  $L_{pp}$  is the length between perpendiculars, and  $T$  the draft of the ship. Though the current ( $U$ ) varies over the depth, a uniform flow field may be assumed for typical drafts.

Wave-current drag will be discussed in the section on wave forces.

**WIND:**

The equations for wind loads have a similar form.

$$F_{x,win} = \frac{1}{2} C_{x,w} \rho_a V^2 A_T$$

$$F_{y,win} = \frac{1}{2} C_{y,w} \rho_a V^2 A_L$$

$$M_{xy,win} = \frac{1}{2} C_{xy,w} \rho_a V^2 A_L L_{pp}$$

The values of  $A_T$  and  $A_L$  (the transverse and lateral windage area, respectively) should be treated with caution as the geometry of FPSO superstructure tends to be irregular.

A wind velocity measurement at an elevation of 10m above the water surface is required for use in the wind load equations [OCIMF, 1997]. The coefficients were developed based on a steady state wind condition. For wind velocities obtained at a different elevation, adjustments to the equivalent 10m velocity are necessary and can be made with the following formula:

$$V_z = v_w (h_0/h)^{1/7}$$

where  $V_z$  is wind velocity at elevation  $h_0=10m$ , and  $v_w$  the wind velocity at elevation  $h$ . Figures 3.1 and 3.2 below show the curves of the wind and current coefficients according to OCIMF.

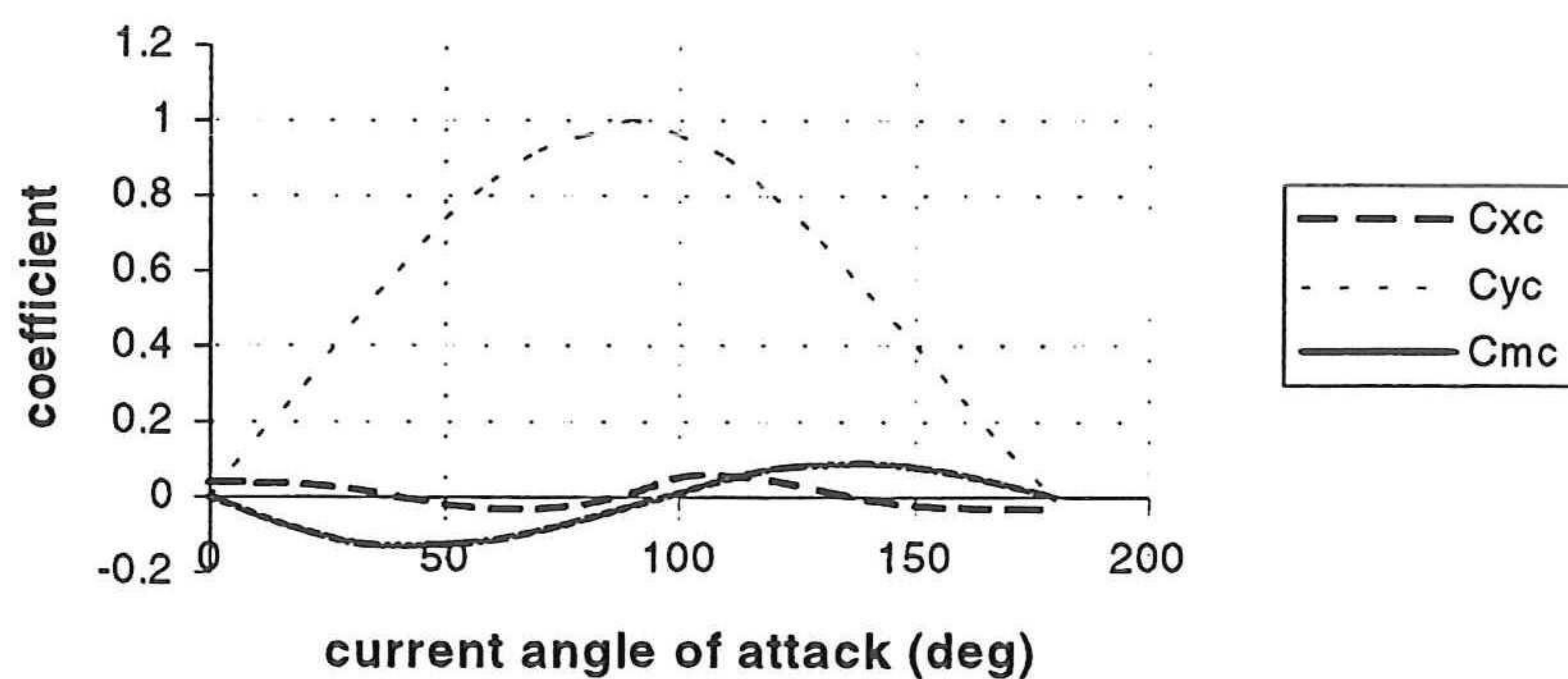


figure 3.1 OCIMF current coefficients

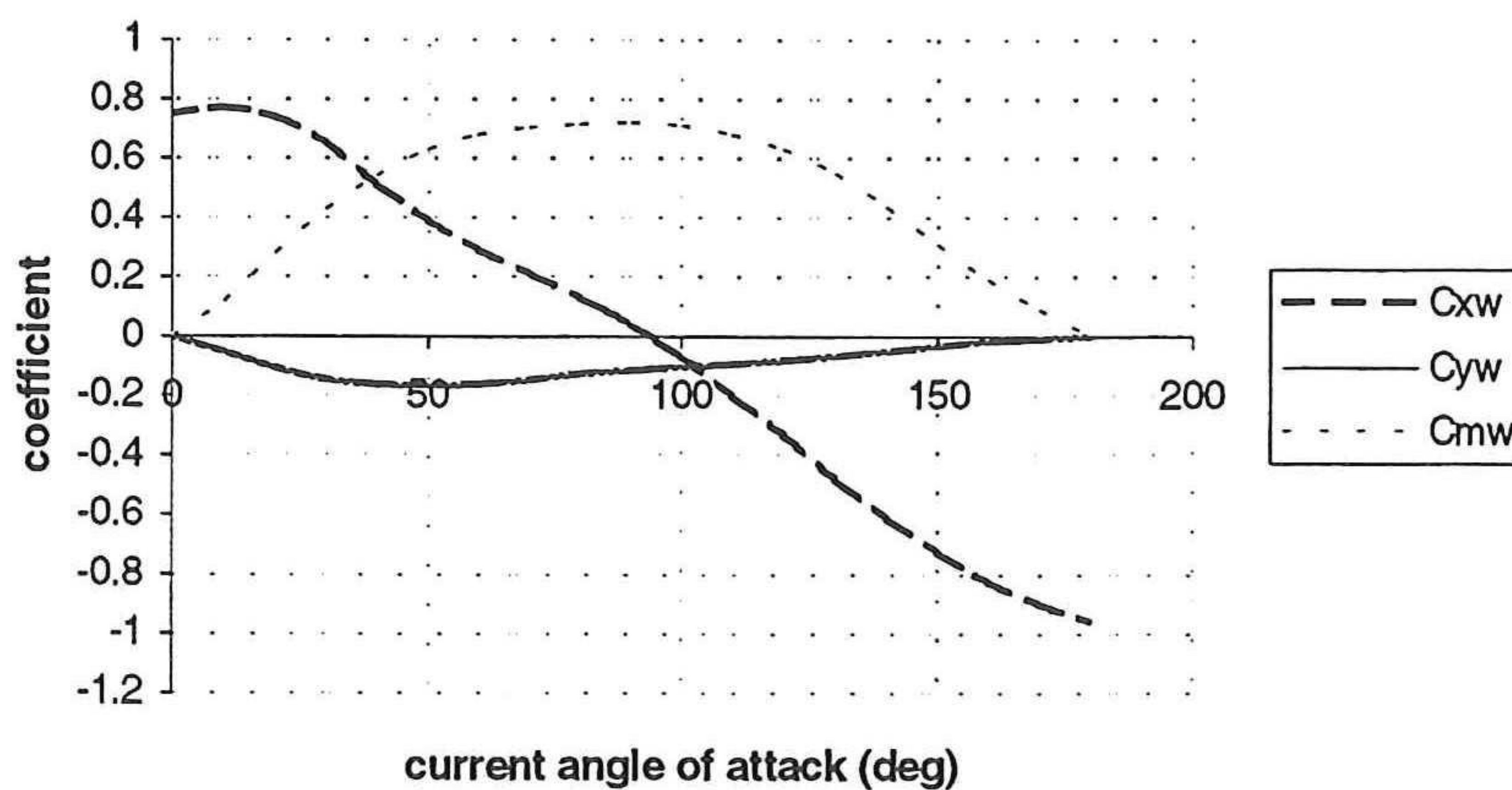


figure 3.2 OCIMF wind coefficients

### 3.2 Waves

Wind waves are the major source of environmental loads on offshore structures. In this study we are interested in the responses of a dynamic system; thus, the frequency at which loads act is at least as significant as their magnitude. The dynamic system consists of a vessel of great mass and a rather soft mooring; the natural frequencies are therefore low and the dynamic response to first order wave action is relatively small. It is however susceptible to resonant excitation from second order, slowly varying forces, or difference frequency forces because these act at a low frequency range which can include the resonant frequencies of the system.

The beam of a tanker is around 50 m. This is significantly greater than the amplitude of the wave induced water particle motion and puts the wave loading in the diffraction regime. That is, diffraction forces will dominate over drag forces due to wave kinematics. Similarly, drag forces arising from wave-current cross terms are also ver small. In consequence, in this study all wave and wave-current drag forces are neglected.

#### 3.2.1 Spectral theory

Within linear wave theory, the sea can be represented by the superposition of many wave components. In this manner, the irregular nature of the sea is approximated. Directional spreading, however, will be left out for the sake of simplicity. A unidirectional wave system will be assumed, represented by the sum of an infinite number of sinusoidal functions as follows:

$$\eta(t) = \sum_n a_n \cos(\varepsilon_n - \omega_n t) \quad (3.1)$$

where  $a_n$ ,  $\omega_n$ ,  $\varepsilon_n$  are respectively the amplitude, frequency and random phase angle of the wave component  $n$ . Faltinsen illustrates this concept with the figure 3.3, given below [Faltinsen, 90]

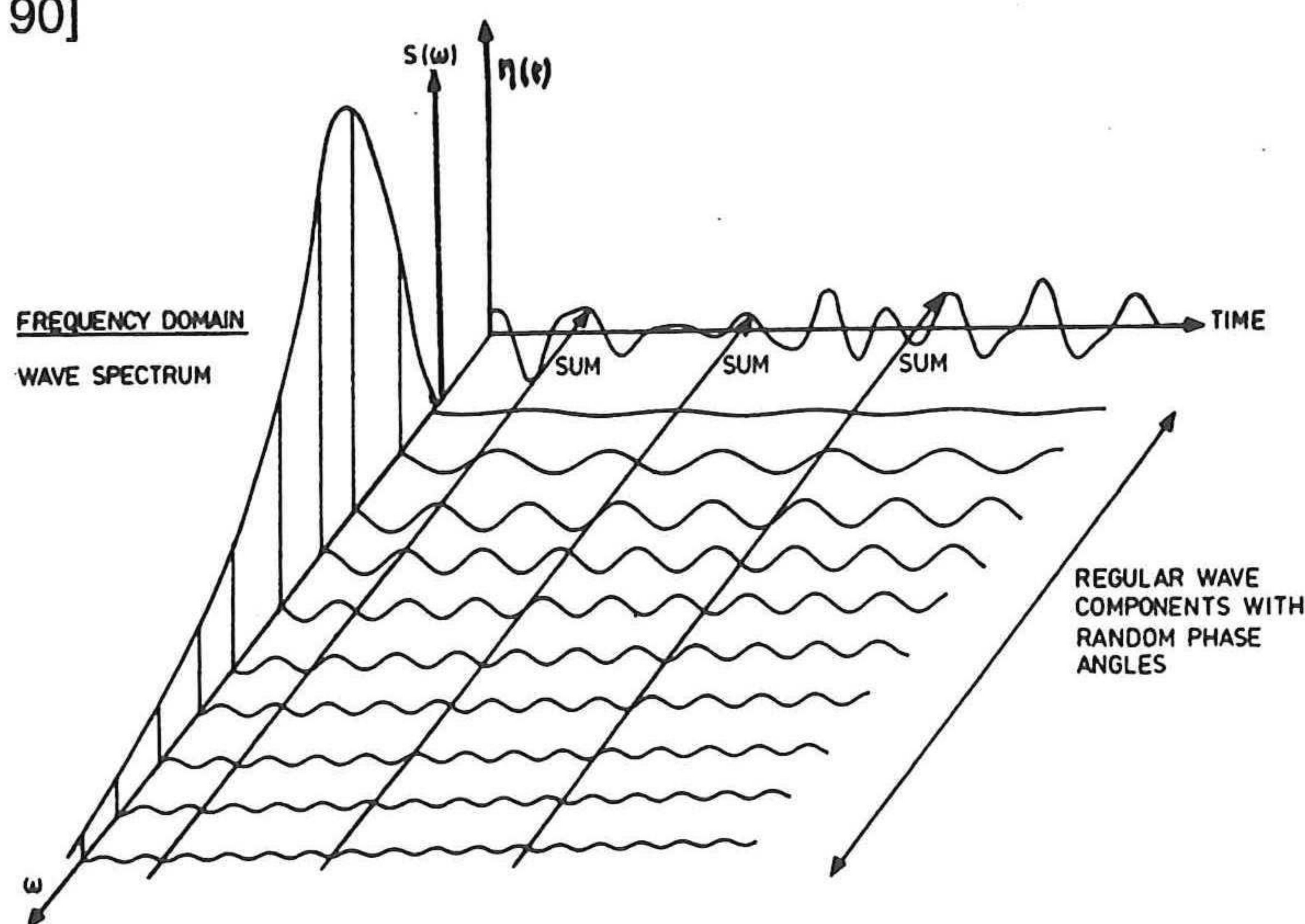


Figure 3.3 relation between the wave components and the spectrum

The stochastic nature of the system has its source in the random phase angle, which has a uniform distribution in the interval  $[0, 2\pi]$ :

$$P(\varepsilon) = \frac{1}{2\pi}, \varepsilon \in [0, 2\pi] \quad (3.2)$$

It may be said that the surface elevation is the sum of many stochastic variables, which, for a great number of wave components ( $n$ ), is normally distributed according to the central limit theorem. The variance of this distribution ( $\eta$ ) is defined as:

$$\sigma_{\eta}^2 = \sum_n \sigma_{\eta_n}^2 \quad (3.3)$$

integrated over the interval over which the random phase is uniformly distributed,

$$= \sum_n \int_0^{2\pi} \eta_n^2(t) p(\varepsilon) d\varepsilon_n =$$

substituting equations 3.1 and 3.2 yields,

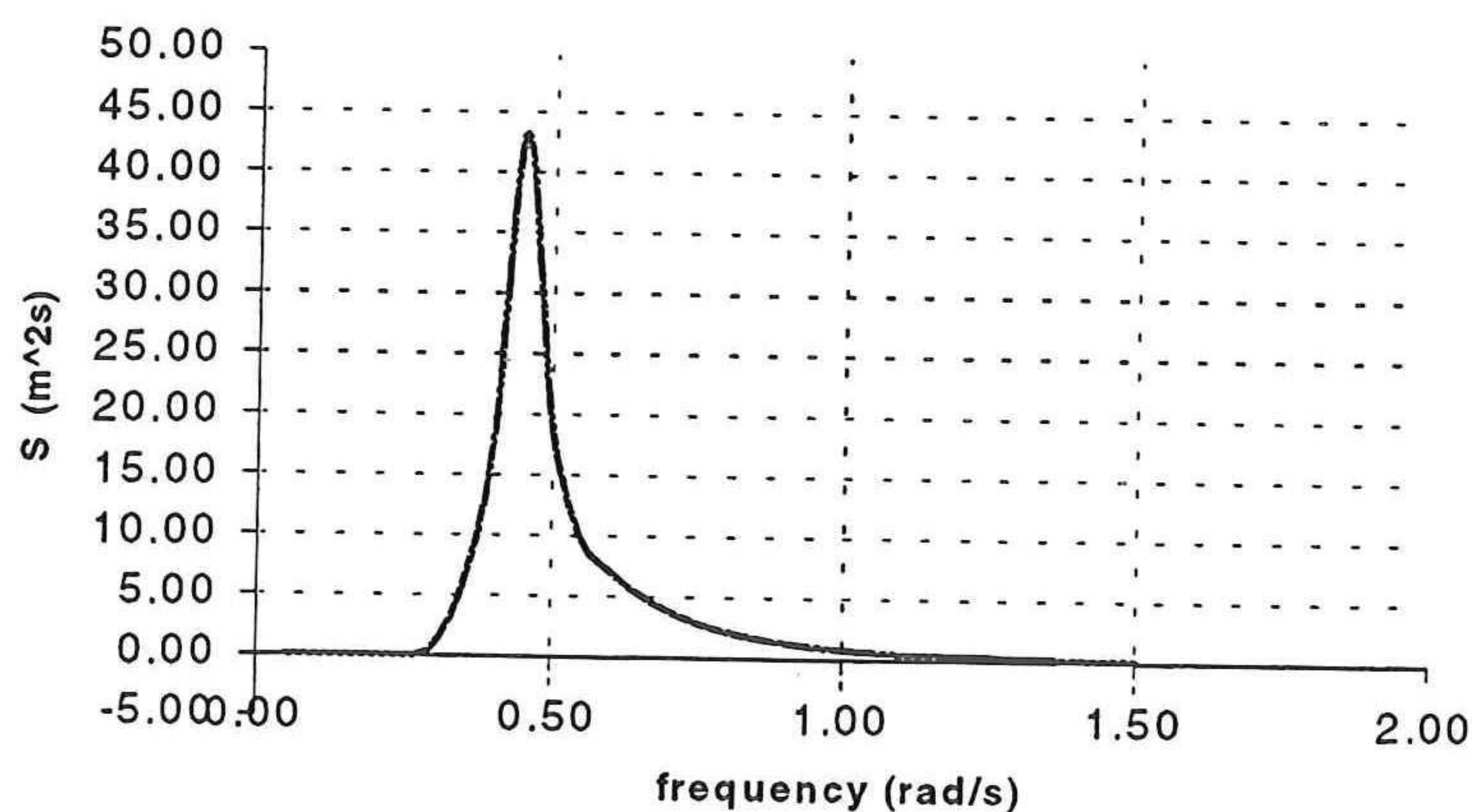
$$= \sum_n \int_0^{2\pi} a_n^2 \cos^2(\varepsilon_n - \omega_n t) \frac{1}{2\pi} d\varepsilon_n =$$

$$\sigma_{\eta}^2 = \sum_n \frac{a_n^2}{2} \quad (3.4)$$

which gives the variance (the standard deviation squared) of the random process, the surface elevation.

The second statistical parameter required for a complete description is the mean,  $\mu_n = 0$ , which is true for all harmonic components.

We now have the statistical properties of the ocean surface: a mean and a standard deviation. But this all needs to be tied to the actual physical process of surface elevation before it can be useful. To do this we need an expression that relates wave amplitude to the frequency so that we can assign to each wave component, defined by its frequency, a standard deviation (the mean will always be zero for these harmonic components). We will have then the statistical parameters (mean and standard deviation) for each component, and thus (because surface elevation is modeled as the sum of a finite number of the these components) the process of surface elevation will be defined.



### 3.4 Jonswap spectrum

The function we are looking for is the wave energy spectrum. It ties the mathematics to the random, physical process in question. The nature of the spectrum is such that its characteristics are independent of time measurement; it describes therefore a stationary process. In practice this assumption only holds for a certain region and duration, often assumed to be three hours, called a sea state. The energy of a wave is related to its amplitude, and the wave spectrum ( $S(\omega)$ ) describes the energy distribution over frequency. This may be expressed as follows, for a single component ( $n$ ) of the process:

$$\sigma_{\eta_n}^2 = \frac{a_n^2}{2} = S(\omega_n)\Delta\omega$$

If a constant interval is taken, the sum (which describes the process) can be expressed as:

$$\sigma_{\eta}^2 = \sum_n S(\omega_n)\Delta\omega$$

When  $\Delta\omega \rightarrow 0$ , the discrete summation can be replaced by a continuous one,

$$\sigma_{\eta}^2 = \int_0^{\infty} S(\omega_n)d\omega \quad (3.5)$$

What can be concluded from equation 3.5 is that the spectrum can also be considered as a distribution of the variances with respect to frequency, and contains all the statistical data required to define the random process of surface elevation.

#### The wave spectrum

The sea states will be described by a Jonswap spectrum in this study, consistent with a North Sea location. Such a spectrum is characterized by two parameters: the significant wave height ( $H_s$ ) and the mean zero crossing period ( $T_z$ ), and is defined as follows [Chakrabarti, 1987]:

$$S(\omega) = \frac{A}{\omega^5} \exp\left[-\frac{B}{\omega^4}\right] \gamma^{\exp\left[-\frac{1}{2\sigma^2}\left(1-\frac{\omega}{\omega_p}\right)^2\right]} \quad (3.6)$$

with,

$$A = 2.626 m_0 B$$

$$B = 5/4 \omega_p^4$$

$$\omega_p = 0.78 \cdot 2\pi/T_z$$

$$m_0 = H_s^2/16$$

$$\gamma = 3.3$$

$$\omega \Rightarrow \text{the wave frequency in rad/s}$$

where  $\omega_p$  is the peak frequency and  $m_0$  the zeroeth moment of the spectrum or the surface area of the wave spectrum.

Furthermore,  $\sigma$  follows from:

$$\sigma = 0.07 \text{ for } \omega < \omega_p$$

$$\sigma = 0.09 \text{ for } \omega > \omega_p$$

In figure 3.4 above, this spectrum is shown for  $H_s = 11m$  and  $T_z = 12s$ .

### 3.2.2 First order wave forces

Calculation of wave forces on structures with dimensions that span a significant proportion of the wavelength ( $>0,2\lambda$ ) must account for the fact that the wave flow will be influenced by the presence of the body. In addition to the boundary condition at the free surface and the sea bed, the condition of no flow through the body surface will result in additional component waves: radiated and scattered waves. The total wave force on the structure is therefore due to both incident as well as radiated and scattered waves. A structure floating in waves experiences forces and moments which can be determined if the velocity potential of the water motion around the structure is known. The velocity potential  $\phi(x,y,z)$  is simply a mathematical expression, whose gradient in  $x$ ,  $y$ , and  $z$  gives the velocity of the flow in  $x$ ,  $y$  and  $z$  respectively. The pressure can be obtained from the Bernoulli equation for non-steady flow in terms of this velocity potential:

$$p = p_0 - \rho \frac{\partial \phi}{\partial t} - \rho g z - \frac{\rho}{2} V^2$$

where  $p$  is the pressure,  $p_0$  is the atmospheric pressure,  $\phi$  the velocity potential,  $g$  the acceleration of gravity,  $V$  the velocity of water motion,

$$V^2 = \left( \frac{\partial \phi}{\partial x} \right)^2 + \left( \frac{\partial \phi}{\partial y} \right)^2 + \left( \frac{\partial \phi}{\partial z} \right)^2$$

By integrating the pressure in a particular direction over the hull of the structure, the force component can be determined.

But before the forces and moments on a structure can be calculated, the velocity potential must be determined; this may be done by writing the velocity potential as the sum of incident, scattered and radiated potentials. Potential flow theory is used to describe water movement in gravity waves. The basic assumptions about this flow are that it is irrotational, and that the water is inviscid and incompressible. The potential ( $\phi$ ) then satisfies the Laplace equation:

$$\frac{\partial^2 \phi}{\partial x^2} + \frac{\partial^2 \phi}{\partial y^2} + \frac{\partial^2 \phi}{\partial z^2} = 0 \quad (3.7)$$

which is solved for a particular set of boundary equations, namely:

- *Sea bed boundary condition:* the velocity in the direction  $z$  is zero
- *Free surface boundary conditions:* the pressure is equal to the atmospheric pressure, and the velocity of water particles normal to the surface is equal to the velocity of the surface in the same direction.
- *Body surface boundary condition:* which requires that, at a point on the surface of the structure, the velocity of a water particle normal to the body surface be equal to the velocity of the structure in the same direction.

With the velocity potential determined, the first order forces then follow from the dynamic part of Bernoulli's linearized equation,

$$p = -\rho \frac{\partial \phi}{\partial t} \quad (3.12)$$

In first order wave theory the second term of Bernoulli's equation, the quadratic velocity term, is assumed negligible, so that we are left with only the linear term, as in equation 3.12.

Integrating the pressure over the immersed body surface yields the force; as such, the first order dynamic force can now be written:

$$F^{(1)} = -\int_S \rho \frac{\partial \phi}{\partial t} n dS = -\int_S p^{(1)} n dS$$

and the first order dynamic moment

$$M^{(1)} = -\int_S p^{(1)} (rxn) dS$$

where  $n$  is the normal vector at a point on the immersed body surface  $S$  and taken as positive out of the body, and  $r$  is the position vector of that point.

An analytical solution is only feasible for structures with simple geometry; a tanker type ship is not one of those, so that a numerical calculation is necessitated of this three-dimensional potential theory problem. The solution of this problem can express the force as the wave amplitude times a frequency dependent function, called a transfer function. The force would then be expressed as:

$$\begin{aligned} F_i^{(1)} &= I_{i,\Delta\psi} a \cos(\varepsilon - \omega t + \delta_i) = & i=1,2,6 & (3.12) \\ & I_{i,\Delta\psi} a \cos(\varepsilon - \omega t) \cos(\delta_i) - I_{i,\Delta\psi} a \sin(\varepsilon - \omega t) \sin(\delta_i) \end{aligned}$$

where  $i=1$  refers to surge,  $i=2$  refers to sway, and  $i=6$  refers to yaw, and  $I_{i,\Delta\psi}$  denotes the first order transfer function which depends on the frequency ( $\omega$ ), the DOF ( $i$ ), and the heading of the ship ( $\Delta\psi$ ) relative to the incident wave. And  $\delta_i$  is the phase shift.

The total force is the sum (in linear theory) of all the force components resulting from  $n$  waves:

$$F_i^{(1)} = \sum_n I_{i,\Delta\psi} a_n \cos(\varepsilon_n - \omega_n t) \cos(\delta_i) - I_{i,\Delta\psi} a_n \sin(\varepsilon_n - \omega_n t) \sin(\delta_i) \quad (3.13)$$

Both the first order transfer functions as well as their corresponding phase shift in this study are obtained from existing hydrodynamic data files. These files cover a wide range of different types of tankers and draft to depth ratios.

### 3.2.3 Second order wave drift forces

A simple way to consider the second order forces is by looking at how they relate to first order forces. First order forces are those forces that act on the structure as a result of the incident waves only, as though the ship were held in place, and only the incident waves moved. This is of course not realistic because the ship is set in motion by the incident waves and, being such a large structure, the ship has a capacity to generate waves of its own, namely, scattered and radiated waves, which are responsible for the second order forces.

Second order forces are of significant influence in this problem, not on account of their magnitude which is small relative to first order forces, but because of their low frequency range of action, to which the mooring system, with its low natural frequency, is susceptible. Because these are slowly varying forces the radiation damping will not be substantial, even at resonance. Clearly, low frequency forces cannot be disregarded in designing a mooring system.

Mathematically, a simple way to illustrate second order forces is by considering the quadratic velocity term in Bernoulli's equation:

$$-\frac{\rho}{2}|\nabla\phi|^2 = -\frac{\rho}{2}(V_x^2 + V_y^2 + V_z^2)$$

where  $V$  is the velocity vector.

In an idealised sea state of two wave components with frequencies  $\omega_1$  and  $\omega_2$  the velocity can be written as:

$$V_1 = A_1 \cos(\varepsilon_1 - \omega_1 t) + A_2 \cos(\varepsilon_2 - \omega_2 t)$$

From this follows,

$$-\frac{\rho}{2}V_1^2 = -\frac{\rho}{2}\left[\frac{A_1^2}{2} + \frac{A_2^2}{2} + \frac{A_1^2}{2}\cos(2\varepsilon_1 - 2\omega_1 t) + \frac{A_2^2}{2}\cos(2\varepsilon_2 - 2\omega_2 t) + A_1 A_2 \cos(\varepsilon_1 - \varepsilon_2 - (\omega_1 - \omega_2)t) + A_1 A_2 \cos(\varepsilon_1 + \varepsilon_2 - (\omega_1 + \omega_2)t)\right]$$

We can distinguish 3 parts to this expression:

1. a constant part, referred to as mean drift, given by the term:

$$-\frac{\rho}{2}\left[\frac{A_1^2}{2} + \frac{A_2^2}{2}\right]$$

2. Terms contributing to high frequency oscillation; these are the sum frequency terms, and those oscillating at twice the frequency.
3. Terms contributing to low frequency oscillation, with frequencies expressed here as the difference of two incident wave frequencies, given by:

$$-\frac{\rho}{2}\left[A_1 A_2 \cos(\varepsilon_1 - \varepsilon_2 - (\omega_1 - \omega_2)t)\right]$$

We will be concerned with only mean drift (1), and the low frequency (3) or difference frequency forces. The latter are non-linear interaction terms that can produce slowly varying excitation forces in surge, sway and yaw motions of a moored structure [Faltinsen. 1990]. Forces with frequency oscillations higher than the dominant frequency components in a wave spectrum will not have a significant effect in the relevant degrees of freedom.

### 3.2.3.1 Low frequency wave drift forces

The action of second order, low frequency forces is associated with the phenomenon of wave groups, which can only occur in irregular waves. The superposition of two different wave components, as is given in the example in section 3.2.3, leads to a signal that is characterized by a relatively high frequency fluctuation, and one that is lower and that constitutes the envelope of the wave signal. This collective effect is what gives rise to slowly varying forces, or low frequency drift force.

To determine the dynamic second order forces, the second order potential must be solved, The instantaneous wetted surface  $S$  is split into 2 parts, namely, a constant part  $S_0$  up to the static waterline on the hull and an oscillating part  $s$  between the static waterline on the hull and the wave profile along the body. The second order fluid force is found by integrating all

the products of pressure  $p$  and normal vector  $n$  which give second order force contributions over the constant part  $S_0$ , and by integration of first order pressures over the oscillatory parts. [Pinkster. 1980]:

$$F^{(2)} = -\iint_{S_0} (p^{(1)} \cdot N^{(1)} + p^{(2)} \cdot n) dS - \iint_S p^{(1)} \cdot n dS$$

In which the first and second order pressure terms are respectively,

$$p^{(1)} = -\rho \frac{\partial \phi^{(1)}}{\partial t} - \rho g z$$

and

$$p^{(2)} = -\frac{\rho}{2} |\nabla \phi^{(1)}|^2 - \rho \frac{\partial \phi^{(2)}}{\partial t}$$

The second order forces are proportional to the square of the wave elevation; it is possible, therefore, to express these forces in terms of a transfer function that relates the second order forces to the wave amplitude squared. We assume that the surface elevation can be approximated, as in eq. 3.1, by

$$\eta(t) = \sum_n a_n \cos(\varepsilon_n - \omega_n t)$$

and the square of the surface elevation is:

$$\eta^2(t) = \sum_{j=1}^N \sum_{k=1}^N \frac{1}{2} a_j a_k \left[ \cos((\omega_j - \omega_k)t + (\varepsilon_k - \varepsilon_j)) + \cos((\omega_j + \omega_k)t + (\varepsilon_k + \varepsilon_j)) \right]$$

All the pressure terms, first and second order, can be expressed in terms of this wave height squared

$$F^{(2)}(t) = \sum_{j=1}^N \sum_{k=1}^N \frac{1}{2} a_j a_k \left[ T_{jk}^- \cos((\omega_j - \omega_k)t + (\varepsilon_k - \varepsilon_j) + \delta_{jk}^-) + T_{jk}^+ \cos((\omega_j + \omega_k)t + (\varepsilon_k + \varepsilon_j) + \delta_{jk}^+) \right] \quad (3.14)$$

where  $j, k$  are the incident wave indices;  $a$  the amplitude of these waves;  $T_{jk}^-$  and  $T_{jk}^+$  and the quadratic transfer functions for difference and sum frequency components, respectively. These transfer functions are independent of amplitude but dependent on frequency, which means they lend themselves very well to spectral analysis.

As we are only interested in slowly varying forces, or difference frequency forces, the high frequency components may be discarded leaving only:

$$F^{(2)}(t) = \sum_{j=1}^N \sum_{k=1}^N \frac{1}{2} a_j a_k \left[ T_{jk}^- \cos((\omega_j - \omega_k)t + (\varepsilon_k - \varepsilon_j) + \delta_{jk}^+) \right] \quad (3.15)$$

The hydrodynamic data available does not give a phase shift, but instead expresses the force with in and out of phase transfer functions as follows,

$$F^{(2)}(t) = \sum_{j=1}^N \sum_{k=1}^N a_j a_k \left[ P_{jk} \cos((\omega_j - \omega_k)t + (\varepsilon_j - \varepsilon_k)) + Q_{jk} \sin((\omega_j - \omega_k)t + (\varepsilon_j - \varepsilon_k)) \right] \quad (3.16)$$

where  $P$  and  $Q$  are transfer functions which give that part of the wave drift force which is in-phase and out of phase with the low frequency part of the incident wave elevation [Pinkster, 1980];

Note that the quadratic transfer functions, like the first order transfer functions, are not only frequency dependent but direction dependent as well; in the available hydrodynamic data files these transfer functions are given in 15 degree intervals.

### 3.2.3.2 Mean wave drift forces

The constant force exerted on a structure in harmonically oscillating waves, be they regular or irregular, is called the mean drift force. A major contribution to the horizontal mean wave force is due to the relative motion between the structure and the waves. It can be explained by a structure's ability to generate waves. Generally, only part of the incident wave will be reflected, the rest will be transmitted underneath the structure. All reflected and scattered waves have the same frequency, which means the two components together constitute another regular wave, whose amplitude depends on the amplitude of the reflected and scattered waves. These in turn depend on the amplitude of the incident wave. We may, therefore, write (knowing that the drift force is proportional to the square of the amplitude of the incident wave) [Remery, 71]:

$$\overline{F}^{(2)} = 1/2 \rho g [R(\omega) \xi_a]^2$$

where:

$$\begin{aligned} R(\omega) \xi_a &= \text{amplitude of reflected and scattered wave} \\ \xi_a &= \text{amplitude of incident wave} \\ R(\omega) &= \text{reflection coefficient} \end{aligned}$$

Mean drift forces can also be expressed in the same manner as the low-frequency wave forces in equation 3.16 above, but for equal frequencies of the two incident waves,  $\omega_j = \omega_k$ . This leads to the following expression for mean drift, consistent with the above expression [Pinkster, 1980]:

$$\overline{F}^{(2)} = \sum_i a_i^2 P_{ii} \quad (3.17)$$

where  $a_i$  is the amplitude of incident wave  $i$ , and  $P_{ii}$  the in-phase quadratic transfer function, which is obtained from the main diagonal of the quadratic transfer function matrix  $T_{jk}$  for  $\omega_j = \omega_k$ .

If we consider now that the wave amplitude may also be expressed spectrally as follows,

$$a_i^2 = 2S_{\eta\eta}(\omega_i) d\omega_i$$

and substituting this into equation 3.17 yields:

$$\overline{F}^{(2)} = 2 \int_0^{\infty} S_{\eta\eta}(\omega) P(\omega, \omega) d\omega$$

The hydrodynamic data is given for discrete values of the transfer function; this means that in fact the integration appears in the following discretized form in the computer program:

$$\overline{F}^{(2)} = 2 \sum S_{\eta\eta}(\omega) P(\omega, \omega) \Delta\omega$$

where  $\Delta\omega$  is the frequency interval, given for values in the frequency range 0.2 rad/s to 1.5 rad/s. This range covers the significant part of the wave spectrum.

### 3.3 Unsteady Wind

Another contribution to low frequency loads on ships come from wind gusts. These can be described, as with waves, with a spectrum, the wind spectrum, which expresses statistically the random nature of winds. It is written as follows [API 2T (RP2T), 1992]:

$$\frac{f \cdot S_{uu}(f)}{\sigma(z)^2} = \frac{f / f_p}{[1 + 1.5 \cdot f / f_p]^{5/3}} \quad (3.18)$$

where  $S_{uu}(f)$  is the spectral energy density of the wind at elevation  $z$ ,  $f$  is the frequency in Hz

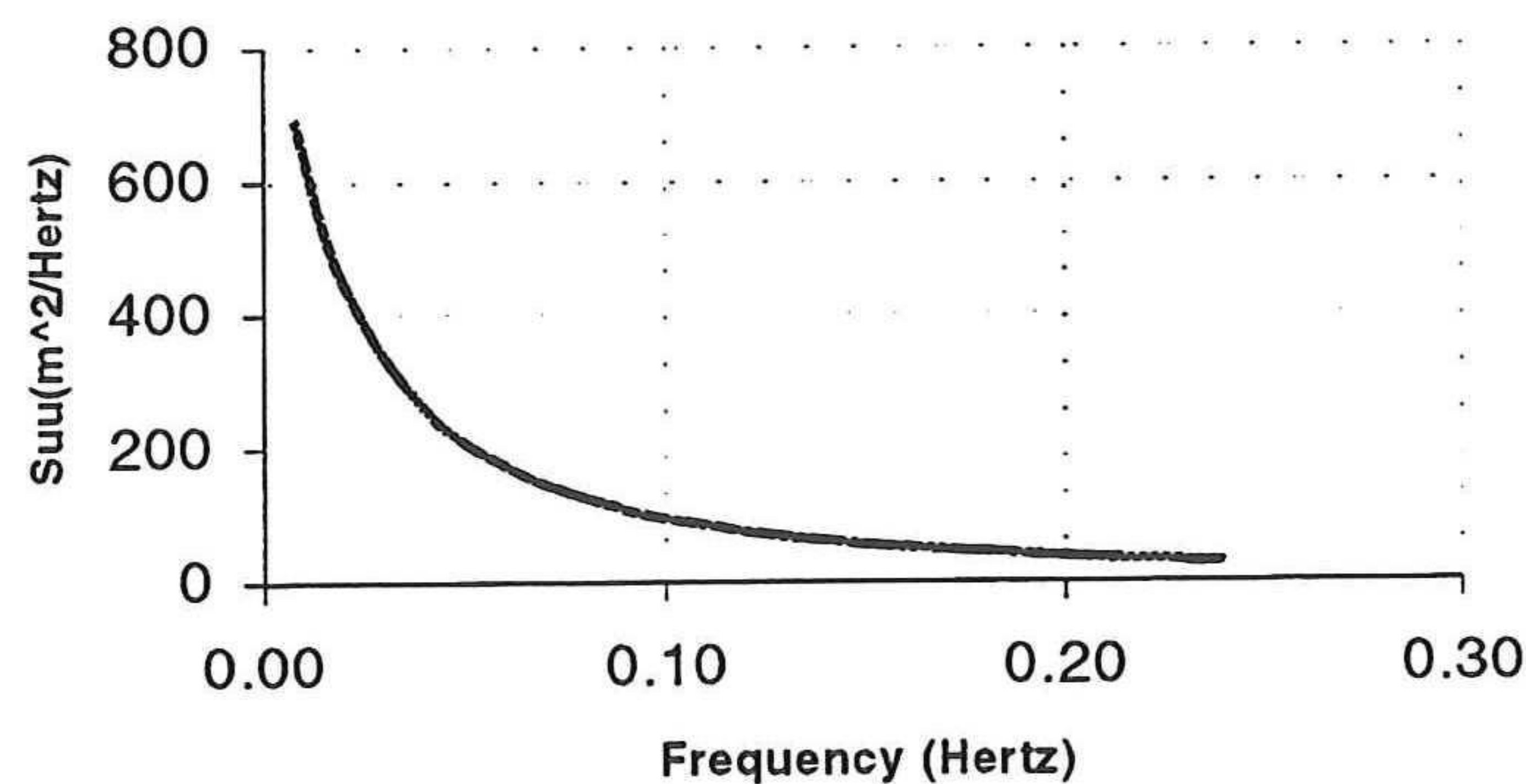


figure 3.6 Wind spectrum

We note that, unlike waves, wind gusts do not obey a dispersion equation.

The standard deviation of the wind speed is given for

$$\sigma(z) = V_z \cdot 0.15(z/20)^{-0.125} \quad \text{for } z \leq 20m$$

$$\sigma(z) = V_z \cdot 0.15(z/20)^{-0.275} \quad \text{for } z > 20m$$

and

$$f_p z / V_z = 0.025$$

Figure 3.6 above gives such a spectrum for  $V_z = 42m/s$ ,  $z = 20$ . To convert the spectrum from Hertz to radians:

$$S_{ww}(\omega) = S(f) / 2\pi$$

### 3.3.1 Wind gust force

The wind velocity can be described as the sum of a steady and unsteady component. We have dealt with steady wind forces in chapter 2, but we will consider the two together again here. The total wind velocity will be written as:

$$W(t) = V_z + w(t)$$

where  $V_z$  (defined in section 3.1) is the mean wind velocity, and  $w(t)$  the gust component.

If we further assume that  $w(t) \ll V_z$ , the square of the velocity is:

$$W|W| = (V_z + w(t))|V_z + w(t)| \approx V_z^2 + 2|V_z|w(t)$$

from which can be derived the linearized dynamic wind force, resulting from gusts (only the second term is included, the first is for steady wind). Consider the surge force:

$$F_{x,win,dyn} = \left(\frac{1}{2} \rho_{air} C_{x,win} A_t\right) 2|V_z|w(t)$$

Defining the wind gust velocity as the sum of sinusoidal velocity components:

$$w(t) = \sum_m w_m \cos(\varepsilon_m - \omega_m t)$$

the dynamic wind force is:

$$F_{x,win,dyn} = \left(\frac{1}{2} \rho_{air} C_{x,win} A_t\right) 2|V_z| \sum_m w_m \cos(\varepsilon_m - \omega_m t) \quad (3.19)$$

In general: 
$$\underline{F}_{win,dyn} = \underline{D} \cdot 2|V_z| \sum_m w_m \cos(\varepsilon_m - \omega_m t) \quad (3.20)$$

where, 
$$\underline{D} = \begin{bmatrix} D_x \\ D_y \\ D_\psi \end{bmatrix} = \begin{bmatrix} 1/2 \rho_{air} C_{x,w} A_t \\ 1/2 \rho_{air} C_{y,w} A_t \\ 1/2 \rho_{air} C_{xy,w} A_t L_{pp} \end{bmatrix}$$

#### 4. STATIC ANALYSIS

The first step in the response analysis is to determine the offset and orientation resulting from the steady forces of *current*, *wind* and *waves*; these are:

1. *Current forces*
2. *Steady wind forces*
3. *Mean wave drift forces.*

All of which have been previously discussed.

These forces depend on the heading of the ship relative to the angle of attack of current, wind and waves; these relative headings are given by  $\Delta\psi_c, \Delta\psi_w, \Delta\psi_\xi$  respectively; this is made clear in figure 4.1 below, and can be expressed as follows

$$\Delta\psi_c = \psi_c - \psi$$

$$\Delta\psi_w = \psi_w - \psi$$

$$\Delta\psi_\xi = \psi_\xi - \psi$$

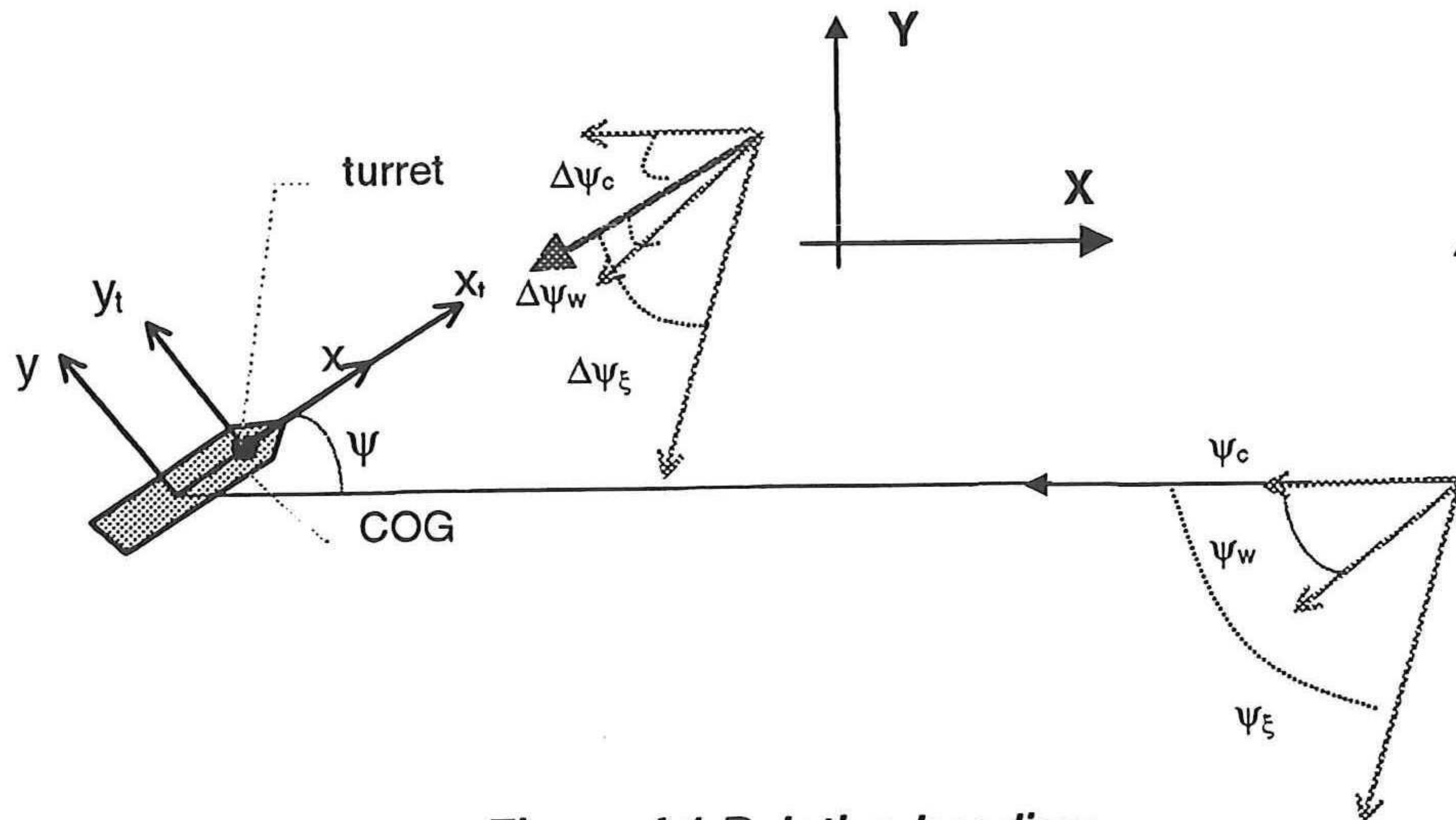


Figure 4.1 Relative heading

The reason mean offset and orientation are determined first is that in the dynamic regime the ship will perform translatory oscillations in surge and sway about this mean offset, and rotational oscillations in yaw about the mean orientation.

##### 4.1 Mean offset and orientation

The mean orientation must be determined first because the loads depend on the relative heading of the ship. The mean offset follows from the moment equilibrium, which is taken about the turret. In addition to the global co-ordinate system, the ship fixed co-ordinate system  $(x_t, y_t)$ , with its origin in the center of the turret, will be used for the static analysis.

The moment equilibrium about the turret can be expressed as:  $\sum M_{turret} = 0$ , which gives,

$$M_{turret} = \left( M_{xy,cur}(\Delta\psi_c) + M_{xy,win}(\Delta\psi_w) + \overline{F}_{xy,drift}^{(2)}(\Delta\psi_\xi) \right) - A_{turret} \cdot \left( F_{y,cur}(\Delta\psi_c) + F_{y,win}(\Delta\psi_w) + \overline{F}_{y,drift}^{(2)}(\Delta\psi_\xi) \right) = 0 \quad (4.1)$$

where  $A_{turret}$  is the arm: the length separating the COG and the center of the turret; the significance of the other terms is given in chapters 2 and 3.

The wind and current coefficients are given per 10 degree interval of the relative heading in the OCIMF files; figures 3.1 and 3.2 show these in detail.

From the moment equilibrium follows the mean orientation of the ship, loaded only with the steady forces from current, wind and waves. This mean orientation will be referred to as  $\psi_{mean}$ . With this value known, we can now determine the forces in the local co-ordinate system as follows:

for  $x_t$ :

$$F_{x_t} = F_{x,cur} (\psi_c - \psi_{mean}) + F_{x,win} (\psi_w - \psi_{mean}) + \overline{F}_{x,drift}^{(2)} (\psi_\xi - \psi_{mean})$$

for  $y_t$ :

$$F_{y_t} = F_{y,cur} (\psi_c - \psi_{mean}) + F_{y,win} (\psi_w - \psi_{mean}) + \overline{F}_{y,drift}^{(2)} (\psi_\xi - \psi_{mean})$$

These forces generate displacements in the mooring which are more conveniently treated in the global co-ordinate system. Therefore, these forces will be transformed into forces ( $F_X, F_Y$ ) in that co-ordinate system. The transformation is:

$$\begin{aligned} F_X &= F_{x_t} \cos(\psi_{mean}) - F_{y_t} \sin(\psi_{mean}) \\ F_Y &= F_{y_t} \cos(\psi_{mean}) + F_{x_t} \sin(\psi_{mean}) \end{aligned} \quad (4.2)$$

The mean offset of the turret can now be written,

$$\begin{aligned} X_t &= F_X / c \\ Y_t &= F_Y / c \end{aligned}$$

Where  $c$  is the spring constant of the mooring system.

Note that what has been calculated is the global displacement of the *turret* with respect to its initial position; in order to determine the position of the COG in the global co-ordinate system (which is necessary for the dynamic analysis), account must be taken of the length that separates the COG from turret, the arm ( $A_{turret}$ ). The transformation from  $X_t, Y_t$  to  $X_g, Y_g$  is the following

$$\begin{aligned} Y_g &= Y_t - A_{turret} \sin(\psi_{mean}) \\ Y_g &= X_t + A_{turret} [1 - \cos(\psi_{mean})] \end{aligned}$$

Figure 4.2 shows these relationships.

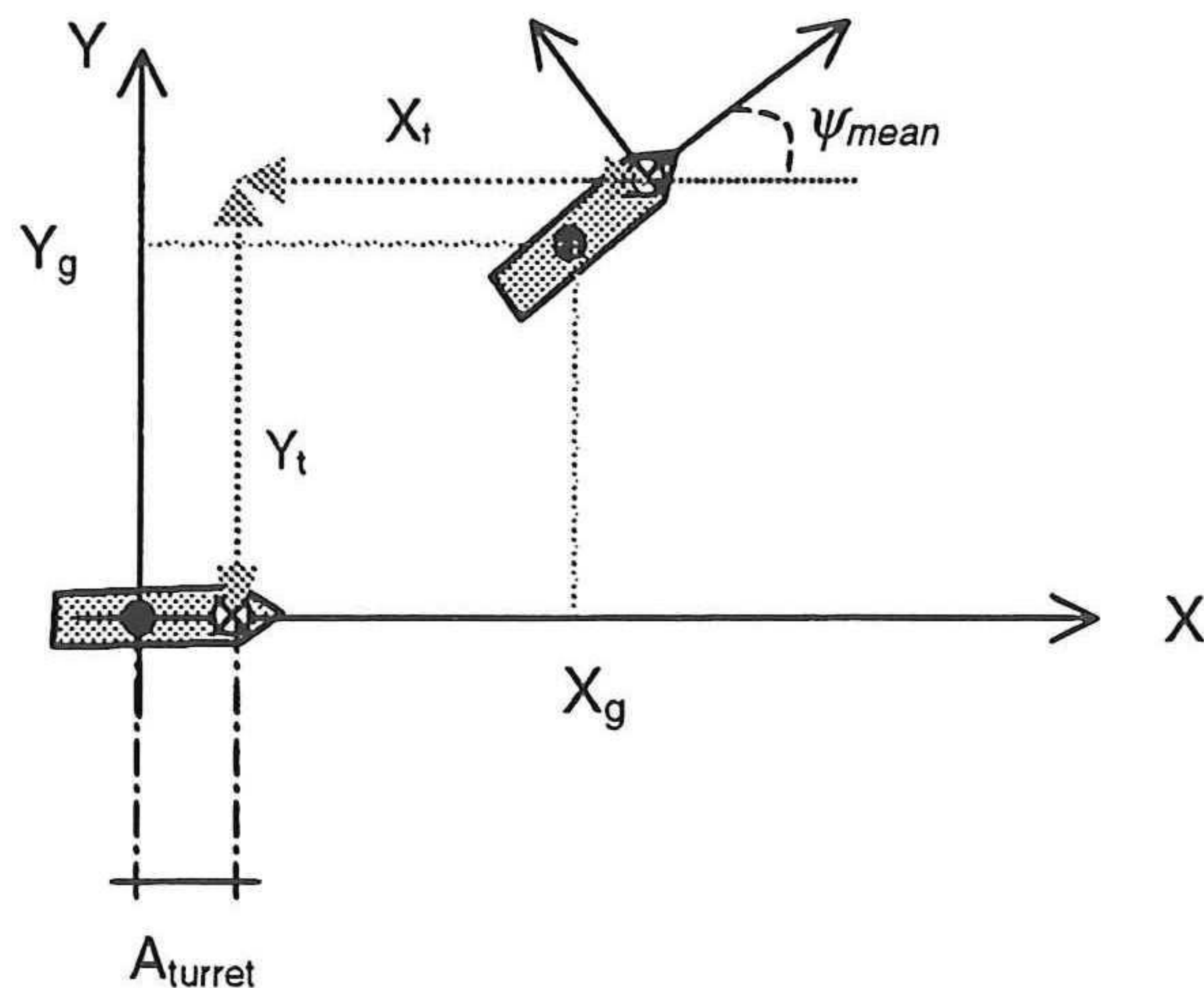


Fig 4.2 Global co-ordinate system

## 4.2 Program

The computer program TURRETSTAT, written in FORTRAN, calculates the mean offset and orientation. The input data is drawn from three separate files: *input.dat* (user defined data related to ship geometry, water depth, sea state etc.), *m1lc1wd2.hyd* (hydrodynamic data for the determination of mean drift), and *ocimf.dat* (the steady wind and current force coefficients).

In short, the basic structure of the program is the following:

1. An initial value of  $\psi_{mean}$  is approximated as the average of  $\psi_w$ ,  $\psi_c$  and  $\psi_d$
2. The value of the moment  $M_{turret}$  is determined
3. The values of the angle between which a zero crossing of the moment  $M_{turret}$  occurs are determined by 10 degree increment or decrease of the angle.
4. The exact value of the angle ( $\psi_{mean}$ ) at the zero crossing point is determined by interpolation. We now have  $\psi_{mean}$ .
5. Because the coefficients for wind, current, and the transfer functions for drift are given for discrete values of the angle, the exact value of these coefficients are also determined by interpolation relative to the exact value of  $\psi_{mean}$ .
6. With the exact coefficients the offset is determined.

### 4.3 Results

The results of the static analysis can be compared to those calculated by the static module of the DYNFLOAT package. Figure 4.3 below compares the offset of the center of gravity (COG) as calculated by DYNFLOAT, and the static module that was written for this project, TURRETSTAT. The case considered is co-linear wind (30.9 m/s) and wave ( $H_s=10m$ ;  $T_z=11s$ ), with a cross current (1.6 m/s) acting at a variable angle with respect to the wind and waves (i.e.  $\psi_w=\psi_\xi=0$ ,  $\psi_c=\psi$ ). The offset is the vectorial sum of the static sway and surge response ( $[x_{cog}^2+y_{cog}^2]^{1/2}$ ). Note that because the vessel weathervanes around the turret to a static equilibrium, the offset of the COG is much greater than that of the turret.

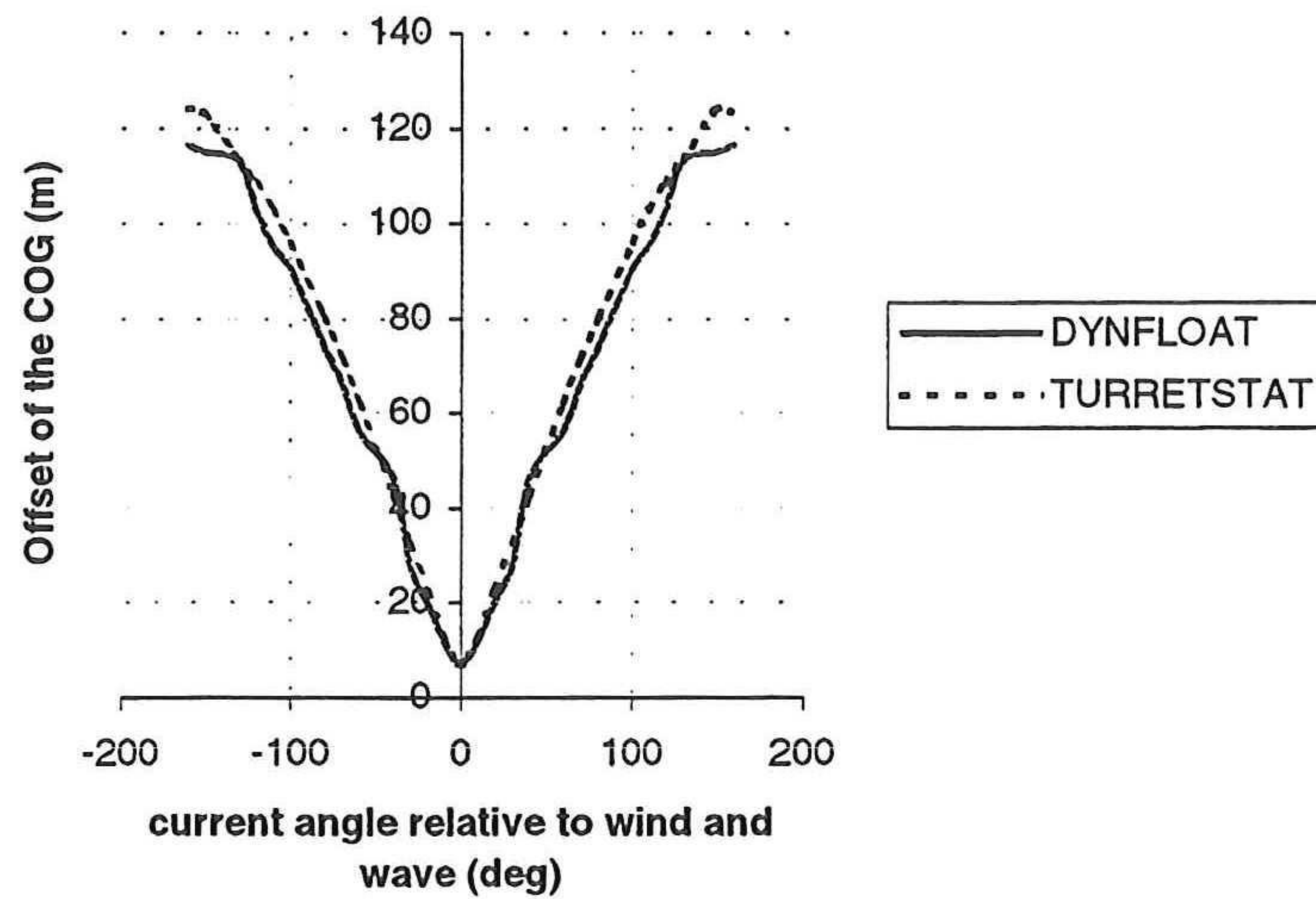


Figure 4.3 Offset of the COG

Another aspect to compare is the equilibrium heading that results from the case as in figure 4.3. Figure 4.4 below compares results for the two programs. Again the results show good correspondence. The sharp peak that occurs around 160 degrees is the sudden shift from one equilibrium position to another more stable one in the opposite quadrant.

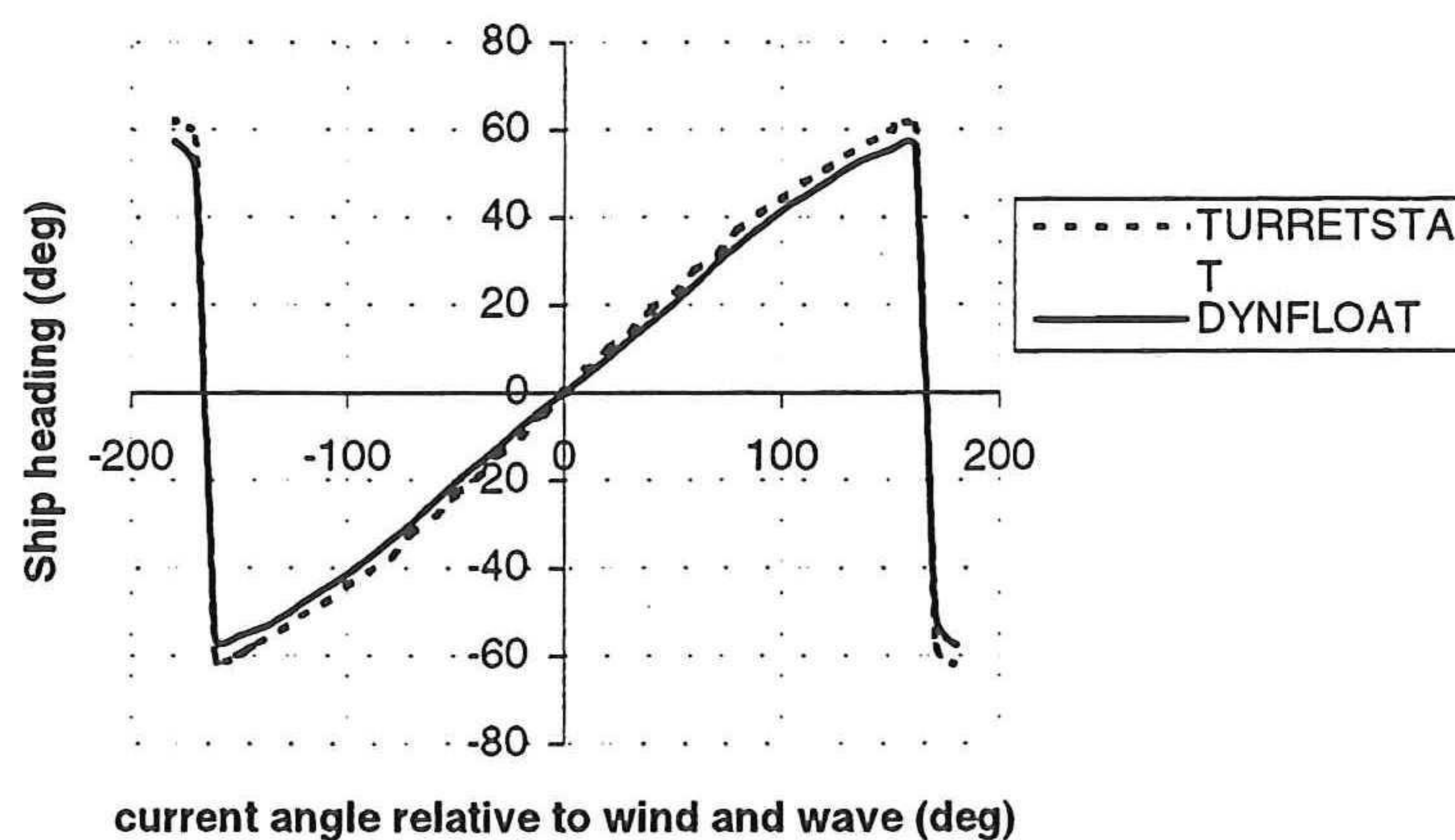
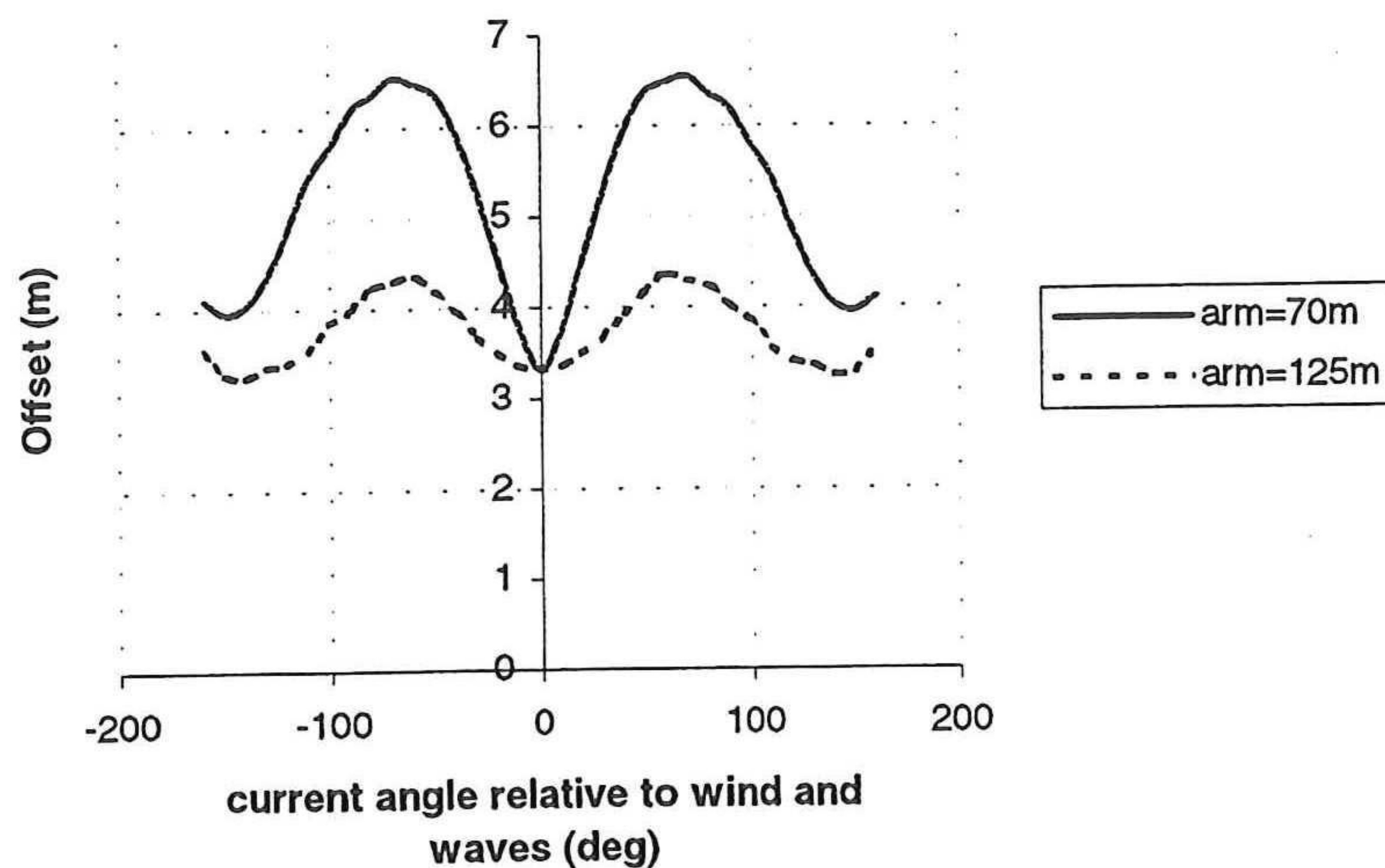


Figure 4.4 Mean heading ( $\psi_{mean}$ )

The offset of the COG best demonstrates how much the ship weathervanes. However if we are interested in the relative amount of static force exerted on the structure, it is best to consider the offset of the turret rather than the COG because the offset of the turret is directly related to the force acting on the structure. The influence of the arm (the length between the COG and the center of the turret) on the offset of the turret is considered in figure 4.5. The offset decreases with increasing arm. What happens is that with a greater arm, the lateral forces can produce a greater moment to allow the ship to weathervane into the prevailing environmental forces, which in turn reduces the total load on the ship. The smaller the arm the less the ship will weathervane about the turret, which means more area exposed to the environmental forces, and so the greater the offset.



**Figure 4.5 Influence of the arm**

Figure 4.5 is based on the same wind, wave and current data as figures 4.3 and 4.4

## 5. DYNAMIC ANALYSIS

With static response determined, the dynamic effects of the loads on the system can now be considered. The response of the ship, which oscillates about the mean offset, is the sum of the static and dynamic effects. In this section we will be dealing with the unsteady forces from waves and wind, both of which will be included as random variables to account for their stochastic nature. Firstly, the equations of motion describing the behavior of the system in its various degrees of freedom (DOF) will be considered; modal superposition will then be used to uncouple the equations per DOF; lastly, expressions for the response in surge, sway and yaw will be determined.

### 5.1 Equations of motion

In general, the dynamic response of a floating structure can be described by a damped spring-mass system with 6 DOF in matrix form as [Journee, 1997]:

$$[A]\ddot{\underline{\xi}} + [B]\dot{\underline{\xi}} + [C]\underline{\xi} = \underline{F}(t) \quad (5.1)$$

where  $A$  is the combined mass and added mass matrix,  $B$  the damping matrix,  $\ddot{\underline{\xi}}, \dot{\underline{\xi}}, \underline{\xi}$  respectively, the system acceleration, velocity and displacement vectors.  $F(t)$  is the total dynamic force acting on the structure.

In this study we will confine our attention to surge, sway and yaw, which account for the principal horizontal displacements. Because we are dealing only with horizontal displacement there will be no hydrostatic restoring force, only that from the mooring system; equation 5.1 can accordingly be rewritten as:

$$\begin{aligned} a_{xx}\ddot{x} + b_{xx}\dot{x} &= F_x(t) - c_{xx}x \\ a_{yy}\ddot{y} + b_{yy}\dot{y} + a_{y\psi}\ddot{\psi} + b_{y\psi}\dot{\psi} &= F_y(t) - c_{yy}y - c_{y\psi}\psi \\ a_{\psi y}\ddot{y} + b_{\psi y}\dot{y} + a_{\psi\psi}\ddot{\psi} + b_{\psi\psi}\dot{\psi} &= F_\psi(t) - c_{\psi y}y - c_{\psi\psi}\psi \end{aligned} \quad (5.2-5.4)$$

where  $a_{jk}$  is the combined mass and added mass,  $b_{jk}$  is the damping,  $c_{jk}$  the spring constant of the mooring system.

The coupled equations are in sway ( $y$ ) and yaw ( $\psi$ ). Surge ( $x$ ) is considered uncoupled, and will not be considered further as it can be solved in a straightforward manner as a single DOF system. The coupling in sway and yaw is very clear when considering the forces that result at the turret following motions in those DOFs.

### 5.2 Modal superposition

To facilitate the response analysis it is best to uncouple the two simultaneous differential equations (5.3 and 5.4) using modal superposition, in which the response is expressed in terms of the undamped mode shapes. The response is then obtained solving a set of independent differential equations [Timoshenko. 1974]. Let us first consider these two equations in matrix form.

$$\begin{bmatrix} a_{yy} & a_{y\psi} \\ a_{\psi y} & a_{\psi\psi} \end{bmatrix} \begin{bmatrix} \ddot{y} \\ \ddot{\psi} \end{bmatrix} + \begin{bmatrix} b_{yy} & b_{y\psi} \\ b_{\psi y} & b_{\psi\psi} \end{bmatrix} \begin{bmatrix} \dot{y} \\ \dot{\psi} \end{bmatrix} + \begin{bmatrix} c_{yy} & c_{y\psi} \\ c_{\psi y} & c_{\psi\psi} \end{bmatrix} \begin{bmatrix} y \\ \psi \end{bmatrix} = \begin{bmatrix} F_y(t) \\ F_\psi(t) \end{bmatrix} \quad (5.5)$$

The steady state response is based on the undamped mode shapes. These can be solved from the undamped homogeneous equations:

$$\begin{bmatrix} a_{yy} & a_{y\psi} \\ a_{\psi y} & a_{\psi\psi} \end{bmatrix} \begin{bmatrix} \ddot{y} \\ \ddot{\psi} \end{bmatrix} + \begin{bmatrix} c_{yy} & c_{y\psi} \\ c_{\psi y} & c_{\psi\psi} \end{bmatrix} \begin{bmatrix} y \\ \psi \end{bmatrix} = \begin{bmatrix} 0 \\ 0 \end{bmatrix} \quad (5.6)$$

(which can also be written otherwise as:  $[A]\ddot{\underline{x}} + [C]\dot{\underline{x}} = \underline{0}$ )

Which, for the solution  $\underline{x}(t) = \underline{\hat{x}} \sin(\omega t + \phi)$ , resolves into the eigenvalue problem:

$$[\omega^2 A + C]\underline{\hat{x}} = \underline{0} \quad (5.7)$$

Setting the determinant of the matrix equal to zero allows for the natural frequencies, the eigenvalues, to be solved. Substituting these back into equation 5.7 resolves the eigenvectors ( $\underline{\hat{x}}$ ), the mode shapes. We have now a set of normalized eigenvectors, and their corresponding natural frequency per mode. As we are dealing with only two DOFs we can expect only two modes shapes. These normalized mode shapes will be defined as follows:

$$\begin{bmatrix} \hat{x}_{11} & \hat{x}_{12} \\ \hat{x}_{21} & \hat{x}_{22} \end{bmatrix} = \begin{bmatrix} \underline{\hat{x}}_1 & \underline{\hat{x}}_2 \end{bmatrix} = E \quad (5.8)$$

and the eigenvalues as:

$$\Omega = \begin{bmatrix} \omega_1 & 0 \\ 0 & \omega_2 \end{bmatrix} \quad (5.9)$$

Sway and yaw are coupled because the turret is not at the center of gravity. If we reduce the distance between the center of the turret and the center of gravity it may be expected that the natural frequencies tend to a single value, while if we increase the distance the difference between the two natural frequencies should increase. This is demonstrated in figure 5.1 below. With an arm=0, there is no more coupling between sway and yaw through the spring system and so the natural frequency for sway is the same as for surge

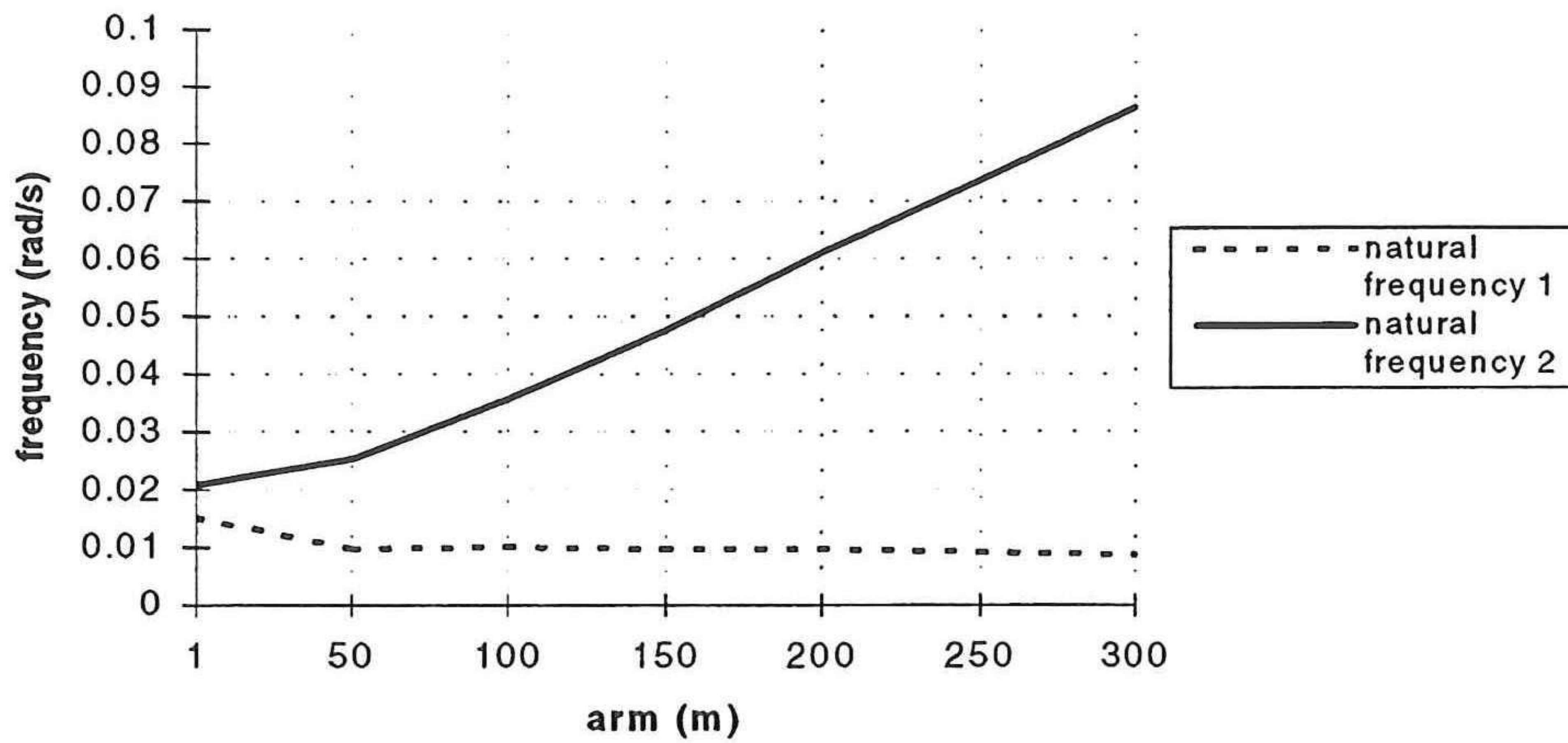


**Figure 5.1 Influence of arm on modal natural frequencies**

In this case this natural frequency would be approximately 0.02 rad/s.

### 5.2.1 Steady state response

Having determined the characteristics of the system in its free, undamped oscillation, it is possible now to determine the response of the system under forced oscillation. For this we will again consider the particular equation:

$$[A]\ddot{x} + [B]\dot{x} + [C]x = F(t) \quad (5.10)$$

And we will assume, in accordance with modal superposition, that the solution (analogous to that of the homogeneous equation) can be expressed as the sum of eigenvectors, each multiplied by a yet undetermined function of time [Spijkers, Dieterman, Klaver, Vrouwenvelder, 1995]. The proposed solution for harmonic loading has the form:

$$\underline{x}(t) = E\underline{u}(t) = \sum_{i=1} \hat{x}_i u_i(t) = \hat{x}_1 \cdot \hat{u}_1 \cos(\omega t + \phi_1) + \hat{x}_2 \cdot \hat{u}_2 \cos(\omega t + \phi_2) \quad (5.11)$$

where the frequency is that of the load.

Substituting eq 5.11 into eq. 5.10 yields:

$$AE\underline{u} + BE\dot{\underline{u}} + CE\underline{u} = F(t) \quad (5.12)$$

These equations can be uncoupled on the basis of the orthogonality relationships with respect to the mass, spring and damping matrices by multiplying through by the transpose of the eigenvector matrix.

$$E^T AE\underline{u} + E^T BE\dot{\underline{u}} + E^T CE\underline{u} = E^T F(t)$$

or,

$$A^* \underline{u} + B^* \dot{\underline{u}} + C^* \underline{u} = E^T F(t) \quad (5.13)$$

where  $A^*$ , and  $C^*$  are diagonal matrices, which follows if  $A$  and  $C$  are symmetric about the main diagonal. The damping matrix  $B^*$  is chosen to be diagonal in order to satisfy the requirements of modal analysis. Matrices  $B$  and  $A$  can be obtained from the hydrodynamic files.

The equations are now uncoupled into their modal counterparts:

$$\ddot{u}_i + 2\xi_i \omega_i \dot{u}_i + \omega_i^2 u_i = \frac{\hat{x}_i^T \underline{F}(t)}{\hat{x}_i^T \underline{A} \hat{x}_i} \quad i=1,2 \quad (5.14)$$

$$\text{with } 2\xi_i \omega_i = \frac{\hat{x}_i^T \underline{B} \hat{x}_i}{\hat{x}_i^T \underline{A} \hat{x}_i} \quad (5.15)$$

These equations can be solved as a set of regular single DOF systems; the same generalities apply. If we define the first order load vector as a sinusoidal function:

$$\underline{F}(t) = \underline{\hat{F}} \cos(\varepsilon - \omega t)$$

In a linear system solutions can be calculated separately and then superimposed. The response is a sinusoidal function with the same frequency, but a different phase angle:

$$u_i(t) = \hat{u}_i \cos(\varepsilon - \omega t + \phi_i)$$

with,

$$\begin{aligned} \hat{u}_i &= \frac{1}{\sqrt{\left(1 - \left(\frac{\omega}{\omega_i}\right)^2\right)^2 + \left(2\xi_i \frac{\omega}{\omega_i}\right)^2}} \frac{1}{\omega_i^2} \frac{\hat{x}_i^T \underline{\hat{F}}}{\hat{x}_i^T \underline{A} \hat{x}_i} \\ &= DAF \frac{1}{\omega_i^2} \frac{\hat{x}_i^T \underline{\hat{F}}}{\hat{x}_i^T \underline{A} \hat{x}_i}. \end{aligned} \quad (5.16)$$

$DAF$  is the dynamic amplification factor, a function of the load frequency ( $\omega$ ), and the natural frequency ( $\omega_i$ ) for mode  $i$ .

$$\text{and, } \tan(\phi_i) = \frac{2\xi_i \frac{\omega}{\omega_i}}{1 - \left(\frac{\omega}{\omega_i}\right)^2} \quad \text{is the phase shift (from force to response)} \quad (5.17)$$

To return now to the principal co-ordinates  $(y, \psi)$  and define the response functions for these, recall that :

$$\underline{x}(t) = E\underline{u}(t) = \sum_{i=1} \hat{x}_i u_i(t) = \hat{x}_1 \cdot \hat{u}_1 \cos(\varepsilon - \omega t + \phi_1) + \hat{x}_2 \cdot \hat{u}_2 \cos(\varepsilon - \omega t + \phi_2)$$

So that the sway  $(y)$  and yaw  $(\psi)$  response functions may also be written as:

$$\begin{aligned} y(t) &= \hat{x}_{y1} \cdot \hat{u}_1 \cos(\varepsilon - \omega t + \phi_1) + \hat{x}_{y2} \cdot \hat{u}_2 \cos(\varepsilon - \omega t + \phi_2) \\ \psi(t) &= \hat{x}_{\psi 1} \cdot \hat{u}_1 \cos(\varepsilon - \omega t + \phi_1) + \hat{x}_{\psi 2} \cdot \hat{u}_2 \cos(\varepsilon - \omega t + \phi_2) \end{aligned} \quad (5.18)$$

### 5.1.2.1 First order dynamic response

The first order dynamic response arises from the following force vectors:

- First order wave forces:

$$\underline{F}^{(1)} = \sum_n I_{i,\Delta\psi} a_n ( \cos(\varepsilon_n - \omega_n t) \cos(\delta_i) - \sin(\varepsilon_n - \omega_n t) \sin(\delta_i) )$$

- Wind gust forces :

$$\underline{F}_{win,dyn} = \underline{D} \cdot 2 \cdot |V_z| \sum_m w_m \cos(\varepsilon_m - \omega_m t)$$

These are vectors for forces in yaw and sway. The corresponding responses are expressed as:

$$\underline{\xi} = \begin{bmatrix} \xi_y \\ \xi_\psi \end{bmatrix}$$

- The response as a result of first order wave forces can now be expressed as:

$$\underline{\xi}^{(1)} = \sum_i \hat{x}_i \cdot \frac{1}{\omega_i^2} \frac{\sum_n DAF_i \cdot \hat{x}_i^T [I_{i,\Delta\psi} a_n ( \cos(\varepsilon_n - \omega_n t) \cos(\delta_i + \phi_i) - \sin(\varepsilon_n - \omega_n t) \sin(\delta_i + \phi_i) )]}{\hat{x}_i^T A \hat{x}_i} \quad (5.19)$$

- And the wind gust response for sway and yaw can be written as.

$$\underline{\xi}_{win,dyn} = \sum_i \hat{x}_i \cdot \frac{1}{\omega_i^2} \frac{\sum_m \hat{x}_i^T [DAF_i \cdot \underline{D} \cdot 2 \cdot |V_z| w_m \cos(\varepsilon_m - \omega_m t + \phi_i)]}{\hat{x}_i^T A \hat{x}_i} \quad (5.20)$$

Modal superposition can be recognized in these expressions where summation occurs for over the modes  $i=1,2$ .

### 5.1.2.2 Second order dynamic response

Second order dynamic response results from low frequency drift forces on the structure. The expression for the low-frequency wave force was determined already as (eq: 3.15)

$$F^{(2)}(t) = \sum_{j=1}^N \sum_{k=1}^N a_j a_k \left[ P_{jk} \cos((\omega_j - \omega_k)t + (\varepsilon_k - \varepsilon_j)) + Q_{jk} \sin((\omega_j - \omega_k)t + (\varepsilon_k - \varepsilon_j)) \right]$$

Because the frequency is the difference between two frequency components ( $j,k$ ), the *DAF* will have to be defined accordingly as:

$$DAF^{(2)} = \frac{1}{\sqrt{\left(1 - \left(\frac{\omega_j - \omega_k}{\omega_i}\right)^2\right)^2 + \left(2\xi_i \frac{\omega_j - \omega_k}{\omega_i}\right)^2}}$$

where  $\omega_i$ , is the natural frequency (for modes  $i=1,2$ ), and  $\omega_j$  and  $\omega_k$  are frequencies of the two wave components.

The response can be defined in much the same way as with the first order forces:

$$\underline{\xi}^{(2)} = \sum_i \hat{x}_i \cdot \frac{1}{\omega_i^2} \frac{\sum_{j=1}^N \sum_{k=1}^N DAF_i^{(2)} \cdot \hat{x}_i^T a_j a_k \left\{ \begin{array}{l} [P_{jk} \cos((\omega_j - \omega_k)t + (\varepsilon_k - \varepsilon_j) + \phi_i) + \\ Q_{jk} \sin((\omega_j - \omega_k)t + (\varepsilon_k - \varepsilon_j) + \phi_i)] \end{array} \right\}}{\hat{x}_i^T M \hat{x}_i} \quad (5.20)$$

this expression can be written in a different form by using the following trigonometric relations:

$$\begin{aligned} & \cos[(\varepsilon_k - \omega_k t) - (\varepsilon_j - \omega_j t) + \phi_i] = \\ & \cos[(\varepsilon_k - \omega_k t) - (\varepsilon_j - \omega_j t)] \cos(+\phi_i) - \sin[(\varepsilon_k - \omega_k t) - (\varepsilon_j - \omega_j t)] \sin(+\phi_i) = \\ & \cos(\varepsilon_k - \omega_k t) \cos(\varepsilon_j - \omega_j t) \cos(+\phi_i) + \sin(\varepsilon_k - \omega_k t) \sin(\varepsilon_j - \omega_j t) \cos(+\phi_i) - \\ & \sin(\varepsilon_k - \omega_k t) \cos(\varepsilon_j - \omega_j t) \sin(+\phi_i) + \cos(\varepsilon_k - \omega_k t) \sin(\varepsilon_j - \omega_j t) \sin(+\phi_i) \end{aligned} \quad (5.21)$$

and,

$$\begin{aligned} & \sin[(\varepsilon_k - \omega_k t) - (\varepsilon_j - \omega_j t) + \phi_i] = \\ & \sin[(\varepsilon_k - \omega_k t) - (\varepsilon_j - \omega_j t)] \cos(+\phi_i) + \cos[(\varepsilon_k - \omega_k t) - (\varepsilon_j - \omega_j t)] \sin(+\phi_i) = \\ & \sin(\varepsilon_k - \omega_k t) \cos(\varepsilon_j - \omega_j t) \cos(+\phi_i) - \cos(\varepsilon_k - \omega_k t) \sin(\varepsilon_j - \omega_j t) \cos(+\phi_i) + \\ & \cos(\varepsilon_k - \omega_k t) \cos(\varepsilon_j - \omega_j t) \sin(+\phi_i) + \sin(\varepsilon_k - \omega_k t) \sin(\varepsilon_j - \omega_j t) \sin(+\phi_i) \end{aligned} \quad (5.22)$$

Substituting these relations into equation 5.20 yields:

$$\underline{\xi}^{(2)} = \sum_i \hat{x}_i \cdot \frac{1}{\omega_i^2} \frac{\sum_{j=1}^N \sum_{k=1}^N DAF_i^{(2)} \cdot \hat{x}_i^T a_j a_k \left\{ \begin{array}{l} \left[ P_{jk} \left\{ \cos(\varepsilon_k - \omega_k t) \cos(\varepsilon_j - \omega_j t) \cos(+\phi_i) + \right. \right. \\ \sin(\varepsilon_k - \omega_k t) \sin(\varepsilon_j - \omega_j t) \cos(+\phi_i) - \\ \sin(\varepsilon_k - \omega_k t) \cos(\varepsilon_j - \omega_j t) \sin(+\phi_i) + \\ \left. \left. \cos(\varepsilon_k - \omega_k t) \sin(\varepsilon_j - \omega_j t) \sin(+\phi_i) \right\} + \right. \\ \left. Q_{jk} \left\{ \sin(\varepsilon_k - \omega_k t) \cos(\varepsilon_j - \omega_j t) \cos(+\phi_i) - \right. \right. \\ \cos(\varepsilon_k - \omega_k t) \sin(\varepsilon_j - \omega_j t) \cos(+\phi_i) + \\ \cos(\varepsilon_k - \omega_k t) \cos(\varepsilon_j - \omega_j t) \sin(+\phi_i) + \\ \left. \left. \sin(\varepsilon_k - \omega_k t) \sin(\varepsilon_j - \omega_j t) \sin(+\phi_i) \right\} \right]}{\hat{x}_i^T A \hat{x}_i} \end{array} \right.}{\hat{x}_i^T A \hat{x}_i} \quad (5.23)$$

### 5.3 Coefficients of the equation

**Radiation damping and added mass:** the radiation damping and added mass terms are given in the hydrodynamic datafiles, arranged by frequency and DOF.

**Mass:** the vessel mass terms for surge and sway are equal and may be written as,

$$M_x = M_y = \rho \nabla$$

where  $\nabla$  is the displaced water volume, and  $\rho$  the water density.

The moment of inertia is expressed in terms of the radius of gyration, which is the distance away from the COG where, if all the mass were concentrated at that distance, the body would have the same moment of inertia as it does with mass distributed. This is expressed for yaw as follows,

$$J_\psi = k_z^2 \rho \nabla$$

where  $k_z$  is the radius of gyration.

**Stiffness:** The stiffness is a key factor in the determination of the system response; it is essential therefore that it be modeled with accuracy. Having to do away with the non-linearity of the spring characteristics detracts considerably from this accuracy. In this project, however, a linear spring will be used in both the static and dynamic parts as this facilitates comparison with existing programs for testing purposes.

We will, however, present a method of including a non-linear spring in the static part for possible future application. :

- Force-displacement data is generated by a program based on the catenary equation (such as MOOR40) for the system of lines used.
- This data is then stored in an array used in the static analysis to match the global forces in  $x$  and  $y$  with displacements in those directions (linear interpolation is used as necessary).

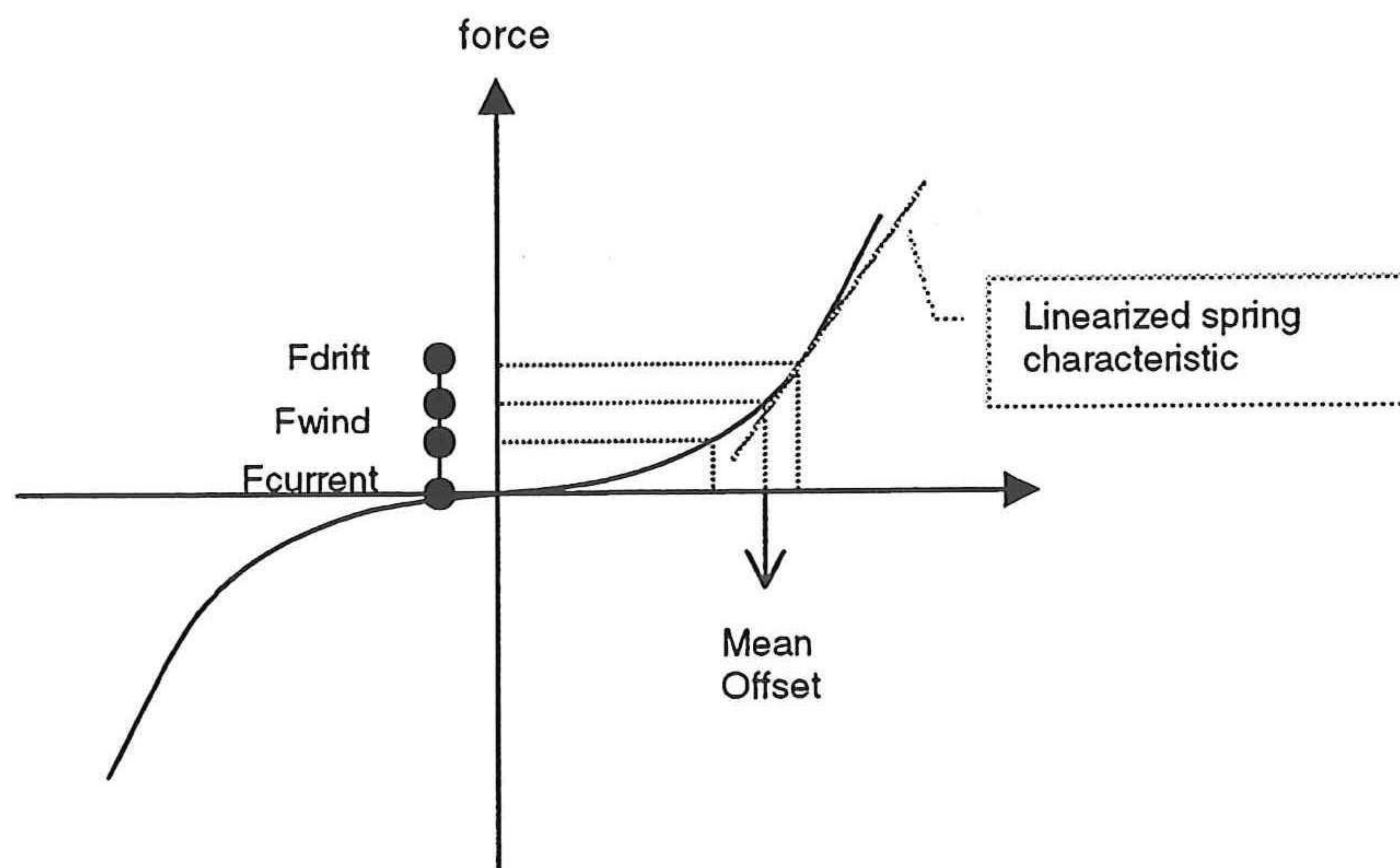


figure 5.1 Force-displacement curve for the mooring system

- The mean offset is then based on a non-linear force-displacement curve in the static regime. A linear spring is determined about the mean offset, which is the cumulative offset of the current, wind and mean wave drift response, as is shown in figure 5.1 above.
- However, the offset that is carried on into the dynamic analysis is comprised of only the influence of wind and current, to avoid double counting mean wave drift because the dynamic equations of wave motion account for the mean wave drift.

With this linearized spring coefficient ( $c_{lin}$ ) the components of the stiffness matrix may be written,

$$\begin{bmatrix} c_{yy} & c_{y\psi} \\ c_{\psi y} & c_{\psi\psi} \end{bmatrix}$$

Assuming the stiffness is not dependent on direction, in other words,  $C_{xx}=C_{yy}$ , we may write,

$$\begin{aligned} c_{xx} &= c_{yy} = c_{lin} \\ c_{y\psi} &= c_{\psi y} = c_{lin} \cdot A \\ c_{\psi\psi} &= c_{lin} \cdot A^2 + c_{env} \end{aligned} \tag{5.24-5.26}$$

where  $A$  is the arm, the distance between the COG and the center of the turret.

The second term of equation 5.26 ( $c_{env}$ ) refers to the “environmental stiffness”; it accounts for the restoring moment from the environmental forces which act when there is a departure from the equilibrium orientation. This restoring coefficient does not depend on the mooring system.

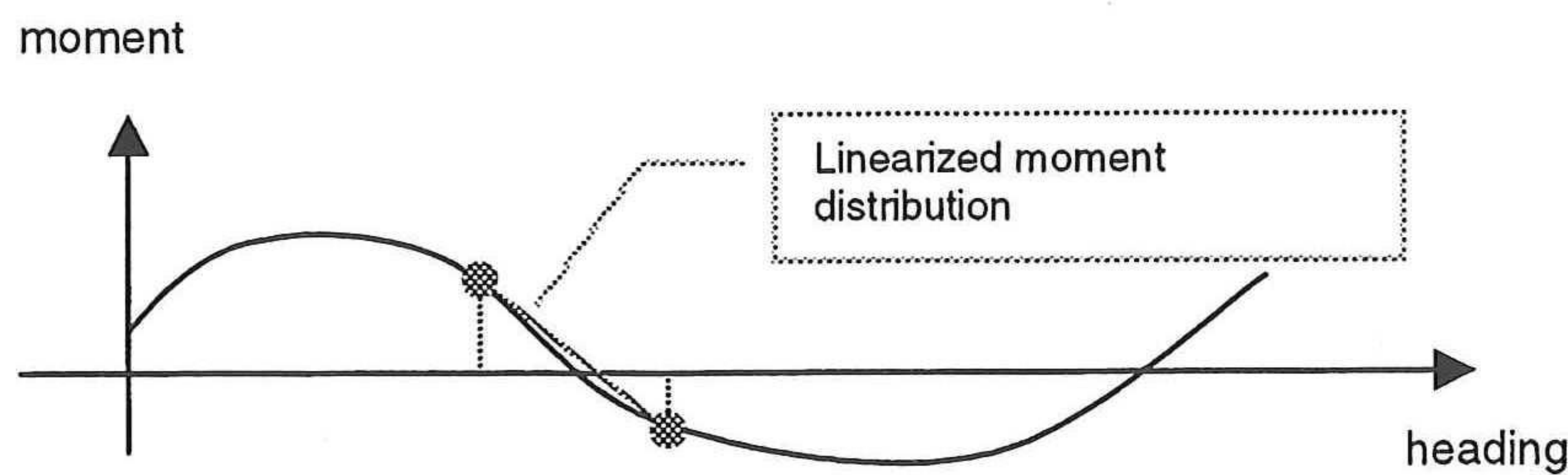


**Figure 5.2 static moment distribution**

Recall that the mean orientation of the ship was derived from the moment equilibrium. The “environmental” rotational stiffness ( $c_{env}$ ) then follows from the gradient of the linearized moment distribution about the mean ( $M=0$ ) as is shown in figure 5.2.

Viscous damping: the viscous damping term is very significant in this project because the low natural frequency of the system causes a low frequency response where radiation damping is virtually negligible; viscous damping is therefore the only restraint on resonant dynamic amplification.

Viscous damping is proportional to the square of the velocity of the structure relative to the instantaneous velocity of the fluid. The latter will be assumed to be constant and equal to the velocity of the current (constant), so that we may write for the square of the relative velocity,

$$(u_x + \dot{x})|u_x + \dot{x}| = u_x^2 + 2|u_x|\dot{x} + \dot{x}^2 \quad 5.27$$

Where  $u_x$  is the current component in the direction  $x$ , and  $\dot{x}$  the velocity of the ship in  $x$ .

For the present we shall assume the ship velocity to be relatively small compared to the current. Therefore, the third term may be assumed negligible. We are left then with,

$$u_x^2 + 2|u_x|\dot{x} \quad 5.28$$

where the first term is accounted for in the static analysis.

If the viscous damping force in  $x$  is to be expressed with OCIMF coefficients we may write,

$$F_{x,damp} = \left(\frac{1}{2} |C_{x,c}| \rho_c L_{pp} T\right) 2|U|\dot{x}$$

where  $U$  is the magnitude of the current velocity, and the component in  $x$  ( $u_x$ ) is now accounted for by  $UC_{c,x}$  (the OCIMF coefficients are depend on the heading of the ship and are given for each degree of freedom) .

The viscous damping terms may now be expressed as follows,

$$\begin{aligned}b_{visc,x} &= \left(\frac{1}{2} |C_{x,c}| \rho_c L_{pp} T\right) 2|U| \\b_{visc,yy} &= \left(\frac{1}{2} |C_{y,c}| \rho_c L_{pp} T\right) 2|U| \\b_{visc,\psi\psi} &= \left(\frac{1}{2} |C_{xy,c}| \rho_c L_{pp}^2 T (1/4 L_{pp})\right) 2|U|\end{aligned}\tag{5.29}$$

These will play a significant role in the calculation.

## 6. FIRST ORDER RELIABILITY METHOD

We have expressed the response of the system in terms of the incident wave and wind gust components in the previous chapter. Each of these components (and there is a finite number) is a stochastic variable that can be characterized by a Gaussian distribution. The application of a probabilistic method allows a certain event (say a prescribed offset) to be coupled to a probability of exceedance; conversely, a probability of exceedance can also be coupled to a certain event, such as an extreme offset. The latter possibility is what will be considered in this project.

### 6.1 Transformations

The variables can only be compared if they are of comparable form; they need to be standardized with respect to the standard deviation of the frequency components of the surface elevation. We will then have random variables of unit-variance and mean zero,  $N(0,1)$ . A single wave and wind gust component were defined as, respectively,

$$\eta_n(t) = a_n \cos(\varepsilon_n - \omega_n t) \quad (6.1)$$

$$w_m(t) = w_m \cos(\varepsilon_m - \omega_m t) \quad (6.2)$$

These are both Gaussian distributed. We will define their standardized counterparts as,

$$x_n = \frac{\eta_n - 0}{\sigma_n} = \frac{\eta_n}{\sigma_n} \quad (6.3)$$

and

$$x_m = \frac{w_m - 0}{\sigma_m} = \frac{w_m}{\sigma_m} \quad (6.4)$$

We may also write:

$$\sigma_n x_n = a_n \cos(\varepsilon_n - \omega_n t) \quad (6.5)$$

and

$$\sigma_m x_m = w_m \cos(\varepsilon_m - \omega_m t) \quad (6.6)$$

There is however another set of basic variables that are uncorrelated and have the same properties [Tromans and van Dam, 1996]. These are shifted with 90 degrees with respect to expressions 6.5 and 6.6, namely,

$$\sigma_n \tilde{x}_n = a_n \sin(\varepsilon_n - \omega_n t) \quad (6.7)$$

and,

$$\sigma_m \tilde{x}_m = w_m \sin(\varepsilon_m - \omega_m t) \quad (6.8)$$

which are the Hilbert transforms of  $x_n$  and  $x_m$ .

We now have all the basic variables with which to define the response in the unit-variance normal space.

## 6.2 Standardized response

We can now also transform the response equations in accordance with the above standard normal variables:

- The first order wave response was:

$$\underline{\xi}^{(1)} = \sum_i \hat{x}_i \cdot \frac{1}{\omega_i^2} \frac{\sum_n DAF_i \cdot \hat{x}_i^T \left[ I_{i,\Delta\psi} a_n \left( \cos(\varepsilon_n - \omega_n t) \cos(\delta_i + \phi_i) - \sin(\varepsilon_n - \omega_n t) \sin(\delta_i + \phi_i) \right) \right]}{\hat{x}_i^T A \hat{x}_i}$$

we may now write:

$$\underline{\xi}^{(1)} = \sum_i \hat{x}_i \cdot \frac{1}{\omega_i^2} \frac{\sum_n DAF_i \cdot \hat{x}_i^T \left[ I_{i,\Delta\psi} \left( \sigma_n x_n \cos(\delta_i + \phi_i) - \sigma_n \tilde{x}_n \sin(\delta_i + \phi_i) \right) \right]}{\hat{x}_i^T A \hat{x}_i}$$

- The dynamic wind gust response was:

$$\underline{\xi}_{win,dyn} = \sum_i \hat{x}_i \cdot \frac{1}{\omega_i^2} \frac{\sum_m \hat{x}_i^T \left[ DAF_i \cdot \underline{D} \cdot 2 \cdot |V_z| w_m \left( \cos(\varepsilon_m - \omega_m t) \cos(\phi_i) - \sin(\varepsilon_m - \omega_m t) \sin(\phi_i) \right) \right]}{\hat{x}_i^T A \hat{x}_i}$$

we may now write:

$$\underline{\xi}_{win,dyn} = \sum_i \hat{x}_i \cdot \frac{1}{\omega_i^2} \frac{\sum_m \hat{x}_i^T \left[ DAF_i \cdot \underline{D} \cdot 2 \cdot |V_z| \left( \sigma_m x_m \cos(\phi_i) - \sigma_m \tilde{x}_m \sin(\phi_i) \right) \right]}{\hat{x}_i^T A \hat{x}_i}$$

- And lastly, the second order, drift response was:

$$\underline{\xi}^{(2)} = \sum_i \hat{x}_i \cdot \frac{1}{\omega_i^2} \frac{\sum_{j=1}^N \sum_{k=1}^N DAF_i^{(2)} \cdot \hat{x}_i^T a_j a_k \left\{ \begin{array}{l} \left[ P_{jk} \left\{ \cos(\varepsilon_k - \omega_k t) \cos(\varepsilon_j - \omega_j t) \cos(\phi_i) + \right. \right. \\ \sin(\varepsilon_k - \omega_k t) \sin(\varepsilon_j - \omega_j t) \cos(\phi_i) - \\ \sin(\varepsilon_k - \omega_k t) \cos(\varepsilon_j - \omega_j t) \sin(\phi_i) + \\ \left. \left. \cos(\varepsilon_k - \omega_k t) \sin(\varepsilon_j - \omega_j t) \sin(\phi_i) \right\} + \right. \\ \left. Q_{jk} \left\{ \sin(\varepsilon_k - \omega_k t) \cos(\varepsilon_j - \omega_j t) \cos(\phi_i) - \right. \right. \\ \cos(\varepsilon_k - \omega_k t) \sin(\varepsilon_j - \omega_j t) \cos(\phi_i) + \\ \cos(\varepsilon_k - \omega_k t) \cos(\varepsilon_j - \omega_j t) \sin(\phi_i) + \\ \left. \left. \sin(\varepsilon_k - \omega_k t) \sin(\varepsilon_j - \omega_j t) \sin(\phi_i) \right\} \right]}{\hat{x}_i^T A \hat{x}_i}$$

we may now write:

$$\underline{\xi}^{(2)} = \sum_i \hat{x}_i \cdot \frac{1}{\omega_i^2} \frac{\sum_{j=1}^N \sum_{k=1}^N DAF_i^{(2)} \cdot \hat{x}_i^T \left\{ \begin{array}{l} P_{jk} \{ \sigma_k x_k \sigma_j x_j \cos(\phi_i) + \sigma_k \tilde{x}_k \sigma_j \tilde{x}_j \cos(\phi_i) - \\ \sigma_k \tilde{x}_k \sigma_j x_j \sin(\phi_i) + \sigma_k x_k \sigma_j \tilde{x}_j \sin(\phi_i) \} + \\ Q_{jk} \{ \sigma_k \tilde{x}_k \sigma_j x_j \cos(\phi_i) - \sigma_k x_k \sigma_j \tilde{x}_j \cos(\phi_i) + \\ \sigma_k x_k \sigma_j x_j \sin(\phi_i) + \sigma_k \tilde{x}_k \sigma_j \tilde{x}_j \sin(\phi_i) \} \end{array} \right.}{\hat{x}_i^T A \hat{x}_i}$$

These expressions are written out fully in the appendix, and the distinction between whether a term is a function of mode or degree of freedom, or both, is made clear.

### 6.3 The unit-variance normal space and the reliability index

If we consider two random variables  $x$  and its Hilbert transform  $\tilde{x}$ ; their respective probability density functions can be plotted out in the unit-variance normal space as in figure 6.1. If we now plot out the projections of the contours at certain heights, we will have concentric circles centered on origin, designating points of equal probability density; this is shown in figure 6.2.

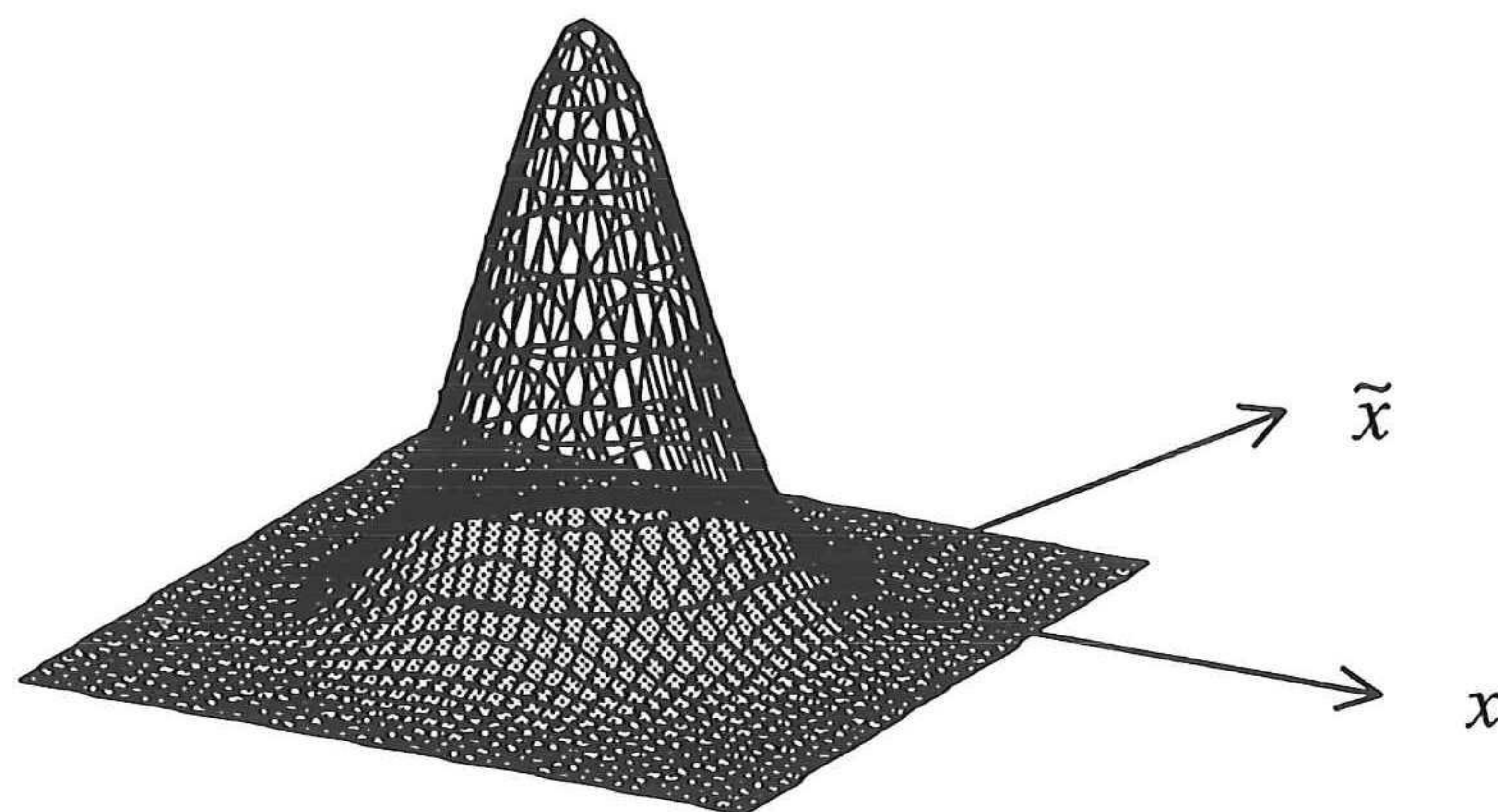


Figure 6.1  $x$  and  $\tilde{x}$  in the unit variance normal space.

The response function can be expressed in terms of the unit-variance variables and plotted in the unit-variance normal space. A constant value of this function defines a surface called the limit-state surface ( $g(x)$ ); 'limit-state' because it constitutes the limit between two areas, namely, the failure set and the non-failure set.

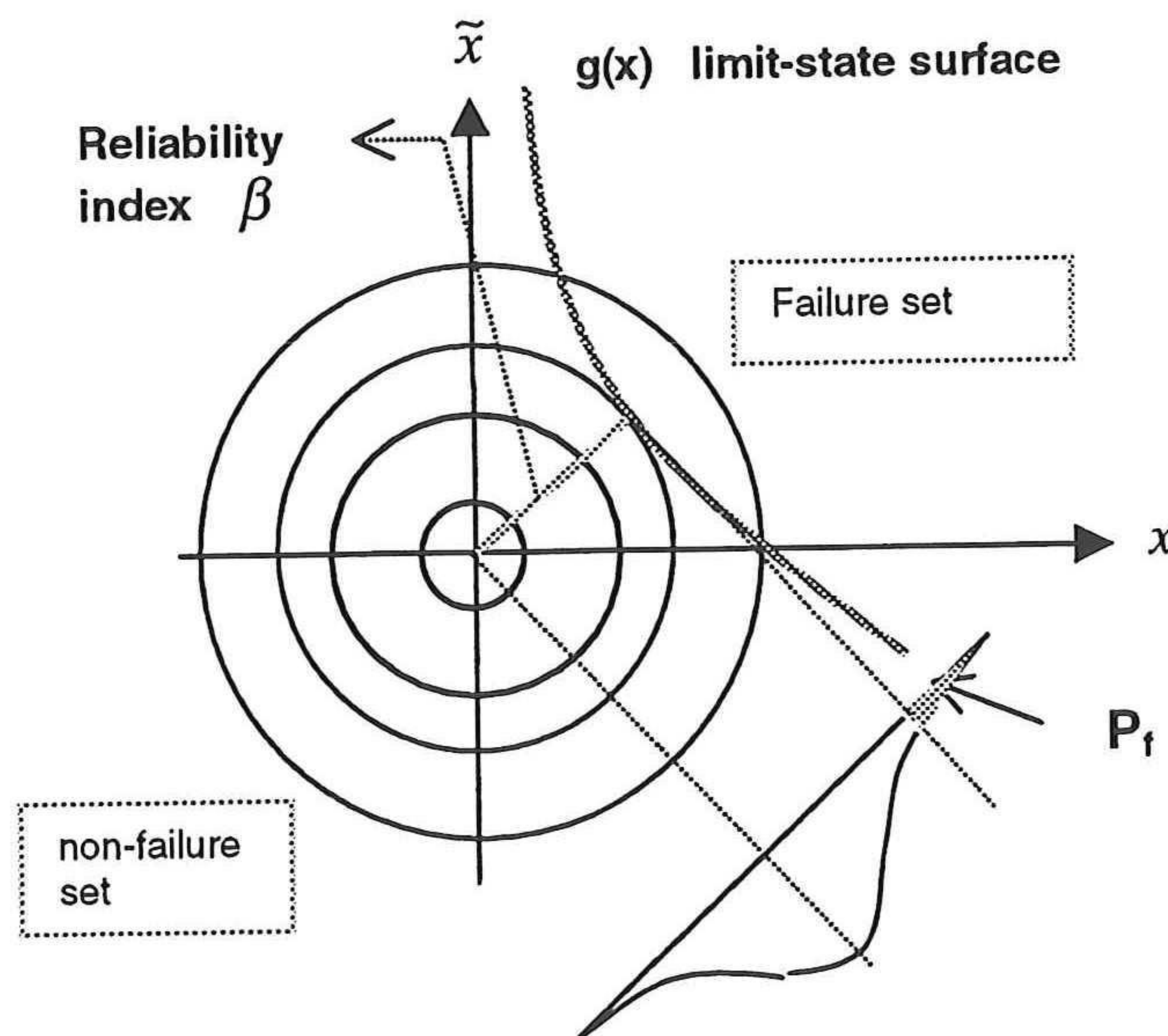


Figure 6.2 The limit-state surface and the probability of exceedance

The smallest distance between the origin and the limit-state surface is defined as the reliability index ( $\beta$ ). The design point represents the point of greatest probability density on the limit-state. Therefore, the volume near it makes the greatest contribution to the failure probability  $P_f$ .

The probability of falling in the failure set is approximated by:

$$P_f = 1 - \Phi(\beta) \quad (6.9)$$

where  $\Phi$  denotes the standardized Gaussian distribution function.  $\beta$ , the reliability index, is a measure of distance from the origin measured in standard deviations. A greater  $\beta$  means a greater safety.

When the limit-state function is non-linear (as is the case here) the 1st and 2nd moments ( $\mu, \sigma$ ) can no longer be obtained exactly. This is because non-linear combinations of the standardized normal distributions does not lead to a normal distribution of the for the function  $g(x)$ . [Melchers, 1987]. To solve the problem of non-linearity of the limit-state surface, it is linearized about a certain point (see figure 6.3). The value of  $\beta$  then depends on the point that is chosen for the linearization. The linearized limit-state surface is called the tangent hyperplane

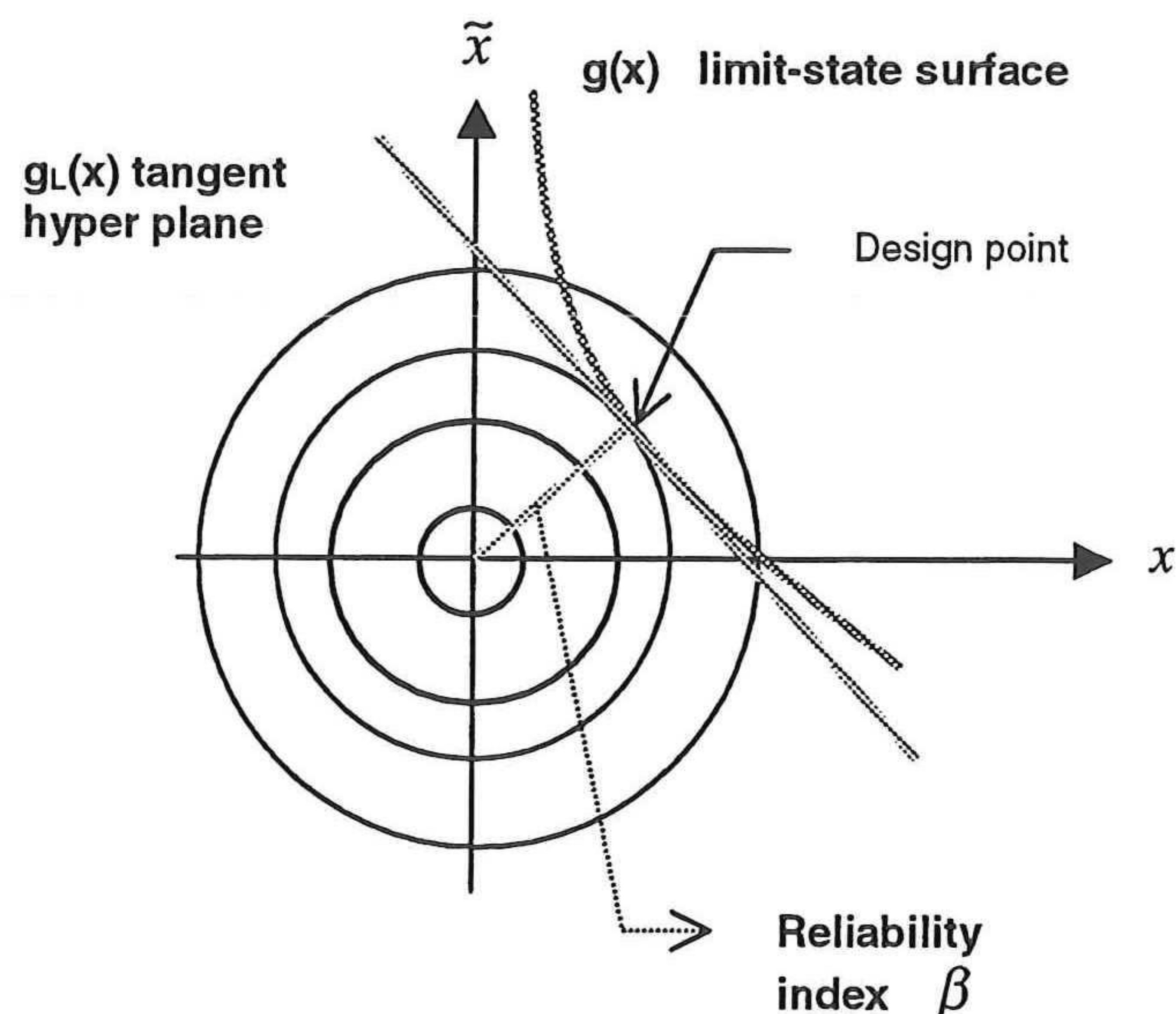


**Figure 6.3** The linearized limit-state function.

The probability of falling outside the limit-state surface into the failure set can be well approximated by the probability of falling outside the tangent hyperplane because most of the probability volume is located behind the design point, perpendicular to the tangent hyperplane.

#### 6.4 Determining the design point

Section 6.3 considered the case for two variables, while in our problem there are  $2^{*(n+m)}$  random variables ( $n$  wave components,  $m$  wave gust components; and their Hilbert transforms). The distance  $\beta$  from the origin to the design point can be written as:

$$\beta = \left( \sum_n (x_n^2 + \tilde{x}_n^2) + \sum_m (x_m^2 + \tilde{x}_m^2) \right)^{1/2} = \left( \sum_{i=1}^{2(n+m)} (x_i^2) \right)^{1/2} \quad (6.10)$$

for  $i=n,m$

The limit-state function  $g(X)$  ( $g(x_1, x_2, \dots, x_i)$ ) is expressed in terms of these variables. Finding the shortest  $\beta$  is a minimalization problem that can be solved by introducing a Lagrangian multiplier  $\lambda$  [Melchers, 1987].

$$\beta - \lambda g(X) = \min(\Delta) \quad (6.11)$$

where we seek to minimize  $\Delta$ , this can be achieved by solving for the stationary

$$\begin{aligned} \text{points } \frac{\partial \Delta}{\partial \lambda} = 0 \text{ and } \frac{\partial \Delta}{\partial x_i} = 0 \\ \frac{\partial \Delta}{\partial x_i} = \frac{\partial \beta}{\partial x_i} - \lambda \frac{\partial g(x)}{\partial x_i} = 0 \\ \frac{\partial \Delta}{\partial \tilde{x}_i} = \frac{\partial \beta}{\partial \tilde{x}_i} - \lambda \frac{\partial g(x)}{\partial \tilde{x}_i} = 0 \end{aligned}$$

which can be written in shorter form as

$$\frac{\partial \Delta}{\partial X} = \frac{\partial \beta}{\partial X} \beta - \lambda \frac{g(X)}{\partial X} = 0 \quad (6.12)$$

where, using equation 6.10,

$$\frac{\partial \beta}{\partial x_i} = \frac{\partial \left( \sum_i^{2(n+m)} x_i^2 \right)^{1/2}}{\partial x_i} = x_i \left( \sum_i^{2(n+m)} x_i^2 \right)^{-1/2} = \frac{x_i}{\beta} \quad (6.13)$$

substituting this equation into 6.12 leads to an expression for the design point  $X^*(x_1, x_2, \dots, x_i)$ :

$$X^* = \lambda \frac{g(X)}{\partial X} \beta \quad (6.14)$$

or,

$$\lambda \frac{g(X)}{\partial x_i} = \frac{x_i}{\beta} \quad (6.15)$$

Multiplying both sides with  $x_i$  and summing over all  $i$ , yields:

$$\sum_i \lambda \frac{g(X)}{\partial x_i} x_i = \frac{\sum_i x_i^2}{\beta} = \frac{\beta^2}{\beta} = \beta \quad (6.16)$$

The Langrangian multiplier can now be expressed as:

$$\lambda = \frac{\beta}{\sum_i \lambda \frac{g(X)}{\partial x_i} x_i} \quad (6.17)$$

The design point follows from an iterative solution of the equations 6.14, 6.16 and 6.17.

### 6.5 The first estimate of the design point

The design point  $X^*$  is not known a priori, nor is the Lagrangian multiplier; a solution is obtained by convergence of the iteration. However, a first estimate is necessary to start the iteration. It seems from the calculation that it hardly matters what is input as a first estimate; the solution converges almost irrespective of the initial values. Certain initial values require a few iterations more. For purposes of insight, however, it is interesting to consider what first estimates might approach the design point better than others. One possibility is to assign to each component ( $x$ ) (weight in accordance with its weight in the wave or wind spectrum. In other words,  $x_n$  is proportional to the standard deviation assigned to frequency component  $n$ ,

$$x_n = c\sigma_n$$

and this for all components.

Renorming : Before running the initial iteration, the values of  $x$  must be renormed, which means that the vectorial sum is to be made equal to the prescribed reliability index. Each component is therefore multiplied by a factor such that,

$$\sum_n (x_n^2 + \tilde{x}_n^2)^{1/2} = \beta$$

This is essential because the reliability index fixes the probability of exceedance of the extreme response.

### 6.6 Extreme response

As much as it is possible to determine the probability of exceedance that accompanies a certain event described by the limit-state function (such as a maximum offset or force etc...) it is also possible to calculate a most probable extreme response that corresponds to a certain prescribed probability of exceedance.

The probability that an arbitrary maximum is outside the tangent hyperplane is approximated by a Rayleigh distribution, which is generally used to characterize the statistics of maxima:

$$Q = \exp(-\beta^2 / 2) \quad (6.18)$$

from which follows,

$$\beta = (-2 \ln Q)^{1/2} \quad (6.19)$$

What we determine in this project is the extreme response that follows from a prescribed probability of exceedance,  $Q$ . Prescribing a certain  $Q$ , the reliability index follows from equation 6.19. Following the reliability method as described above, the design point can be obtained by solving equations 6.14, 6.16 and 6.17 iteratively.

### 6.7 FORM: an optimization

The procedure is essentially a process of optimization around the response of the system. We begin with a number of stochastic variables each expressed as a variable ( $x$ ) and a standard deviation, as in equation 6.5,

$$\sigma_n x_n = a_n \cos(\varepsilon_n - \omega_n t)$$

The standard deviation is derived for each frequency component from the wave or wind spectrum. We are interested in the response that corresponds to a prescribed probability of exceedance. From equation 6.19 we know that this probability of exceedance can be related to a certain reliability index. What the optimization process does is calculate for all the variables ( $x$ ) values such that the response is maximum, and the vectorial sum of these values is equal to the reliability index, which ensures that the response corresponds to the prescribed probability of exceedance. Basically, the components are given relative "weight" according to how they influence the response. Thus, a component whose frequency is close to a natural frequency of the system is likely to be assigned a greater value than another that is further away.

### 6.8 Wave and wind histories

Once the design point is determined, the corresponding surface elevation and response time series may be obtained. In accordance with equation 6.5 we may write,

$$x_n = \frac{a_n}{\sigma_n} \cos(\varepsilon_n - \omega_n t)$$

$$\tilde{x}_n = \frac{a_n}{\sigma_n} \sin(\varepsilon_n - \omega_n t)$$

The wave amplitude associated with frequency  $n$  can be determined as follows,

$$x_n^2 + \tilde{x}_n^2 = \frac{a_n^2}{\sigma_n^2} ( \cos^2(\varepsilon_n - \omega_n t) + \sin^2(\varepsilon_n - \omega_n t) ) = \frac{a_n^2}{\sigma_n^2}$$

hence,

$$a_n = \sigma_n \sqrt{x_n^2 + \tilde{x}_n^2} \quad (6.20)$$

The phase angle can be calculated in the following way

$$\frac{\tilde{x}_n}{x_n} = \frac{\sin(\varepsilon_n - \omega_n t)}{\cos(\varepsilon_n - \omega_n t)} = \tan(\varepsilon_n - \omega t) \quad (6.21)$$

with the extreme response occurring at  $t=0$ ,

$$\varepsilon_n = \arctan\left(\frac{\tilde{x}_n}{x_n}\right) \quad (6.22)$$

The surface elevation can now be obtained with,

$$\eta(t) = \sum_n a_n \cos(\varepsilon_n - \omega_n t) \quad (6.23)$$

Similarly, the wind gust speed amplitude  $w_m$  and the corresponding phase shift follows from,

$$w_m = \sigma_m \sqrt{x_m^2 + \tilde{x}_m^2} \quad (6.24)$$

$$\varepsilon_m = \arctan\left(\frac{\tilde{x}_m}{x_m}\right) \quad (6.25)$$

The wind gust speed time series can be obtained from,

$$w(t) = \sum_m w_m \cos(\varepsilon_m - \omega_m t) \quad (6.26)$$

## 7. RESULTS AND ANALYSIS

In section 6 the probabilistic method used in this project is described; it was concluded that what we are dealing with is an optimization of response with the constraint of a fixed probability of exceedance  $Q$ . We will look more closely now at what this produces.

### 7.1 The limit state function

The limit state function defines the area of interest; it can be force, stress, or, as in this case, motion response. For the present study of a turret moored ship, the offset of the turret is of particular interest. However, in the interest of easy comparison with DYNFLOAT (a time-domain simulation program) we shall look at the offset of the center of gravity (COG).

There are motions in the  $x$  direction (surge) and in the  $y$  direction (sway and yaw, which will henceforth be referred to as lateral motions), which means that the maximum response is the vectorial sum of these, resulting from first and second order forces. The limit state function may thus be expressed as follows:

$$g(x, \tilde{x}) = \xi_{lim} - \sqrt{(\xi_{x,win} + \xi_{x,wave(1)} + \xi_{x,wave(2)})^2 + (\xi_{y,win} + \xi_{y,wave(1)} + \xi_{y,wave(2)})^2}$$

Where  $g$  is the limit-state function (a function of the unit-variance variables),  $\xi_{lim}$  is the maximum allowable response.

Customarily the first-order, second moment probabilistic method is used to find a probability of exceedance associated with a certain prescribed response. One would set for example a response of 30m (i.e.  $\xi_{lim}=30m$ ) and the algorithm would optimize to find the highest probability density on the limit state surface. The greatest probability density is found at the design-point where,

$$g(x^*, \tilde{x}^*) = 0$$

However, for purposes of design, it is far more relevant to determine the extreme response associated with a probability of exceedance; in this case we fix the probability of exceedance and optimize for the maximum response.

### 7.2 The probability of exceedance ( $Q$ )

There is a relation between the distribution of maxima and the distribution of the extremes. Figure 7.1 below shows this relation. The probability,  $Q$ , of an individual maximum falling outside the limit state is the probability of an individual response maximum in one sea state. This is expressed by equation 6.19,

$$Q = \exp[-\beta^2/2]$$

However, the probability that during a sea state the extreme maximum does not exceed a certain extreme response is given by [Battjes, 92],

$$P = (1 - Q)^N \quad 7.1$$

where  $N$  is the expected number of maxima during a sea state.

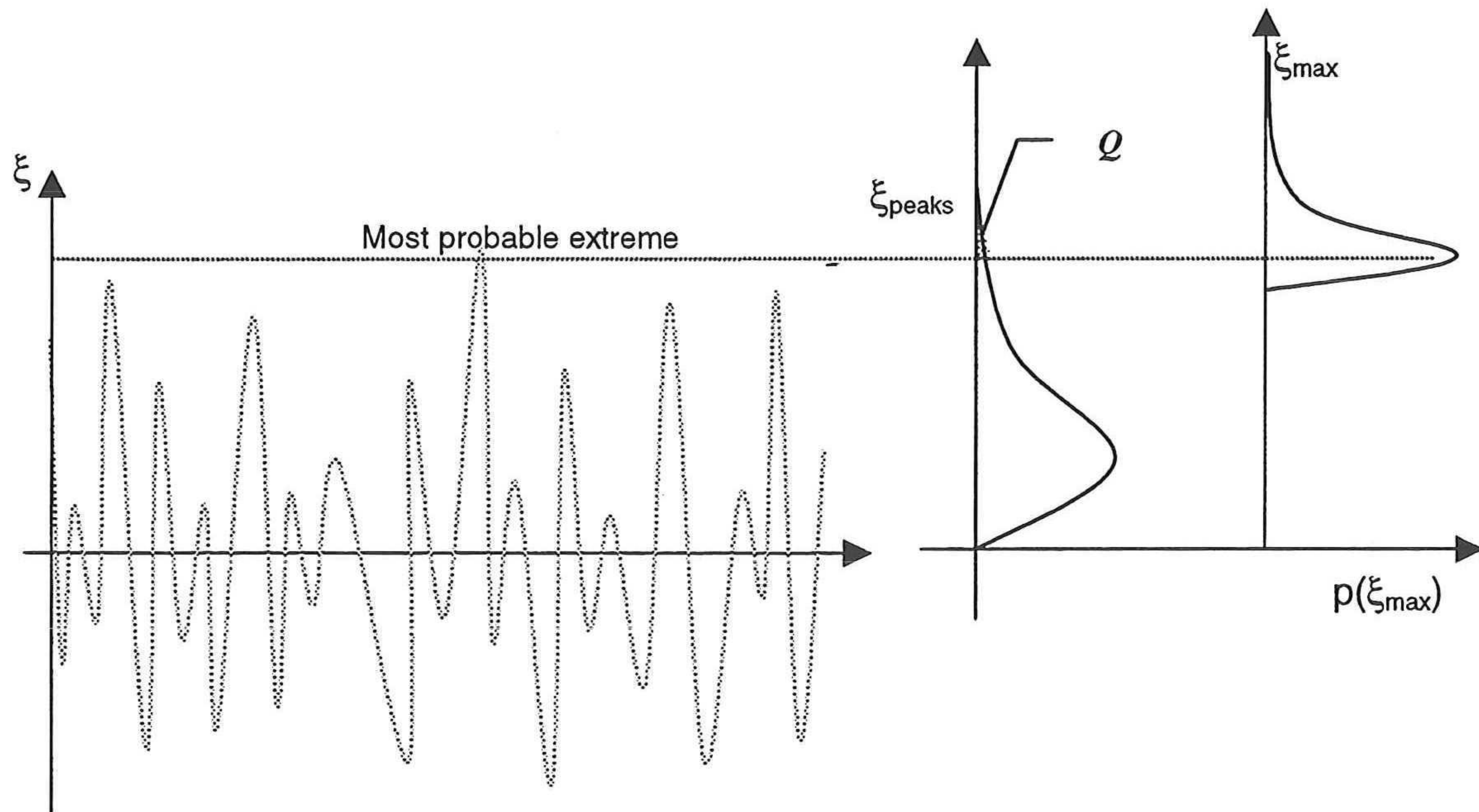


**Figure 7.1 Probability distributions of maxima and extremes for a response signal**

As we are dealing with extreme values where only the range  $Q \ll 1$  is relevant, we may write,

$$P = \exp(-NQ)$$

for a narrow banded process  $N$  can be estimated as,

$$N = T_D / T_{zu} \quad 7.2$$

Where  $T_D$  is the duration of the sea state (3 hours) and  $T_{zu}$  is the mean zero upcrossing period of the associated linear process (the associated linear process is one that has the tangent hyper-plane as a limit state).

Of particular interest is the most probable extreme response. For a large number of peaks a good estimate of the probability of exceedance  $Q$ , associated with the most probable extreme may be estimated as,

$$Q = 1/N \quad 7.3$$

The mean zero up-crossing period has yet not been determined; it can be derived from a weighted average of the frequencies constituting the design-point response,

$$T_{zu} = 2\pi \left[ \frac{\sum_i \omega_i^2 x_i^{*2}}{\sum_i x_i^{*2}} \right]^{-1/2} \quad \text{for } i=m+n \quad 7.4$$

where  $x_i^*$  is the design point.

Because  $T_{zu}$  is not initially known, it is necessary to run the program through once based on an assumed value for the probability of exceedance. The program then calculates a new value for  $N$  based on equations 7.2 and 7.4, and thus a new value for  $Q$  can be determined with equation 7.3. This is to be done iteratively until  $Q$  has converged. Practice has shown that convergence is reached within one or two iterations.

### 7.3 CASE 1

This case will be considered to demonstrate the sensitivities of the program. The results will be compared with those from DYNFLOAT and the object is to make evident certain shortcomings inherent not to the program itself, but to the nature of the method used.

The simplest case of co-linear wind, wave and current will be examined first. The general data related to this case is the following :

```

Draft (m).....:
22.3
Length between PP (m).....:
325
Longitudinal exposed area (m^2).....:
3160
Transverse exposed area (m^2).....:
1130
Water density (Kg/m^3).....:
1025
Air density (Kg/m^3).....:
1.025
Current angle (deg).....:
0.0
Wind angle (deg).....:
0.0
Wave angle (deg).....:
0.0
Current velocity (m/s).....:
1.6
Wind velocity (m/s).....:
30.9
Arm (ship midpoint to center turret).....:
125.0
Significant wave height (m).....:
10.0
Mean wave period (s).....:
11.0
spring (kN/m).....:
915.0
limit on iteration.....:
0.06
Probability of exceedance.....:
0.001280
Mass of the vessels (tons).....:
392400.0
Radius of gyration (m).....:
81.25
Number of components wind/wave.....:
81
    
```

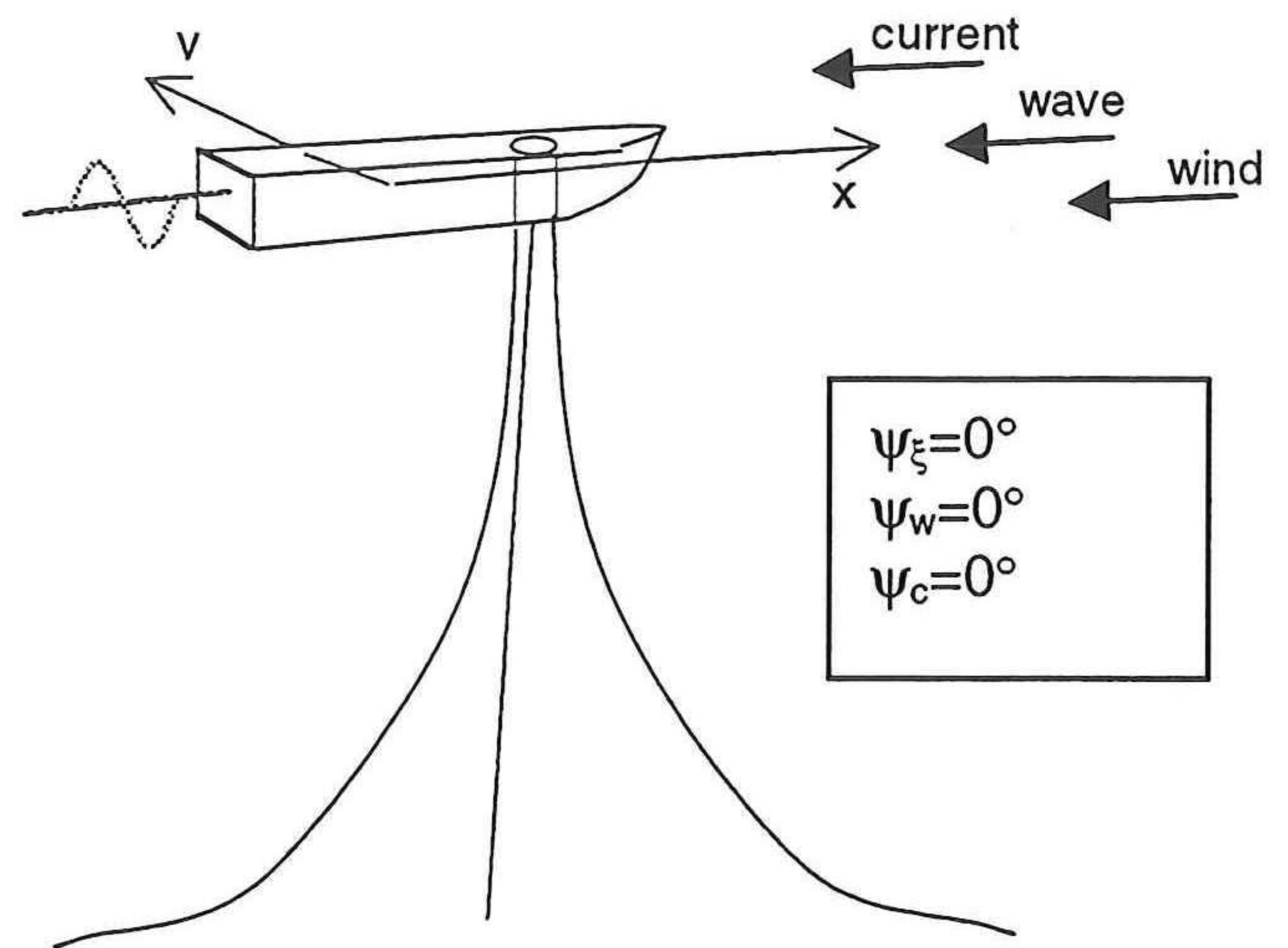


Figure 7.2a Case 1 input data for TURRETDYN

Figure 7.2b Relative direction of the environmental variables with respect to the ship

The ship is fully loaded with a mass of 329400 tons. The water depth is 100m, but because we are dealing with a linear spring, the water depth is not relevant to the mooring system, only to the hydrodynamic data; the latter were chosen (from a set of files) consistent with a 100m water depth and 100% loaded condition. The probability of exceedance corresponds to  $\beta=3.65$ , which converges after a few iterations. *This case will only deal in surge response because all the environmental loads are co-linear.*

Initial iterations have yielded a probability of exceedance of about 0.00128, which corresponds to a reliability index (using  $\beta = (-2\ln Q)^{1/2}$ ) of 3.65. Recall that the reliability index (beta) is the distance of the design point from the origin measured in standard deviations.

Before discussing the results as calculated by TURRETDYN (the program developed for this project) let us first consider the results calculated by DYNFLOAT (time-domain), with which 8 simulation were run with 3 hour simulations. The results are given in figure 7.2 below.

Run	Standard deviation (m)	Maximum dynamic response (m)
1	8.57	-26.71
2	5.64	-17.89
3	6.66	-19.65
4	6.36	-14.43
5	6.33	-24.77
6	6.10	-15.74
7	7.80	-21.59
8	6.29	-17.75
<b>Average</b>	<b>6.7</b>	<b>-19.81</b>

**Figure 7.3 DYNFLOAT dynamic surge response statistics**

What is immediately apparent in these results is the scatter: the standard deviation alone varies from 6.29m to 8.57m, which is a 27% variation, while one might expect there to be much better correspondence in the statistics of the individual runs.

There are several factors that may be responsible for this:

1. *The low natural frequency of the system*
2. *Linearization of the spring*
3. *Statistical effects in time domain simulation*

Some of these these factors cause similar problems in TURRETDYN. These points will serve as basis for comparison with TURRETDYN.

- 1) Case 1, as described above, has a natural frequency of about 0.0463 rad/s, which corresponds to a period of about 136 seconds. This is very low and is attributable to the large mass of the vessel in its fully loaded condition. At such frequencies damping is very low, in particular radiation damping, so that it is almost entirely up to viscous damping to restrain the dynamic amplification. The consequence of this is that the dynamic amplification curve is very peaked. The data for case 1 given in figure 7.2 , shows a case with 81 wave and 81 wind components. This number is not arbitrary but was chosen based on the natural frequency of the system. The range of the spectrum that is considered runs from 0.0 rad/s to 0.75 rad/s; discretizing this spectral range with 81 components gives a frequency interval of,

$$\Delta\omega = (0.75\text{rad/s})/81 = 0.009259 \text{ rad/s}$$

This means that component number 5 corresponds to the natural frequency:

$$\omega_5 = 5 * 0.009259 \text{rad/s} \approx 0.0463 \text{rad/s}$$

The dynamic amplification curve that results from this discretization is given in figure 7.4

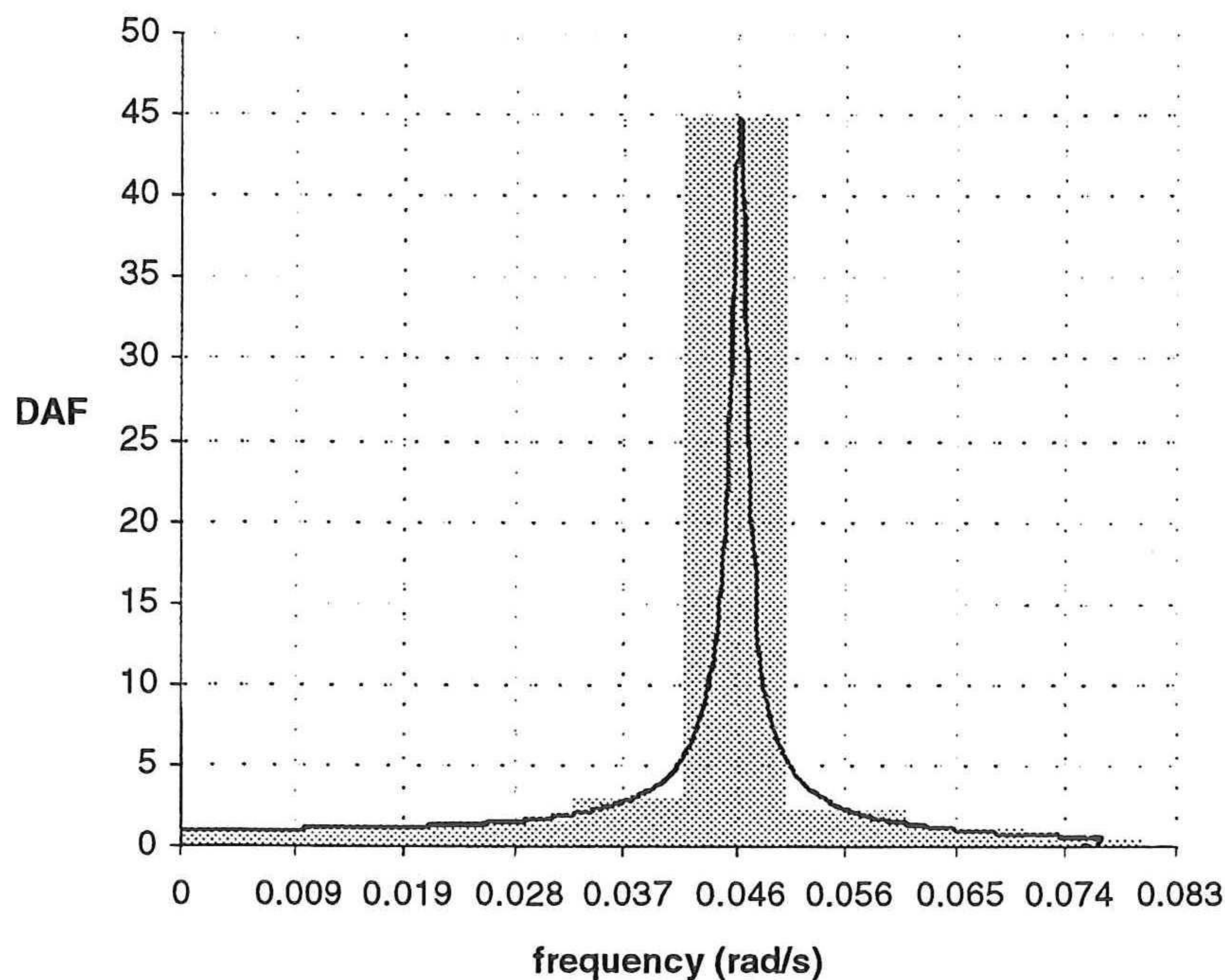


**Figure 7.4 Dynamic amplification curve and the discretized surface area for 81 components**

The shaded area indicates the discretized surface area of the DAF. The results using 81 components, for a frequency range between 0 rad/s and 0.75 rad/s are given in the figure 7.5 below.

Number of components	Frequency interval (rad/s)	Dynamic surge response (m)
81	0.009252	-46.6m

**Figure 7.5 results of TURRETDYN for 81 components**

But if we decide now to take a slightly different interval, using 82 instead of 81 components, the frequency interval is 0.009146 rad/s; the fifth component of this series is 0.045 rad/s which is only slightly removed from the natural frequency of 0.046 but sufficiently to very significantly influence the response because of the peakedness of the dynamic amplification. The results for 82 components are given in figure 7.6.

Number of components	Frequency interval (rad/s)	Dynamic surge response (m)
82	0.009146	-28.4m

**Figure 7.6 results of TURRETDYN for 82 components**

A very small shift in the frequency interval has such an important effect on the response. The dynamic amplification curve is so peaked due to the low damping that unless the discretization of the curve is very accurately done, the results can be misleading.

DYNFLOAT is based on a discretized spectrum as well; the scatter in the standard deviation may in part be attributable to this discretization. DYNFLOAT generates a

random set of components based on the seed number; changing the seed generates a new set of component within a certain frequency range. As has been demonstrated above, a very slight shift away from the resonance frequency can produce large discrepancies.

We have considered now the influence of the low natural frequency on damping and hence on dynamic amplification; let us consider the next point that has been mentioned already, namely, discretization. The only means to achieve reliable results is to discretize the spectrum such that the peakedness is accurately accounted for.

TURRETDYN provides a means to consider the general accuracy of the discretization. This is merely a tool and should not be regarded as a measure of the accuracy. What is done is the discretized dynamic amplification curve is numerically integrated, first with 6000 components (which gives the “real” surface area), this can be written as,

$$A_{DAF,n} = \sum_n DAF(\omega_n) \cdot \Delta\omega$$

For  $n=6000$  components  $A_{DAF,6000}=0.27$  rad/s. This result can now be compared with results of  $A_{DAF}$  for various numbers of components given in figure 7.7 below.

Number of components (n)	$A_{DAF,n}$ (rad/s)	Percent difference with $A_{DAF,6000}$
81	0.54	100%
113	0.44	62%
162	0.37	37%
324	0.29	7%

**Figure 7.7 Influence of number of components on the surface area of the discretized dynamic amplification curve**

If we now run TURRETDYN with 324 components for wind and for waves, for which we know the accuracy is significantly better, the results should be far more representative. These results are given in figure 7.8 below.

Number of components	Frequency interval (rad/s)	Dynamic surge response (m)
324	0.002315	-16.57

**Figure 7.8 results of TURRETDYN for 324 components**

Indeed, what occurs is that where an accurate discretization is made, accounting well for the peakedness of the DAF, the results are stable around -16m and correspond much better with the average of the DYNFLOAT maxima.

- 2) The next point to consider is the influence of the linearized spring on the sensitivity of the results. The linear spring is merely a model, and though it may not be a realistic one it is not inherently wrong, however it dictates that resonance occurs at one frequency only for a co-linear case. This project does not put in question the accuracy of DYNFLOAT, which is meant to be run to its full capacity including the non-linear spring characteristics of the mooring system; what may additionally cause it to yield misleading results is the introduction of the linear spring. A non-linear spring is susceptible to resonant oscillation over a range of frequencies, which makes for a less peaked dynamic amplification curve, and so the problem of discretization would not be as significant as with a linear spring. What may therefore be said about TURRETDYN, foremost, is that if it is too sensitive at low frequencies, introducing a non-linear spring could, to some extent, resolve that

problem by reducing the peakedness of the DAF and so reducing the sensitivity to discretization.

- 3) Finally, we discuss the effect of sampling in time domain simulation. Time domain simulation is often regarded as accurate because of the potential to include much physical detail. It is easy to forget the effects of sample size on derived results. For a normal process with zero mean and duration  $T$ , the variance in the mean square of the signal is given by Bendat and Piersol as,

$$\frac{2}{T} \int_{-\infty}^{\infty} C_x^2(\tau) d\tau$$

where  $C_x$  is the auto-covariance of the process. For the present study, we do not know the auto-covariance for the surge response or if the process is normal. However, we might estimate the expression to be roughly  $2\sigma^4 T_n / T$ , where  $T_n$  is the natural period. Thus, the coefficient of variation of the estimate of the standard deviation of dynamic surge is order 10 per cent for a three hour simulation. For the extremes obtained from DYNFLOAT, we should note that the average of the extremes is an estimate of the expectation of the extreme response. Assuming the usual type of extreme value distribution, the expectation will be a little greater than the most probable value given by our TURRETDYN calculations. In view of the small number (8) of simulations, even this estimate of the expectation will be subject to significant uncertainty and bias.

7.4 CASE 2

In this section we will examine the same vessel as in case 1, but in a 40% loaded condition. This influences the vessels mass, the draft, the windage area; in short, all the factors that determine the forces that act on the vessels. Additionally, the lowered mass will lead to a higher natural frequency; this means an increase in the relative importance of radiation damping, and a less peaked dynamic amplification curve. Figure 7.9 gives the data for this case.

7.4.1 Co-linear case

Draft (m)	8.92
Length between PP (m)	325
Longitudinal exposed area (m <sup>2</sup> )	7425.62
Transvers exposed area (m <sup>2</sup> )	2270.13
Water density (Kg/m <sup>3</sup> )	1025.0
Air density (Kg/m <sup>3</sup> )	1.025
Current angle (deg)	0.0
Wind angle (deg)	0.0
Wave angle (deg)	0.0
Current velocity (m/s)	1.6
Wind velocity (m/s)	30.9
Arm (ship midpoint to center turret)	125.0
Significant wave height (m)	10.0
Mean wave period (s)	11.0
spring (kN/m)	915.0
limit on iteration	0.06
Probability of exceedance	0.0011626
Mass of the vessels (tons)	155400.0
Radius of gyration	81.25
Number of components wind/wave	200

Figure 7.9a Input data for case 2 colinear

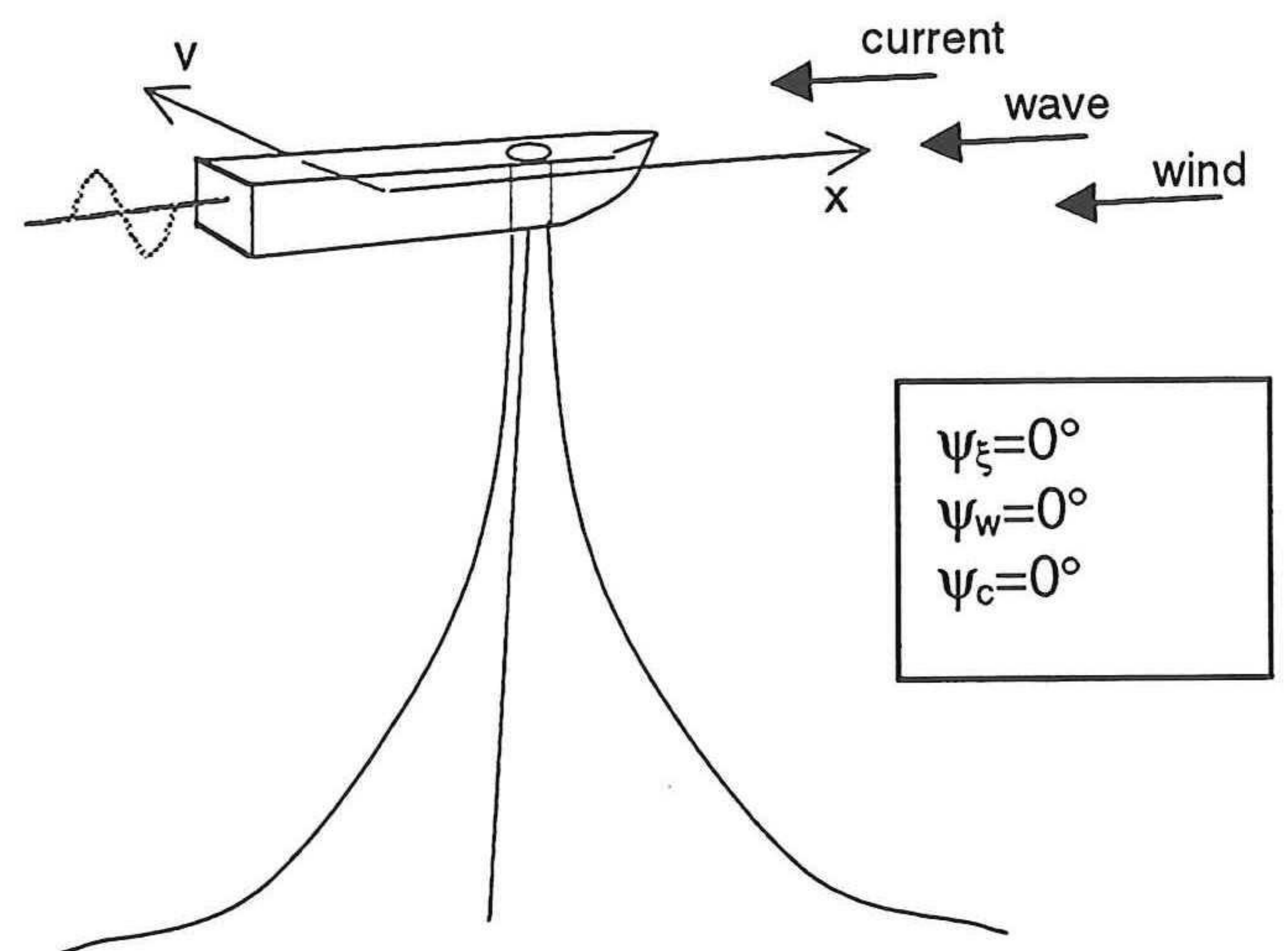


Figure 7.9b Relative direction of the environmental variables with respect to the ship

We first consider the co-linear case, with wind, wave and current aligned at zero degrees with respect to the ship ( $\psi_w=\psi_c=\psi_{\xi}=0^{\circ}$ ); in section 7.4.2 a cross current case will be examined with also wind acting at an angle ( $\psi_w=45^{\circ}$ ,  $\psi_c=100^{\circ}$ ,  $\psi_{\xi}=0^{\circ}$ ).

The probability of exceedance proves to be slightly different for this case, corresponding to a  $\beta$  of 3.67.

This case was run with 200 components, which yields a surface area of the discretized dynamic amplification curve of 0.50 rad/s, compared with the “real” surface area of 0.45 rad/s; this is a difference of about 10%. The results are given in figure 7.10

Static offset (m)	First order wave surge (m)	Second order wave surge (m)	Wind surge (m)	Total (m)
-2.5	0.365	-15.21	-1.52	-18.87

**Figure 7.10 Results for co-linear case 2 from TURRETDYN**

DYNFLOAT generates comparable data and the scatter is substantially less than in the previous case. This data is given in figure 7.11 below.

Run	Static offset (m):	Standard deviation (m)	Max. dynamic offset (m)
			-2.56
1		5.32	-14.61
2		8.25	-24.07
3		6.16	-17.81
4		7.50	-21.76
5		6.00	-18.41
6		5.17	-16.97
7		5.86	-19.41
8		5.30	-17.04
			Average= -18.76
			<b>TOTAL = -21.32</b>

**Figure 7.11 Results for the co-linear case2 from DYNFLOAT**

Again here TURRETDYN underestimates the response compared with DYNFLOAT; this may be attributable to the factors that were discussed for case 1. The results shown in figure 7.10 show clearly the predominance of second order forces. The natural frequency in surge is in the order of 0.075 rad/s for which there is virtually no available spectral energy to excite the system at wave frequency.

The second order forces however, though they are relatively weak, benefit from the dynamic amplification and the low damping to produce significant response. Figure 7.12 below shows the second order wave surge response. Recall that the natural frequency of the oscillation is about 0.075 rad/s, which corresponds to a period of about,

$$T = \frac{1}{0.075 / 2\pi} \approx 84s$$

and indeed the second order wave surge oscillation clearly has a period of just under 100 seconds. The system is excited in its resonant frequency which allows the relatively weak second order forces to occasion such large offsets.

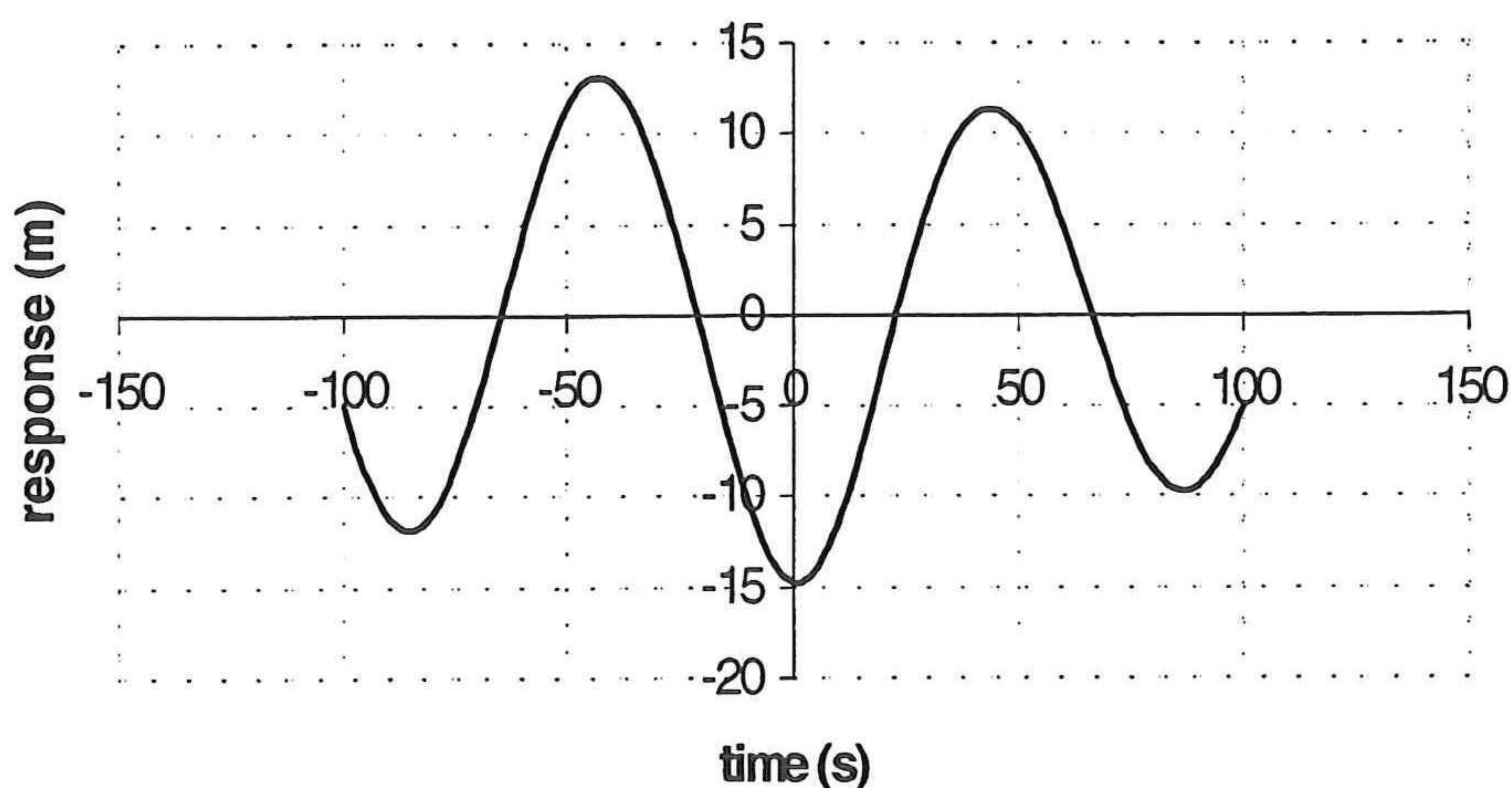


**Figure 7.12 Second order wave surge**

There is virtually no first order wave response because there is very little available energy at 0.075 rad/s. Wind gust energy, however, at this frequency is substantial enough to occasion response as given in figure 7.13 below.

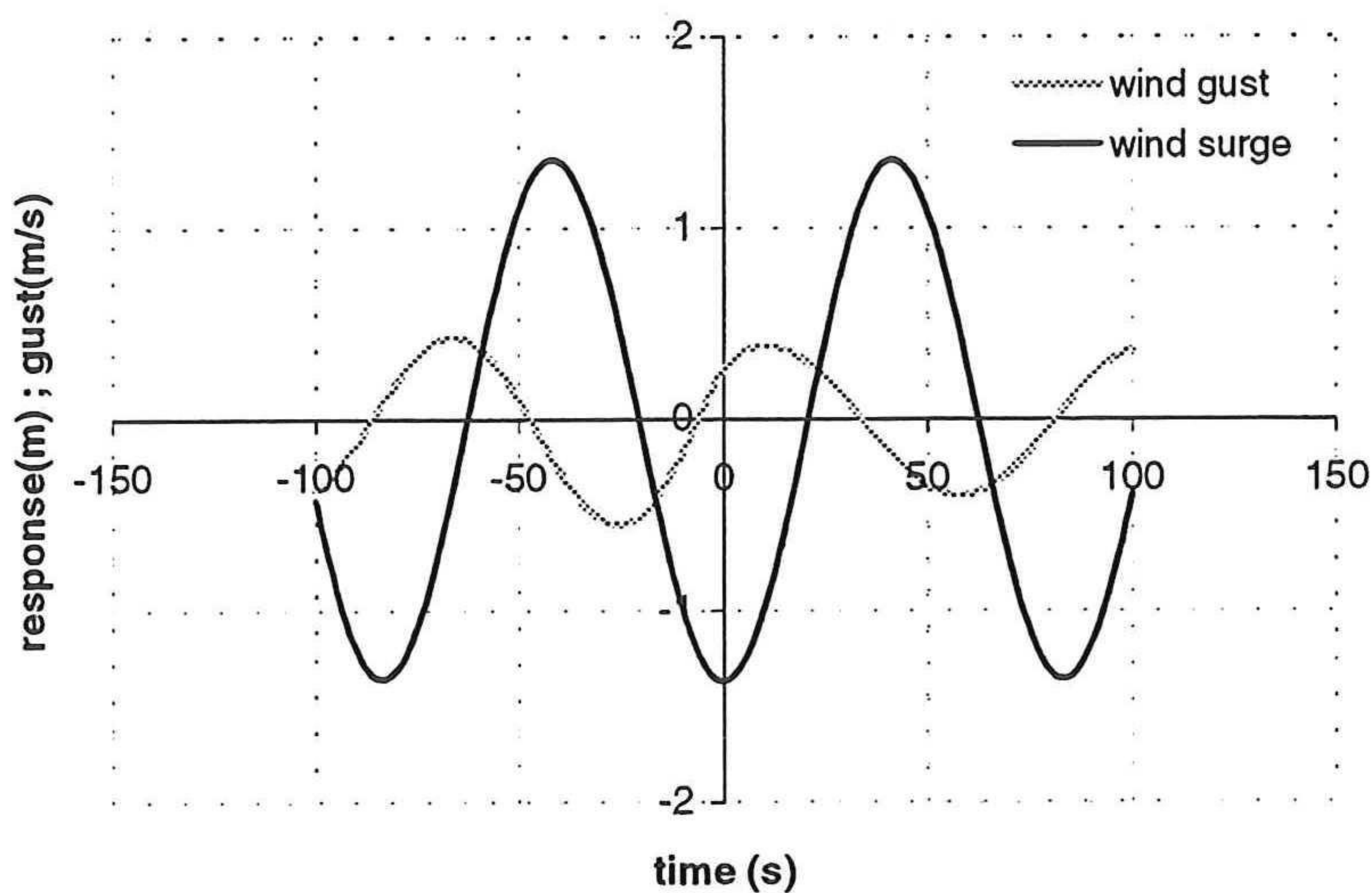


**Figure 7.13 Wind surge response and wind gust history**

Wind gusts also excite the system at resonant frequency ( $T \approx 84s$ ). Note the lag in the surge response with respect to the wind gusts; this is due to the dynamic relation between displacement and velocity.

What is clear is that the extreme response is governed by the natural frequency; the optimization aligns the components with this natural frequency and assigns more “weight” to components that contribute to resonant oscillation

**7.4.2 Cross current case**

The defining feature of the system has not been considered yet, namely the weathervaning capability of the ship around its turret. The same case as above is now considered with changes to the directions of the wind and current, and the velocity of the current is increased to cause a further rotation of the vessel. This data is given in figure 7.14 below.

```

Draft (m).....:
8.92
Length between PP (m).....:
325
Longitudinal exposed area (m^2).....:
7425.62
Transvers exposed area (m^2).....:
2270.13
Water density (Kg/m^3).....:
1025.0
Air density (Kg/m^3).....:
1.025
Current angle (deg).....:
100.0
Wind angle (deg).....:
45.0
Wave angle (deg).....:
0.0
Current velocity (m/s).....:
2.6
Wind velocity (m/s).....:
30.9
Arm (ship midpoint to center turret).....:
125.0
Significant wave height (m).....:
10.0
Mean wave period (s).....:
11.0
spring (kN/m).....:
915.0
limit on iteration.....:
0.07
Probability of exceedance.....:
0.0014916
Mass of the vessels (tons).....:
155400.0
Radius of gyration.....:
81.25
Number of components wind/wave.....:
400
    
```

**Figure 7.14a Input data for TURRETDYN**

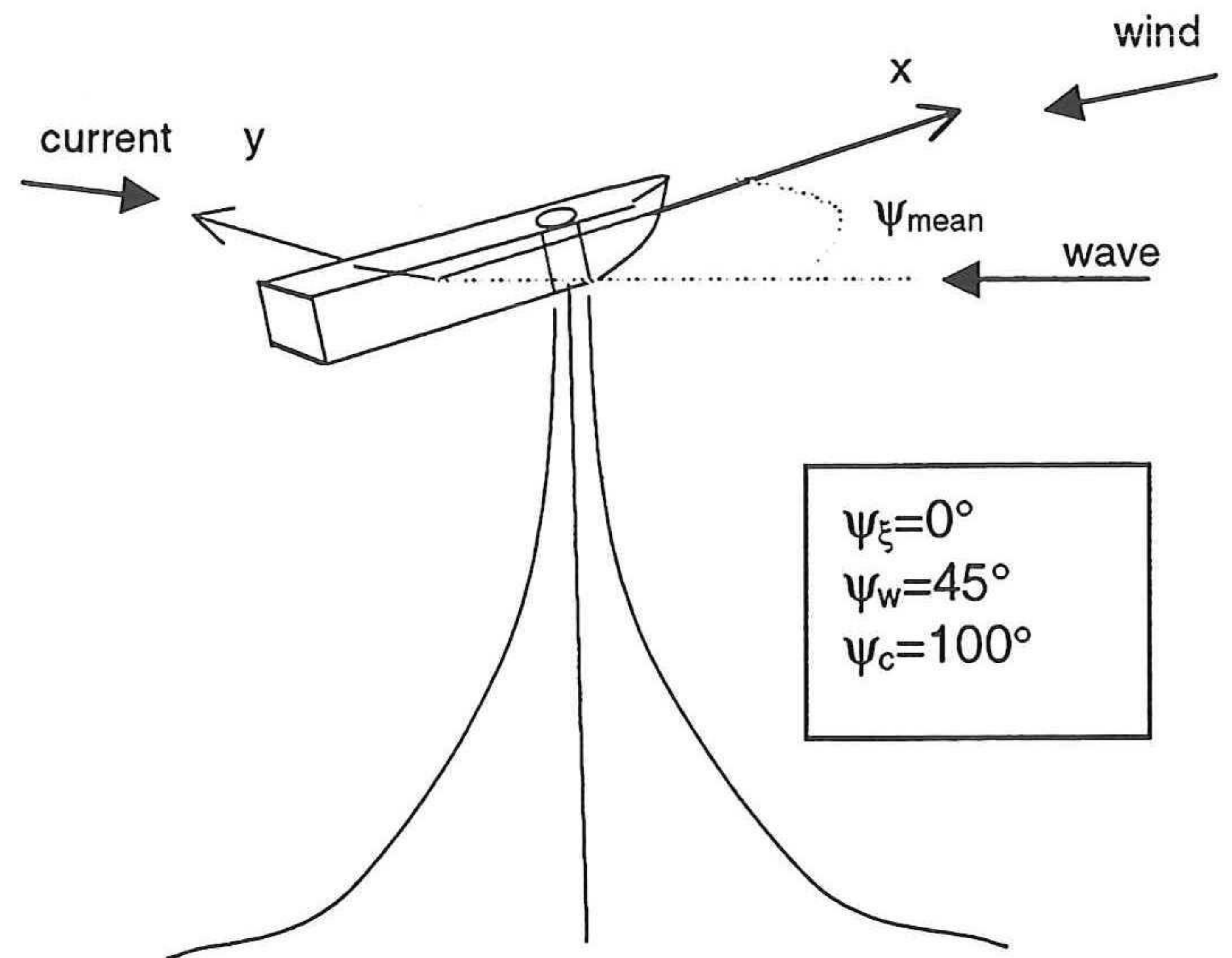


**Figure 7.14b direction of Environmental forces for the cross current case 2**

TURRETSTAT (the static analysis program developed for this project) calculates the mean offset and heading for the input given in figure 7.14a. The static results, given for the center of gravity of the ship, are given in figure 7.15.

*static results*

<b>Mean heading</b>	61°
<b>Mean X<sub>COG</sub></b>	62m
<b>Mean Y<sub>COG</sub></b>	-110m

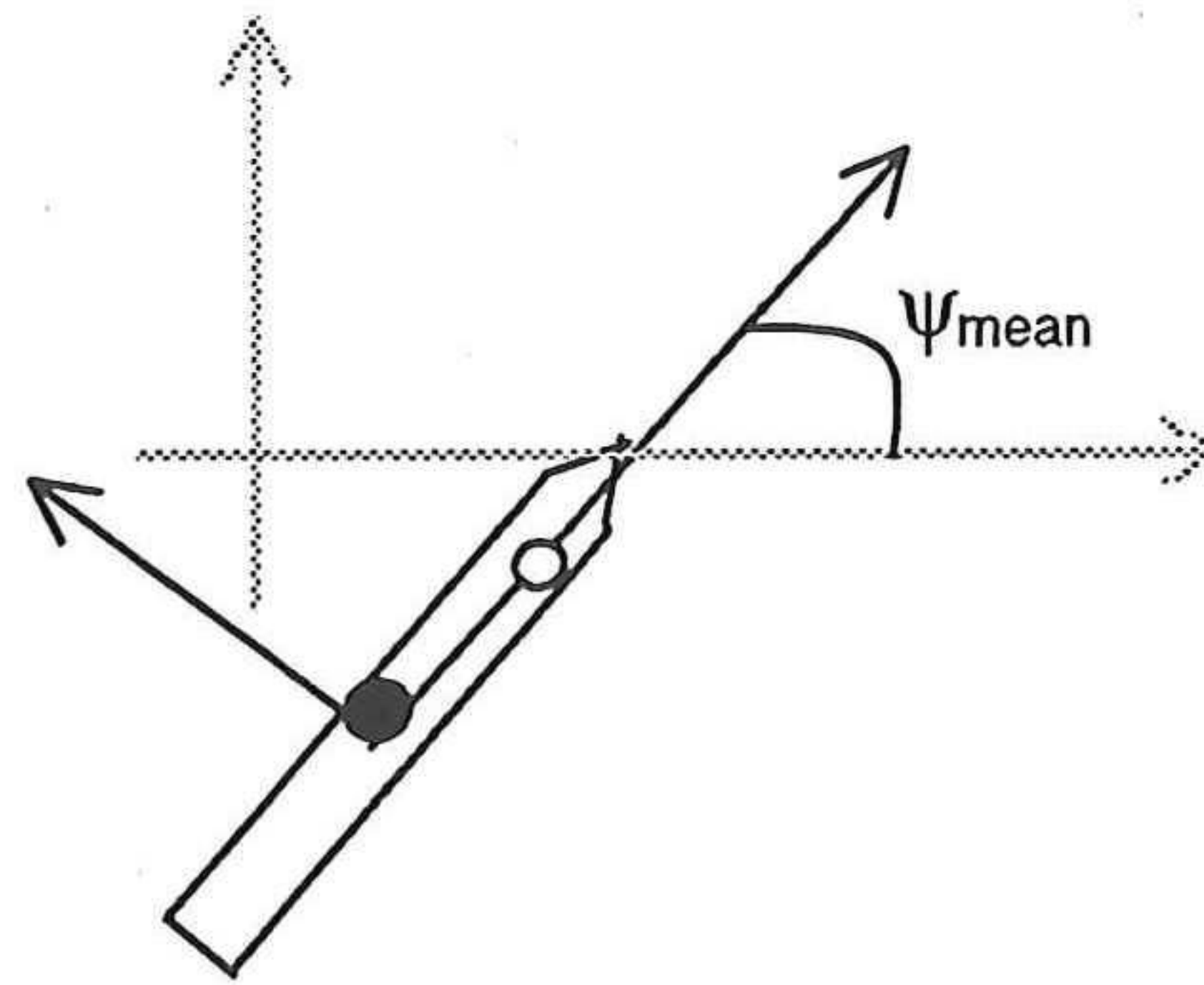


**Figure 7.15 Equilibrium position and heading**

In this case the three degrees of freedom play a role in the dynamic response of the system; this means that there are three natural frequencies to be accounted for: one for the uncoupled surge, and two modal natural frequencies associated with motions in sway and yaw. It is known from the previous example that the natural frequency in surge is about 0.075 rad/s (this value varies per incident wave frequency because the natural frequency depends on the added mass, which is frequency dependent). The ship will oscillate about the mean position and heading as is given figure 7.15 above. The mode shapes that constitute its motion in sway and yaw as calculated by TURRETDYN are shown in figure 7.16. In order to show the mode shapes, a nominal sway offset of 30m is assumed

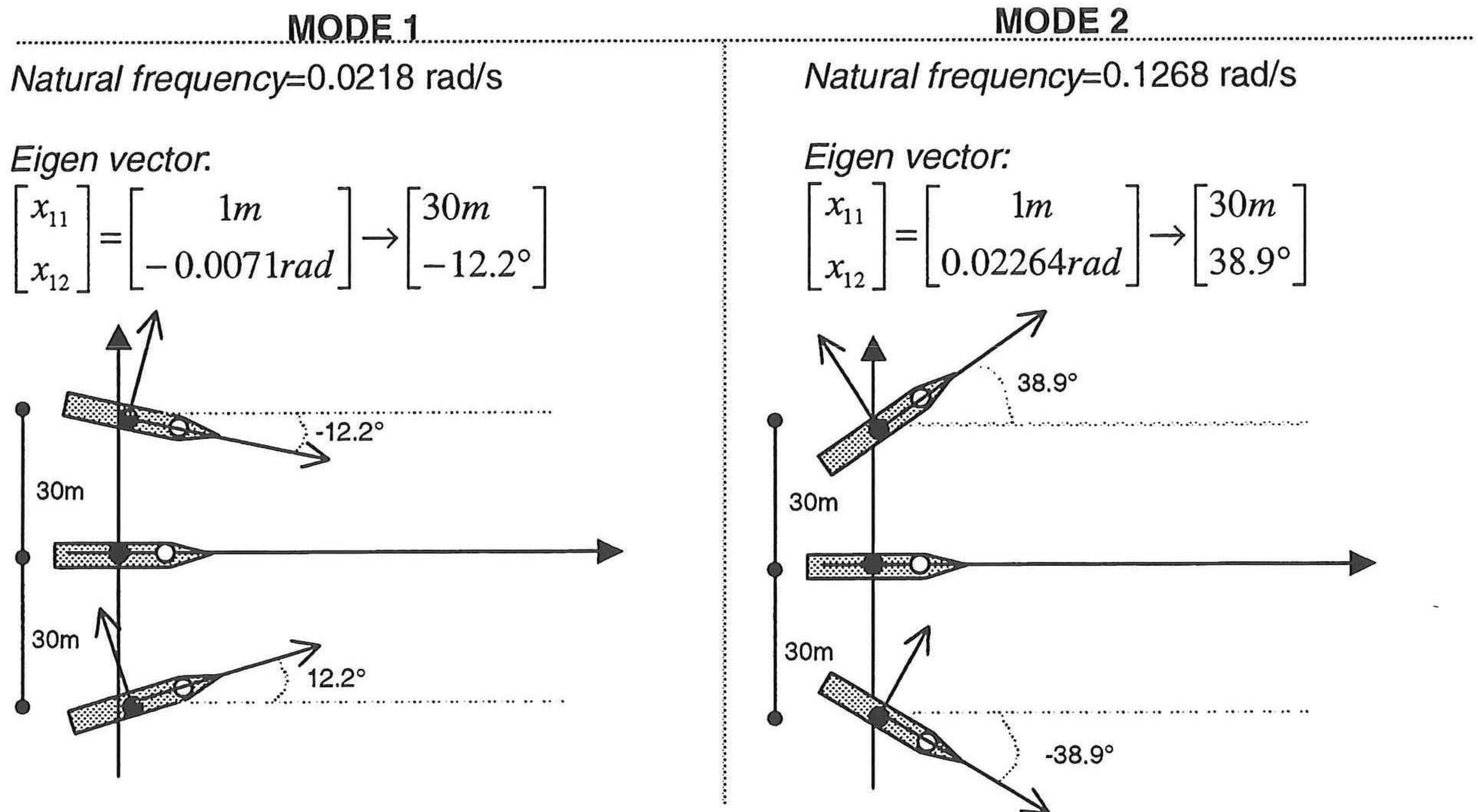


**Figure 7.16 Mode shapes for case 2**

As mentioned, there are three natural frequencies to be account for. In case1 it was demonstrated how significant the discretization of the dynamic amplification factor is. In the co-linear example of case 2, the single natural frequency was accurately accounted for with 200 components; in this case, 400 components are required to accurately define the three dynamic amplification curves. This substantially increases computer time, and makes this development software less competitive with its time-domain counterpart. The results as calculated by TURRETDYN for n=400, are given in figure 7.17a below.

	First order wave response	Second order Wave response	Wind response	Total dynamic response
Surge (m)	-0.554	-0.873	-0.438	-1.86
Sway (m) Y	0.310	-17.92	-0.169	-17.78
Yaw (deg) $\psi$	0.327	13.31	0.0067	13.64

Figure 7.17a Dynamic results for cross-current case 2, as calculated by TURRETDYN

These results are in the local (ship fixed) co-ordinate system, and they are given with respect to the calculated static equilibrium. In other words, the response given in figure 7.17 are oscillations about the mean position and heading. The same is true for the results as calculated by the time domain simulation program DYNFLOAT, which are given in figure 7.17b. Because lateral motion is the dominant response motion in this case, only sway and yaw statistics are given.

Run	Motion	Standard deviation	Maximum dynamic Response
		<b>Static response</b>	<b>X: 65.3 m</b>
			<b>Y: -95.3 m</b>
			<b><math>\psi</math>: 59.5°</b>
1	Y (m)	5.15	-15.71
	$\psi$ (deg)	4.34	-13.90
2	Y (m)	5.33	-21.80
	$\psi$ (deg)	4.35	-14.34
3	Y (m)	5.81	-19.28
	$\psi$ (deg)	4.35	-16.69
4	Y (m)	5.60	-22.84
	$\psi$ (deg)	4.36	-13.28
5	Y (m)	6.20	-16.31
	$\psi$ (deg)	4.89	-16.66
		<b>Average:</b>	<b>Y=-19.19m</b>
			<b><math>\psi</math>=14.9°</b>

Figure 7.17b Dynamic results for cross-current case 2, as calculated by DYNFLOAT

There is fairly good correspondence between the results from TURRETDYN and those from DYNFLOAT, and the latter seem to show less scatter than in the previous cases making them a good basis of comparison with the frequency domain program TURRETDYN.

Again the response is dominated by the second order effect. Surge is relatively small compared to the lateral response, but this does not mean that there is not greater surge response possible; all it means is that the optimization process yields this particular response configuration as the maximum possible for the given probability of exceedance. In figure 7.18 below, the time series for the second order wave surge and lateral responses are given. Indeed, in figure 7.18 the surge response reaches as high as five meters.

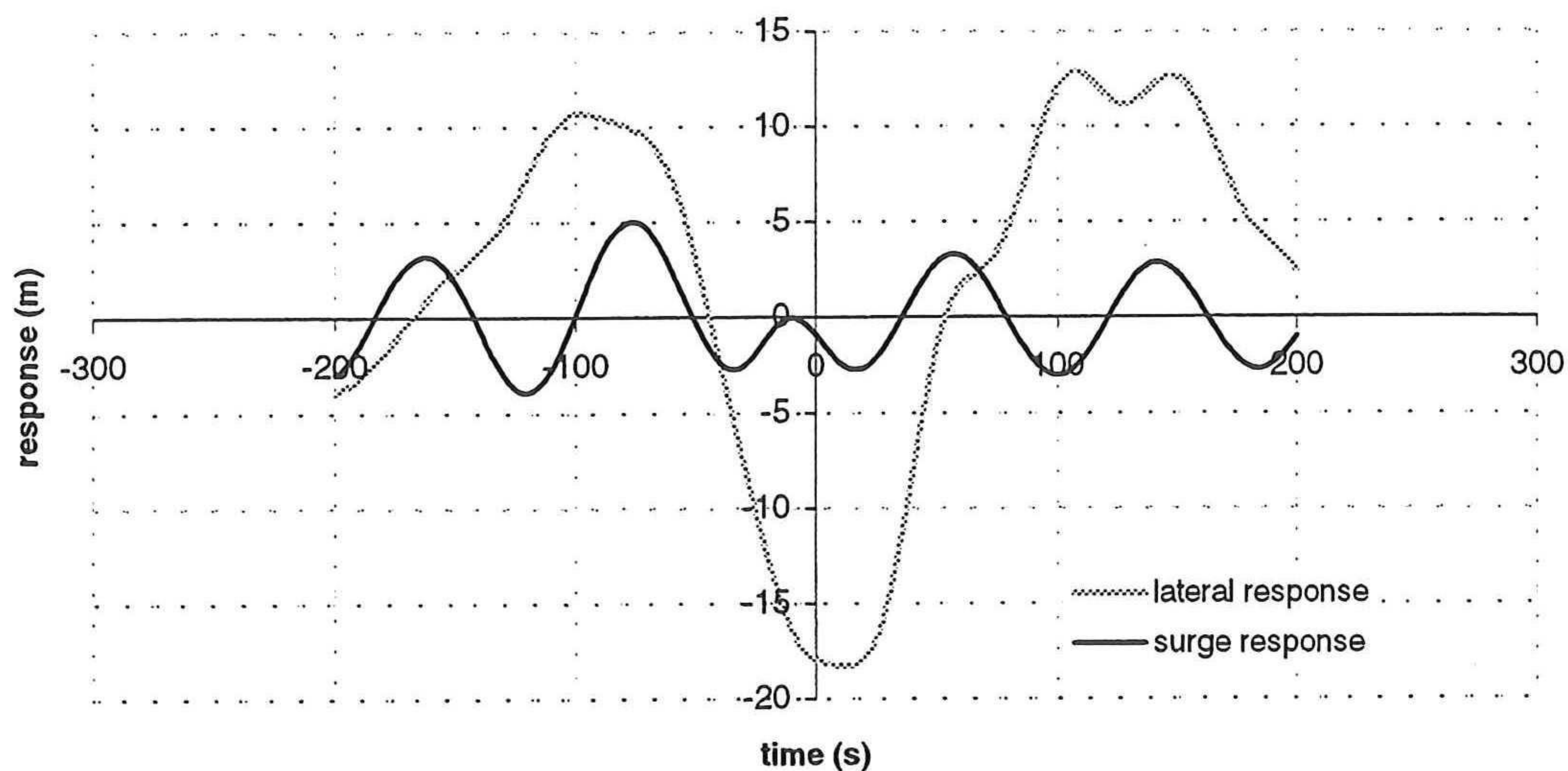


**Figure 7.18 Time series of the second order lateral and surge response**

The surge response in figure 7.18 is considerably more regular than the lateral response. This is because surge motion is not coupled and is therefore governed by only one natural frequency. Indeed, the oscillation in surge has a period of about 80s, which corresponds to the natural frequency of  $0.0752\text{rad/s}$ , as is described in the co-linear case 2 above.

The lateral motion, being constituted of coupled sway and yaw, is governed by two natural frequencies, which results in two modes of oscillation. When we decomposed the lateral motion into its two constituent modes we find that its irregularity in fact results from the superposition of the modal responses, which individually are relatively regular as can be seen in figure 7.19 below.

The maximum lateral response is dominated by mode 1 oscillation, which has a period of approximately 250 seconds; this corresponds very well with the natural frequency associated with mode 1 of  $0.0218\text{rad/s}$  ( $T=288\text{s}$ ). The reason mode 1 dominates is that for the same lateral response, a mode 2 oscillation requires more than twice as much yaw (see figure 7.16); the environmental restoring forces (discussed in section 5.3) counter any departure from the equilibrium. The less the ship yaws, the less it will be “forced” back to its equilibrium position, and therefore mode 1 is more apt to generate lateral response than mode 2.

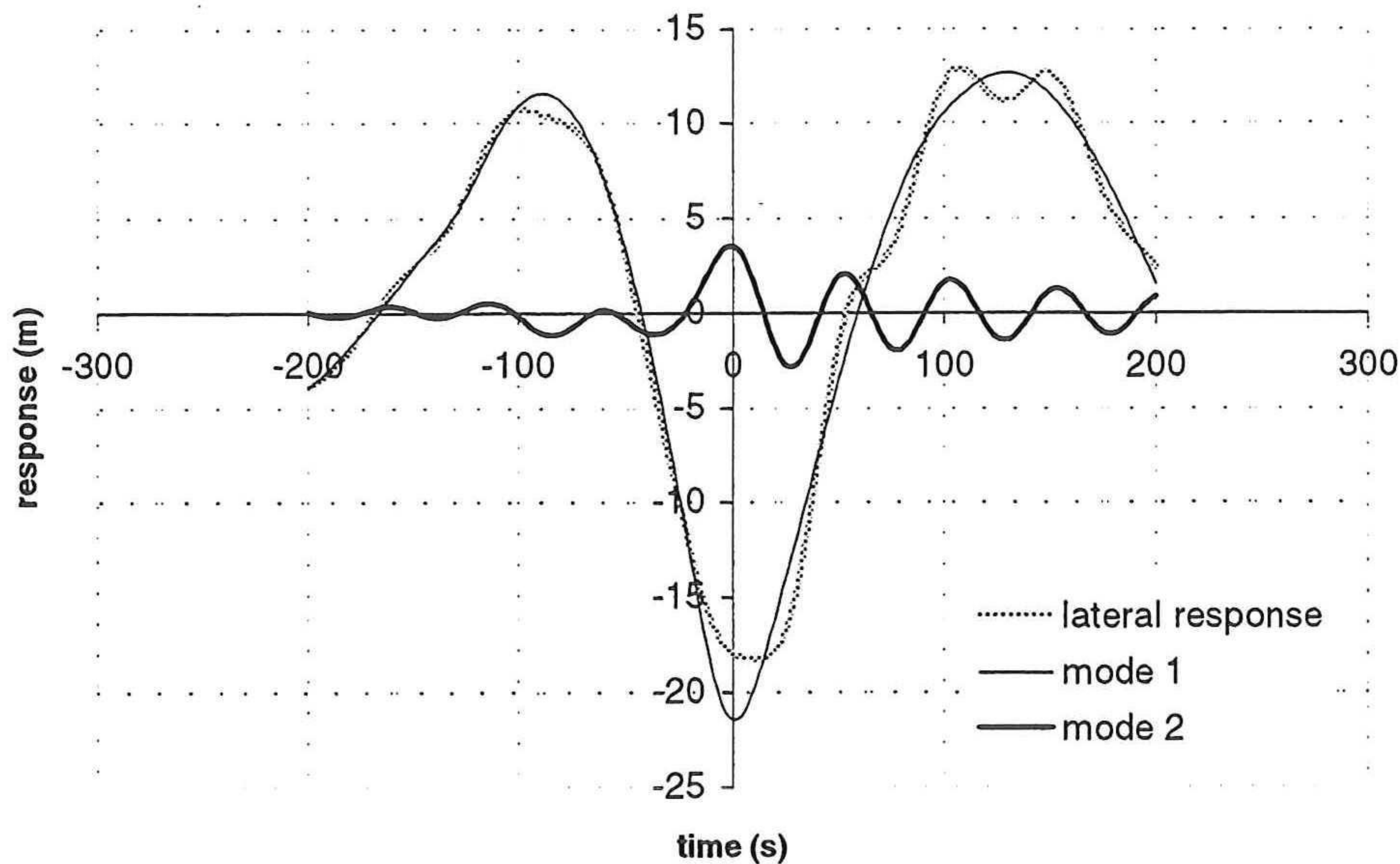


**Figure 7.19** Second order wave sway response decomposed into its constituent modes.

Furthermore, mode 2 oscillates at a frequency of 0.127 rad/s, which corresponds to a period of about 50 s; this is a frequency about 5 times greater than that of mode 1. We may, therefore, expect far more damping in mode 2 than in mode 1.

There are 400 components over a spectral range of 0 to 0.75 rad/s, this gives a frequency interval of 0.001875rad/s, which means the time series repeats itself after 3351s. Figure 7.18 only shows 400s worth of response, but it gives the maximum that occurs during the history. Figure 7.20 gives the wave history over a 800 second range.

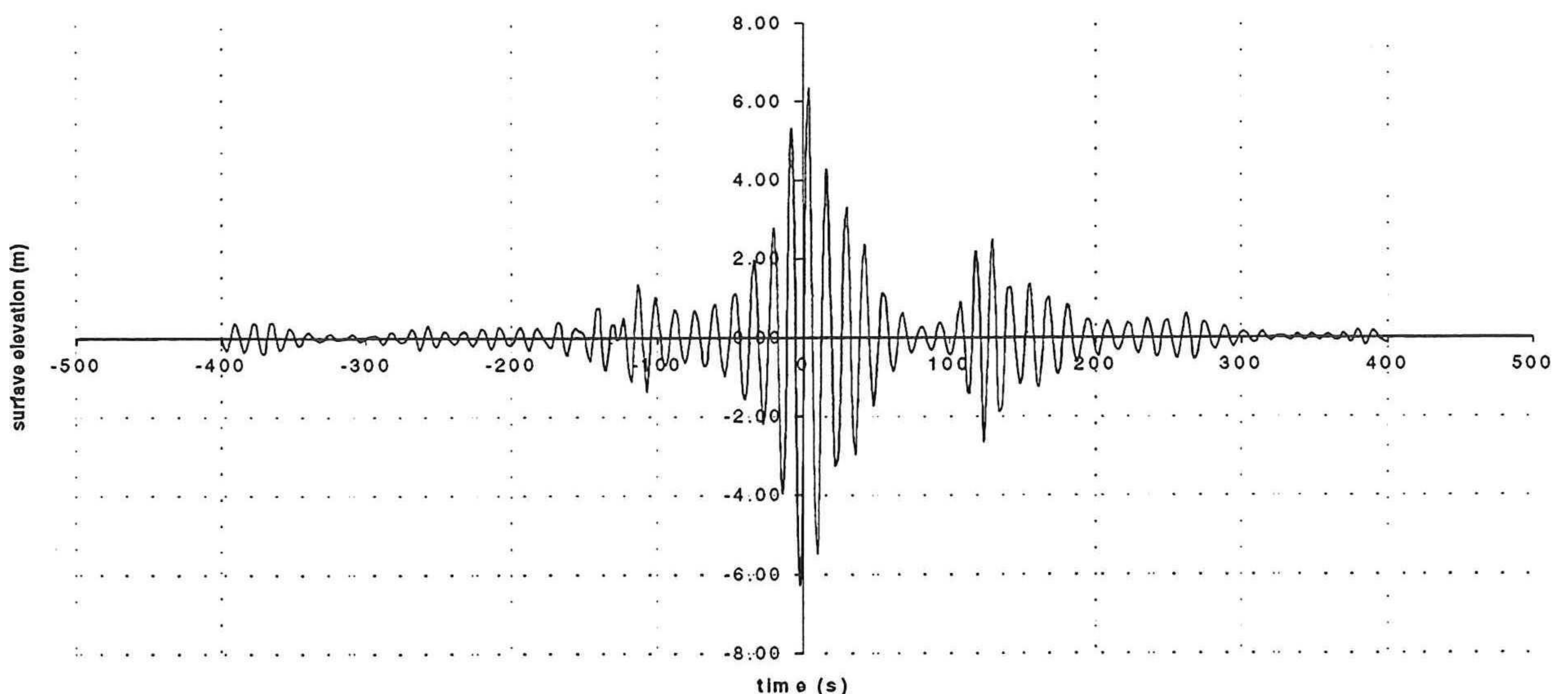


**Figure 7.21** Wave history

Note that though we are dealing with a sea state with a significant wave height of 10m, the wave amplitude associated with the maximum response is only 6m; this again points to the superior importance of frequency, rather than amplitude, in the extreme response: dynamic amplification governs the behavior of the system.

## 7.5 Concluding remarks

Linearization and discretization together work to make the system very sensitive, in certain situations even over-sensitive. The linearized spring at low frequency oscillation gives rise to a very peaked dynamic amplification curve which only viscous damping (radiation damping is virtually insignificant at low frequency) can keep in check. Discretizing such a peak requires very small intervals, and it is not possible to simply increase the refinement around the resonant frequency because it isn't wave frequency response that is predominant but second order forces which rely on a combination of wave components of higher energy; therefore the entire higher energy range of the wave spectrum needs refinement. The object of this method is, among other aims, to win time over the time domain simulation, but calculations with a number of components in excess of 300 (in spite of the provisions made in the program to speed up the calculation by bypassing calculations that contribute insignificantly to the response, either due to low energy content or dynamic amplification) make the frequency domain no longer attractive.

In addition to the fact that a non-linear spring would far better represent the stiffness characteristics of the mooring system, the implementation of a non-linear spring may also reduce the sensitivity problem: the system would no longer be susceptible to only one resonant frequency, so making it very sensitive, but a range of frequencies. The skewed nature of non-linear spring curves would admit larger frequency intervals in the discretization (while retaining the same level of accuracy) so reducing the number of components required.

A second point that needs further attention is the viscous damping, which governs the extent of dynamic amplification at low frequency oscillation and so must be modeled very accurately. In this project the square of the system velocity is assumed negligible- in a zero current case this term becomes essential. This is another non-linearity that needs to be integrated into the method.

The results, however, seem to demonstrate at least that the method is applicable to this type of problem. The shortcomings mentioned above do need further attention, but the basis is sound. If these problems are resolved and the algorithm is sufficiently streamlined to root out any unnecessary computations, then the object may be reached.



## 8. CONCLUSION

A probabilistic method (first-order second-moment) has been applied to the problem of extreme response of turret moored vessels. Though the accent has been put on the advantage of such a method over time domain simulation, it may be considered a very effective one in its own right: it allows limits state criteria (i.e. force, displacement etc.) of any dimension and variables of any distribution; additionally, the method provides a means to retrieve the wind and wave histories that occasioned the extreme response.

With respect to time domain analysis, as has been mentioned already, the time investment is the main distinction between the two methods. However, it must be noted that this advantage is lost in the case of a dynamic amplification curve that is particularly peaked (as with very low frequency oscillations), because the discretization necessitates too great a number of components.

As it stands, the program is not yet fit to be used as a tool for global design. There are two areas in particular that would need to be addressed, namely, the inclusion of non-linearities and the streamlining of the algorithm.

The non-linearities that need to be accounted for are the non-linear spring characteristics and the non-linear viscous damping term; both are crucial for a realistic calculation.

Streamlining might include an effective means to circumvent any response calculation that does not significantly contribute to the total response.

Further development of the program might include the implementation of the remaining degrees of freedom, heave pitch and roll, as well directional wind and wave spectra. This together with the improvements mentioned above would make for accurate and reliable extreme response calculations.



## Nomenclature

a:	incident wave amplitude
A:	added mass matrix
$A_L$ :	lateral wind area
$A_T$ :	transverse wind area
B:	damping matrix
C:	stiffness matrix
$C_c$ :	current force coefficient
$C_{lin}$ :	linear spring constant
$C_{env}$ :	environmental rotational stiffness
$C_w$ :	wind force coefficient
E:	eigen vector matrix
$F^{(2)}$ :	(low frequency) second order wave force
$F^{(1)}$ :	first order wave force
f:	frequency (Hertz)
$F_{cur}$ :	current force
$F_{win}$ :	static wind force
$F_{win,dyn}$ :	Dynamic wind force
$g(x)$ :	limit-state function
g:	gravitational acceleration
$H_s$ :	significant wave height
I:	first order wave force transfer function
$L_{pp}$ :	length between perpendiculars
M:	mass matrix
n:	number of wave frequency components
m:	number of wind frequency components
p:	pressure
$P_n$ :	in phase quadratic transfer function
$P_f$ :	failure probability
$Q_n$ :	out of phase quadratic transfer function
Q:	probability of exceedance
S:	energy density spectrum
$T_z$ :	mean wave period
T:	draft
t:	time
U:	current velocity
$V_z$ :	wind velocity
$v_w$ :	wind velocity at level $h_0$
w:	unsteady wind component
x-tilde:	Hilbert transform of the random variable
x:	surge
$X^*$ :	design point
y:	sway
$\rho_c$ :	water mass density
$\rho_a$ :	air mass density
$\varepsilon$ :	random phase angle
$\omega$ :	circular frequency
$\eta$ :	wave surface elevation
$\phi$ :	velocity potential
$\sigma$ :	standard deviation
$\mu$ :	mean
$\delta$ :	wave elevation to force phase shift
$\Psi_{mean}$ :	mean ship heading

$\psi_c$ :	current angle of attack
$\psi_w$ :	wind angle of attack
$\psi_\xi$ :	wave angle of attack
$\psi$ :	yaw
$\Omega$ :	eigen value matrix
$\phi$ :	phase shift between force and response
$\xi$ :	system response
$\beta$ :	reliability index
$\Phi$ :	Gaussian distribution
$\lambda$ :	Langrangian multiplier

**References:**

- *API Recommended Practice 2T (RP 2T), Supplement 1*: American Petroleum Institute, Washington DC, 1992.
- Battjes, J.A.: *Windgolven* : reader TU-Delft, 1992.
- Bendat, J.S, Pierson, A.G, *Random Data: Analysis and Measurement Procedures*: John Wiley and Sons, New York, 1971.
- Chakrabarti, S.K. : *Hydromechanics of Offshore Structures*: Computational Mechanics Publications, Boston, 1987.
- Faltinsen, O.M.: *Sea Loads on Ships and Offshore Structures*: Cambridge University press, Cambridge: 1990.
- Journee, J.M.J.: *Bewegingen van Constructies in Golven* : Delft University of Technology, 1992.
- Newman, J.N.: *Marine Hydrodynamics* : MIT Press, Cambridge, 1977.
- Patel, M.H. : *Advanced Offshore Engineering*. BPP Technical Services Ltd., 1994.
- Pinkster, J.A.: *Low Frequency Second Order Wave Exciting Forces on Floating Structures*, PhD Thesis, TU-Delft, 1980.
- *Prediction of Wind and Current Loads on VLCC's* : OCIMF Publication, 1994.
- Spijkers, J., Dieterman, H., Klaver, E., Vrouwenvelder, A.C.W.M. *Dynamica van Constructies Deel 1*, reader TU-Delft, 1995.
- Timoshenko, S., Young, D.H., Weaver, jr, W: *Vibration Problems in Engineering, Fourth Edition*, John Wiley & Sons, New York, 1974.
- Vrouwenvelder, A.C.W.M., Klaver, E.C.: *Stochastische Trillingen*: reader TU-Delft, 1994.
- Wichers, J.E.W.: *A Simulation Model For a Single Point Moored Tanker*. PhD Thesis, MARIN 1988.



**APPENDIX**



**First order wave sway and yaw:**

Recall that the eigen vectors are written as follows:

$$E = \begin{bmatrix} \hat{x}_{11} & \hat{x}_{12} \\ \hat{x}_{21} & \hat{x}_{22} \end{bmatrix} = \begin{bmatrix} \underline{\hat{x}}_1 & \underline{\hat{x}}_2 \end{bmatrix}$$

The numerical indices 1 and 2 refer modes 1 and 2; indices n and m refer to wave and wind components, respectively.

The first order wave response in sway can be written based on equation 5.19

$$\zeta_{y,wave}^{(1)} = \hat{x}_{11} \cdot \frac{1}{\omega_1^2} \frac{\sum_n DAF_1 \cdot \left[ \hat{x}_{11} I_y \sigma_n (x_n \cos(\delta_y + \phi_1) - \tilde{x}_n \sin(\delta_y + \phi_1)) + \hat{x}_{21} I_\psi \sigma_n (x_n \cos(\delta_\psi + \phi_1) - \tilde{x}_n \sin(\delta_\psi + \phi_1)) \right]}{\underline{\hat{x}}_1^T A \underline{\hat{x}}_1} +$$

$$\hat{x}_{12} \cdot \frac{1}{\omega_2^2} \frac{\sum_n DAF_2 \cdot \left[ \hat{x}_{12} I_y \sigma_n (x_n \cos(\delta_y + \phi_2) - \tilde{x}_n \sin(\delta_y + \phi_2)) + \hat{x}_{22} I_\psi \sigma_n (x_n \cos(\delta_\psi + \phi_2) - \tilde{x}_n \sin(\delta_\psi + \phi_2)) \right]}{\underline{\hat{x}}_2^T A \underline{\hat{x}}_2}$$

The yaw response is determined by substituting the corresponding mode shape:

$$\zeta_{\psi,wave}^{(1)} = \hat{x}_{21} \cdot \dots + \hat{x}_{22} \cdot \dots$$

**First order wind sway and yaw:**

Similarly, for sway

$$\zeta_{y,wind} = \hat{x}_{11} \cdot \frac{1}{\omega_1^2} \frac{\sum_m DAF_1 \cdot 2 \cdot |V_z| \cdot \sigma_m (X_m \cos(\phi_1) - \tilde{X}_m \sin(\phi_1)) [\hat{x}_{11} D_y + \hat{x}_{21} D_\psi]}{\underline{\hat{x}}_1^T A \underline{\hat{x}}_1} +$$

$$\hat{x}_{12} \cdot \frac{1}{\omega_2^2} \frac{\sum_m DAF_2 \cdot 2 \cdot |V_z| \cdot \sigma_m (X_m \cos(\phi_2) - \tilde{X}_m \sin(\phi_2)) [\hat{x}_{12} D_y + \hat{x}_{22} D_\psi]}{\underline{\hat{x}}_2^T A \underline{\hat{x}}_2}$$

and yaw,

$$\zeta_{\psi,wind} = \hat{x}_{21} \cdot \dots + \hat{x}_{22} \cdot \dots$$

## Second order sway and yaw:

Again, the numerical indices 1 and 2 refer modes 1 and 2; indices j and k refer to the two wave components.

The expression as given in section 6 is the following:

$$\xi_{wave}^{(2)} = \sum_i \hat{x}_i \cdot \frac{1}{\omega_i^2} \frac{\sum_{j=1}^N \sum_{k=1}^N DAF_i^{(2)} \cdot \hat{x}_i^T \left\{ \begin{array}{l} P_{jk} \{ \sigma_k x_k \sigma_j x_j \cos(\phi_i) + \sigma_k \tilde{x}_k \sigma_j \tilde{x}_j \cos(\phi_i) - \\ \sigma_k \tilde{x}_k \sigma_j x_j \sin(\phi_i) + \sigma_k x_k \sigma_j \tilde{x}_j \sin(\phi_i) \} + \\ Q_{jk} \{ \sigma_k \tilde{x}_k \sigma_j x_j \cos(\phi_i) - \sigma_k x_k \sigma_j \tilde{x}_j \cos(\phi_i) + \\ \sigma_k x_k \sigma_j x_j \sin(\phi_i) + \sigma_k \tilde{x}_k \sigma_j \tilde{x}_j \sin(\phi_i) \} \end{array} \right\}}{\hat{x}_i^T A \hat{x}_i}$$

We will define a few expressions to simplify the full equation:

$$\begin{aligned} X_{in,1} &= [x_k x_j \cos(\phi_1) + \tilde{x}_k \tilde{x}_j \cos(\phi_1) - \tilde{x}_k x_j \sin(\phi_1) + x_k \tilde{x}_j \sin(\phi_1)] \\ X_{in,2} &= [x_k x_j \cos(\phi_2) + \tilde{x}_k \tilde{x}_j \cos(\phi_2) - \tilde{x}_k x_j \sin(\phi_2) + x_k \tilde{x}_j \sin(\phi_2)] \\ X_{out,1} &= [\tilde{x}_k x_j \cos(\phi_1) - x_k \tilde{x}_j \cos(\phi_1) + x_k x_j \sin(\phi_1) + \tilde{x}_k \tilde{x}_j \sin(\phi_1)] \\ X_{out,2} &= [\tilde{x}_k x_j \cos(\phi_2) - x_k \tilde{x}_j \cos(\phi_2) + x_k x_j \sin(\phi_2) + \tilde{x}_k \tilde{x}_j \sin(\phi_2)] \end{aligned}$$

we may now write,

$$\begin{aligned} \xi_{y,wave}^{(2)} &= \hat{x}_{11} \cdot \frac{1}{\omega_1^2} \frac{\sum_{j=1}^N \sum_{k=1}^N DAF_1^{(2)} \cdot \left[ \hat{x}_{11} [P_y \sigma_k \sigma_j X_{in,1} + Q_y \sigma_k \sigma_j X_{out,1}] + \right. \\ &\quad \left. \hat{x}_{21} [P_\psi \sigma_k \sigma_j X_{in,1} + Q_\psi \sigma_k \sigma_j X_{out,1}] \right]}{\hat{x}_1^T A \hat{x}_1} + \\ &\quad \hat{x}_{12} \cdot \frac{1}{\omega_2^2} \frac{\sum_{j=1}^N \sum_{k=1}^N DAF_2^{(2)} \cdot \left[ \hat{x}_{12} [P_y \sigma_k \sigma_j X_{in,2} + Q_y \sigma_k \sigma_j X_{out,2}] + \right. \\ &\quad \left. \hat{x}_{22} [P_\psi \sigma_k \sigma_j X_{in,2} + Q_\psi \sigma_k \sigma_j X_{out,2}] \right]}{\hat{x}_2^T A \hat{x}_2} \end{aligned}$$

as above,

$$\xi_{\psi,wave}^{(2)} = \hat{x}_{21} \cdot \dots + \hat{x}_{22} \cdot \dots$$